

The role of crustal-scale shear zones in SW Gondwana consolidation – transatlantic correlation




Renata da S. Schmitt^{1,2*}, Rudolph A. J. Trouw^{1,2}, Evânia Alves da Silva^{1,2},
João Vitor Mendes de Jesus¹, Luis Felipe M. da Costa² and
Claudia R. Passarelli³

¹Departamento de Geologia-IGEO, Universidade Federal do Rio de Janeiro, Rio de Janeiro, Brazil

²Programa de Pós-Graduação em Geologia, IGEO, Universidade Federal do Rio de Janeiro, Rio de Janeiro, Brazil

³Instituto de Geociências, Universidade de São Paulo, Rio de Janeiro, Brazil

 RDSS, 0000-0001-6349-5459; RAJT, 0000-0003-0901-8234;
EADS, 0000-0001-5875-9552; JVMDJ, 0000-0002-1804-3776;
LFMDC, 0000-0002-1659-8233; CRP, 0000-0001-6435-9205

*Correspondence: schmitt@geologia.ufrj.br

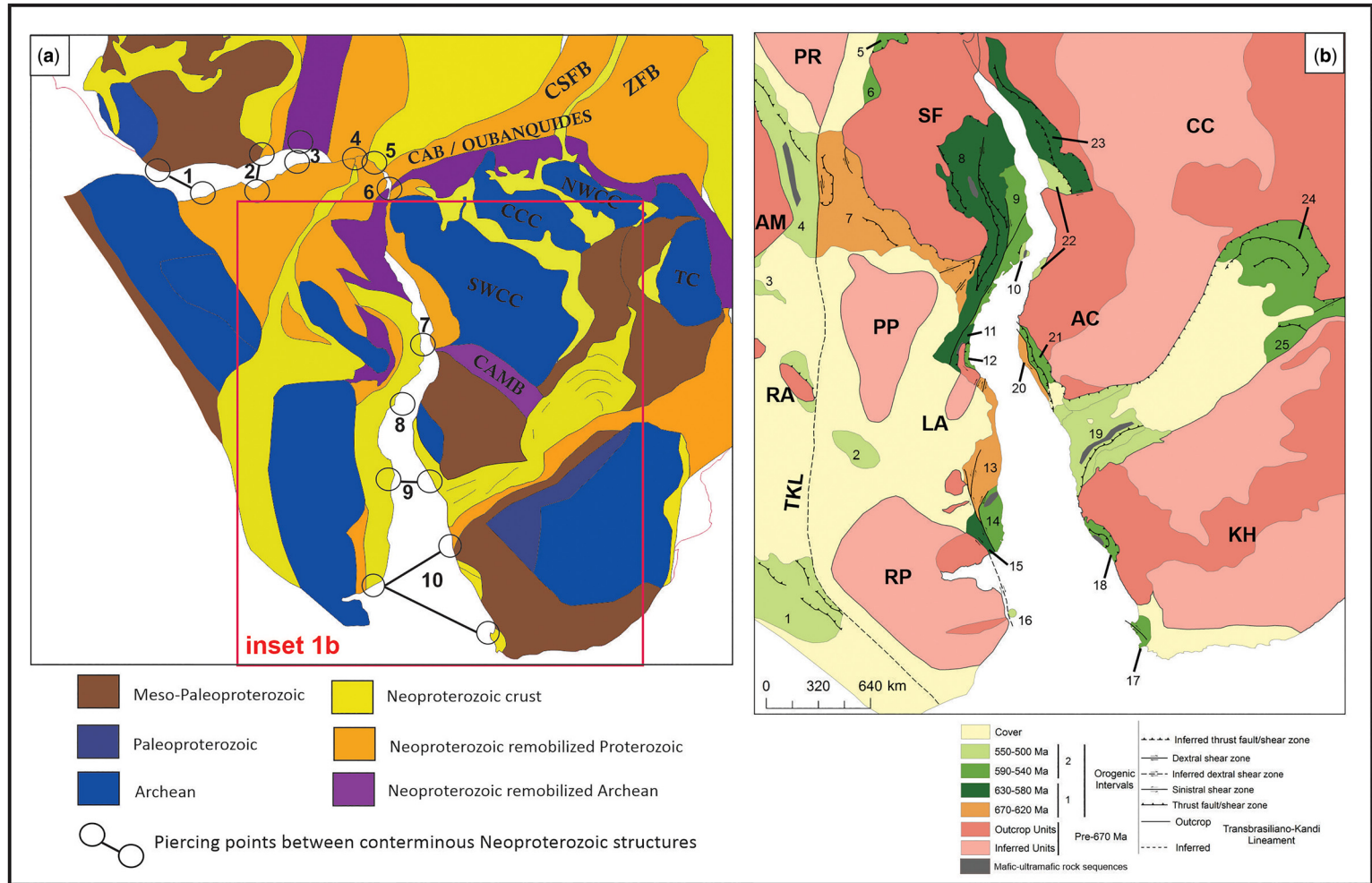
Abstract: We present the first correlation between South American and African shear zones based on a reconstruction model of SW Gondwana continental crust, correlating 57 Brasiliano–Pan-African crustal-scale shear zones that sutured this palaeocontinent at c. 500 Ma. The final amalgamation and consolidation of the SW Gondwana continental crust were attained by an anticlockwise rotation of three cratons (Kalahari, Angola and São Francisco) in relation to the clockwise rotation of the Río de la Plata Craton in the Early Paleozoic. These relative movements were accommodated by transcurrent shear zones active from 585 to 500 Ma within the Pan-African–Brasiliano belts that surround these cratons. This kinematic interaction resulted in the initiation of a long-term active margin starting with the Cambrian Pampean orogeny and ending with the Permian–Triassic Gondwanide orogeny.

Major shear zones play a key role in the dynamic reconstruction of supercontinent amalgamation (de Wit *et al.* 2001; Oriolo *et al.* 2018a, b). They tend to accommodate convergent continental blocks during collision by lateral adjustments and indentation, in response to remnant contractional forces (e.g. Passchier *et al.* 2016; Faleiros *et al.* 2022). The accommodation of stresses during collisional and late collisional intervals occurs not only by the reactivation of high strain zones but also by the formation of new shear zones.

The consolidation of the Gondwana supercontinent involved diachronous convergence of multiple smaller continents over 150 myr (Meert 2003; de Wit *et al.* 2008; Schmitt *et al.* 2018). The result was a complex puzzle of cratons and orogenic belts with a ductile to ductile–brittle fabric anatomically adjusted to the cratons. The convergence of several cratonic blocks, building up the Gondwana continental plate, generated locally tectono-metamorphic interference zones, involving orogenic triple junctions (Trouw *et al.* 2013; Passchier *et al.* 2016). An example is in central to east Brazil, where the evolution of the 620–500 Ma Ribeira Orogen overlaps in space and time with the 690–600 Ma Brasília

Orogen (Peternel *et al.* 2005; Trouw *et al.* 2013), documented by the Ribeira metamorphic isograds that crosscut the Brasília structures, added to the reactivation and formation of strike-slip shear zones. Other orogenic triple junctions are poorly understood within the SW Gondwana crust, especially the belts and cratons that occur near and at the modern Atlantic passive continental margins. De Wit *et al.* (2008) presented connections between the South American and African Precambrian terranes and structures, defining possible piercing points (Fig. 1a). However, the lack of data on the submerged continental crust adds several uncertainties to these connections, compromising the interpretations of the tectonic evolution of the orogenic belts that constitute Gondwana (Basei *et al.* 2005; Konopásek *et al.* 2016; Will *et al.* 2019).

The objective of this paper is to review the role in time and space of the crustal-scale strike-slip shear zones of the Ediacaran–Cambrian Brasiliano–Pan-African collisional orogens located near and at the Atlantic continental margins. Based on a literature compilation and on the experience of many years of field work by the authors, especially in key regions like SSE Brazil, Uruguay and NW Namibia,



Transatlantic SW Gondwana crustal-scale shear zones

we investigate the nature and finite framework of the tectonic terranes in the Dom Feliciano–Ribeira–Kaoko–Damara–Gariép–Saldania orogenic system that led to SW Gondwana’s final amalgamation and consolidation as a continent. After a concise description of the chrono-thermal-kinematic history of 57 crustal-scale shear zones, a step-by-step reconstruction is presented to show how the different pre-Gondwana continents and minor blocks came together and then adjusted along these shear zones until final consolidation. This is the first paper to present the correlation between South American and African shear zones based on a reconstruction model of the SW Gondwana continental crust, by extracting the South Atlantic oceanic lithosphere through plate kinematics methodology, taking into account the intraplate continental deformation including the current passive continental margins. Only with the kinematic reconstruction of the Jurassic (pre-rift) Period is it possible to perform a precise correlation amongst the Brasiliano–Pan-African crustal-scale shear zones that sutured this palaeocontinent at c. 500 Ma. As pointed out by our visionary geologist Maarten de Wit, ‘obtaining a “tight” reconstruction for Gondwana will remain an elusive goal unless better integration between marine geophysics and on-land geology is achieved’ (de Wit *et al.* 2008, pp. 407–408).

Ediacaran–Cambrian Gondwana amalgamation

The convergence of the Neoproterozoic cratons to build up the Gondwana crust was diachronous and is recorded in 680 to 500 Ma orogenic belts. Schmitt *et al.* (2018) compiled 55 orogenic belts over the entire Gondwana related to this amalgamation, grouping them in two main orogenic intervals: (1) 670–575 and (2) 575–480 Ma. During Phase 1, the proto-Gondwana core was formed with few but

long orogenic belts, some more than 2000 km in length (e.g. Ganade de Araujo *et al.* 2014). The second orogenic interval, in the Cambrian and Ordovician, includes more than 40 orogenic belts produced by the convergence and collision of peripheral continental blocks, such as the Kalahari and Río de la Plata cratons, against proto-Gondwana, locus of the South Atlantic rifting during the Cretaceous (Fig. 1b).

SW Gondwana continental crust is partially preserved today in the southern part of South America and Africa. This continental domain was fully amalgamated at the end of the Cambrian, after more than 150 myr of tectonic convergence between six cratonic blocks (Schmitt *et al.* 2018). These Neoproterozoic palaeocontinents were: São Francisco–Congo, Angola, Kalahari, Luís Alves, Paranapanema and Río de la Plata (Fig. 1b). Here, we describe their late Gondwana amalgamation, focusing not on the orogenic belts but on the convergent palaeocontinents, their geometry and timing of collision. The behaviour of the syn- to late-collisional shear zones, which sutured SW Gondwana, resolved cratonic indentation to orthogonal and oblique convergence.

The Río de la Plata Craton is well exposed in the Uruguayan shield, but it is mostly covered by the sedimentary and volcanic units of the younger Gondwana basins (Chacoparaná and Hesperides; Pángaro *et al.* 2016). This craton collided with the Kalahari, Angola and Luís Alves cratons suturing SW Gondwana (Fig. 1b). These collisions are registered in the Dom Feliciano, Kaoko, Gariép and Saldania belts that record at least 200 myr of tectonic activity pre-dating the final consolidation of Gondwana (Goscombe *et al.* 2003a; Goscombe and Gray 2007, 2008; De Toni *et al.* 2020a, b; Hueck *et al.* 2020; Battisti *et al.* 2022). During syn- to late-collisional stages, subduction started along its western margin, recorded by the Pampean and Famatinian orogenies in the latest Proterozoic to

Fig. 1. (a) Simplified geological map of West and Central Gondwana showing the major Neoproterozoic shields with their embedded Precambrian cratons, and their margins that were remobilized in the Pan-African/Brasiliano orogens. Nine Neoproterozoic ‘piercing’ points between once conterminous Pan-Gondwana sub-vertical lineaments are identified along opposite sides of the South Atlantic. In addition, the mid-Phanerozoic (c. 250 Ma) ‘piercing points’ associated with the Cape Fold Belt and the Sierra de la Ventana are also shown. (b) Tectonic map of SW Gondwana with cratons (in pink) and post-670 Ma orogens’ mobile belts (in orange and green) classified by orogenic age, major crustal-scale structures and oceanic-derived units. Cratonic blocks: AC, Angola; AM, Amazonia; CC, Congo; KH, Kalahari; LA, Luís Alves; PP, Paranapanema; PR, Parnaíba; RA, Río Apa; RP, Río de la Plata; SF, São Francisco. Orogenic belts: 1, Pampean; 2, Caapucú High; 3, Paraguay; 4, Araguaia; 5, Borborema (South); 6, Rio Preto; 7, Brasília; 8a, Araçuaí (West); 8b, Ribeira (Paraíba/Embu); 8c, Apiaí to East Araçuaí and Occidental Terrane; 9, Ribeira (Oriental Terrane); 10, Cabo Frio Tectonic Domain; 11, Curitiba Terrane; 12, Paranaguá Terrane; 13, Dom Feliciano; 14, Cuchilla Dionísio; 15, Nico Pérez; 16, Mar del Plata Terrane; 17, Saldania; 18, Gariép; 19, Damara; 20, Kaoko (Coastal); 21, Kaoko (Central–East); 22, Angola; 23, West Congo; 24, Lufilian; 25, Zambezi. CAB, Central Angola Belt; CAMB, Central Angola Mobile Belt; CCC, Cuvette Congo Craton; CSFB, Central Saharan Fold Belt; NWCC, Mboumou–Uganda Craton; SWCC, SW Congo Craton; TC, Tanzania Craton; TKL, Transbrasiliano–Kandi Lineament; ZFB, Zalingai Fold Belt. Source: (a) modified from de Wit *et al.* (2008); de Wit and Linol 2015; (b) modified from Schmitt *et al.* 2018.

Ordovician (Rapela *et al.* 2007; Martino *et al.* 2010; Casquet *et al.* 2018). These orogenies affected the Pampia block, which is partially covered by Cenozoic Andean sediments (Ramos *et al.* 2010). The tectonic contact between the Río de la Plata Craton and the Pampia block coincides with the extrapolation of the Transbrasiliano Lineament (Fig. 1b), a c. 3000 km Ediacaran–Cambrian shear zone, used as a prominent piercing point in the equatorial Atlantic (Fig. 1a). The southern limit of the Río de la Plata Craton remained a passive margin until the Permian, when the Patagonia continental block collided with SW Gondwana during the Gondwanides orogeny (Trouw and de Wit 1999; Tomezzoli and Cristallini 2004; Ramos 2008).

The Paranapanema block is covered by the Parana Basin sedimentary units (Fig. 1b). This inferred craton is based on geophysical data characterized by a distinct P-wave high-velocity anomaly corroborated by geometrical synthetic tests (Mantovani and Brito Neves 2009; Affonso *et al.* 2021). The crustal framework of the basement is interpreted as NE–SW and NW–SE linear structures (Pinto and Vidotti 2019). The Apiaí Terrane, in the southern Ribeira Belt, and the Socorro Guaxupé nappe, in the southern Brasília Belt, have pre-Neoproterozoic basement units that are interpreted as part of the Paranapanema reworked continental margin (Trouw *et al.* 2013; Campanha *et al.* 2016; Tedeschi *et al.* 2018).

The Luís Alves microplate is considered an exotic continental fragment composed of Archean to Paleoproterozoic tonalite–trondhjemite–granodiorite suite, mafic–ultramafic bodies and paragneiss remnants, bounded by major shear zones with no correlation with the adjacent crustal terranes (Passarelli *et al.* 2018). This crustal block was formed by several magmatic and metamorphic events, and since the end of the Paleoproterozoic, it has been cold and stable, being surrounded by terranes produced or intensively reworked during the Neoproterozoic Brasiliano orogenic cycle (Basei *et al.* 2009; Passarelli *et al.* 2018; Heller *et al.* 2021).

The Kalahari Craton is composed of an amalgamation of smaller cratonic blocks and orogenic belts, such as the Kaapvaal Craton, the Zimbabwe Craton and the Choma–Kalomo block, including rocks from the Archean to the Mesoproterozoic (Jacobs *et al.* 2008). Its amalgamation began in the Archean, with episodes in the Paleoproterozoic marked by the occurrence of the intracontinental Bushveld magmatism. During the Mesoproterozoic, subduction zones surrounded the Kalahari proto-craton, giving rise to the Namaqua–Natal orogeny, and during the Neoproterozoic, the final incorporation of the Kalahari Craton into Gondwana (Oriolo *et al.* 2018a). The collision between the Kalahari and the southern Angola cratons generated the Damara Orogen, an

ENE–WSW belt well preserved in southern Africa. Its eastern prolongation defines the Lufilian–Zambesi Belt, and its western prolongation is orthogonally disrupted by the Atlantic rift (Fig. 1). The oldest orogenic ages of the Damara Orogen are 590–580 Ma (Lehmann *et al.* 2016), and the main collisional interval is 540–520 myr (Jung and Mezger 2003; Goscombe *et al.* 2022).

Further north, the Rehoboth inlier is a Mesoproterozoic domain, located in central Namibia, exposed between the Southern Margin Zone and the Southern Foreland of the Pan-African Damara Orogenic Belt (Ziegler and Stoessel 1988; van Schijndel *et al.* 2011). It is comprised of sedimentary to volcanic rock units, intruded by granites that can reach batholithic dimensions, with U–Pb ages from 1210 to 1080 Ma (Becker *et al.* 2005; van Schijndel *et al.* 2011).

The Angola Craton, from west to central Africa, is bordered to the west and south by Neoproterozoic mobile belts (Fig. 1b; e.g. Kaoko and Damara, respectively). The craton is largely covered by the Kalahari sands to the east. Most authors considered the Angola Craton as an Archean to Mesoproterozoic continental block that was part of the larger Congo Craton, but the connection is mostly covered by the Phanerozoic sediments of the Congo Basin (Jelsma *et al.* 2018). De Wit and Linol (2015) proposed that there is a Paleoproterozoic NW–SE mobile belt (Central Angola Mobile Belt; Fig. 1a) separating the Angola Craton from the major Congo Craton. As this belt could have been reworked during the Pan-African orogeny, some authors propose that the Angola Craton was not anchored to the Congo Craton, thereby allowing space for the Neoproterozoic subduction models envisaged to account for the pre-collision calk-alkaline magmatic provinces in the Brasiliano belts, now located along the Atlantic coast (Heilbron *et al.* 2008; Tupinambá *et al.* 2012).

Methods

This work is mainly a compilation from the literature covering data on 57 crustal-scale shear zones of SW Gondwana. We adopt here the broader concept of shear zone, i.e. a tabular zone in which strain is notably higher than in the adjacent rocks (Fossen 2016). The kinematic sense is not reduced to the simple shear mode, but may also include pure shear. Therefore, we considered all oblique tectonic regimes.

The compilation focused on crustal-scale structures, mostly with at least 100 km length (some exceptions to this are explained in the text), that are near or at the Atlantic conjugate continental margins. The database is presented in Table 1 and includes parameters such as length, width,

Transatlantic SW Gondwana crustal-scale shear zones

pressure–temperature (P–T) conditions, rock microstructures, kinematics, displacement, geochronological data and tectonic setting (intra-terrane structure, terrane limiting structure and/or suture zone). The shear zones were vectored on the current geological and tectonic maps of South America and Africa, simplified to scale 1:12 m, from the Gondwana database of the Digital Centre of Gondwana Geoprocessing (DCGG) at the Universidade Federal do Rio de Janeiro (UFRJ) in Brazil.

The reconstruction of SW Gondwana was based on the new geological map of Gondwana (Schmitt *et al.* 2023). This new kinematic reconstruction of the tectonic plates for the South Atlantic region used in part the model proposed by Heine *et al.* (2013) and Richetti *et al.* (2018), modified through the GPlates software (Müller *et al.* 2018), with the South African platelet (100) fixed in the current coordinates (Fig. 2a). The Amazonia (201), Tucano (36), Benue (14) and West Africa (714) platelets were maintained, as well as their rotation poles determined by Heine *et al.* (2013; Fig. 2a), detailed in Table 2. We adjusted and closed the northern African region, modifying the reconstruction model of Richetti *et al.* (2018) by creating new platelets and internal boundaries for the African plate (Fig. 2a). The platelet 711 was created using the Atlas mountain belt as an internal boundary. The platelet 713 (Algeria) was defined considering the Cretaceous deformation recorded on the geology of the Sahara, Gourara, Oued Mya and Illizi–Ghadames basins, providing a better fit with platelet 715 (Nubian shield). In platelet 715, three new subdivisions are presented, generating platelet 716 (Sinai), with anticlockwise rotation; platelet 710 (Danakil), with rotation poles from Collet *et al.* (2000); and platelet 712 (Aisha) with clockwise rotation.

The area examined in this paper involves the fit of three platelets – South Africa (100), Central Brazil (201) and South Brazil + Uruguay + North Argentina (40) – in the new reconstruction model for SW Gondwana proposed herein (Fig. 2b). The internal plate boundaries (platelets) of South America and Africa were modified from Richetti *et al.* (2018) using the geology and the extrapolation of the fracture zones of the oceanic crust. The actual COB (continent–oceanic boundary) lines from the Africa and South America plates were traced based on Karner and Driscoll (1999); Torsvik *et al.* (2009); Franke *et al.* (2010); Soto *et al.* (2011); Gaina *et al.* (2013); Heine *et al.* (2013); Kumar *et al.* (2013); and Stica *et al.* (2014). In order to undo the Cretaceous deformation related to the rifting process, palaeo-COBs were created for the continental margins based on the equidistance between the current coastlines and COBs. Level quota values were assigned for the COBs and the shorelines to build up a digital elevation model (DEM) where

reconstructed COBs were reduced to 30, 50 and 70% from the current shoreline. Depending on the nature of the continental margin (e.g. magma-poor or magma-rich), a different COB reduction was modelled for each segment. For instance, platelet 40 was adjusted with a 50% reduction in the COB and platelet 41 was adjusted with a 70% reduction in the COB for the South American margin and its African counterpart, respectively (Figs 2 & 3).

New rotation poles were calculated for these new platelets (Table 2). The Paraná/La Plata (40) and Valdes (41) platelets were adjusted with the African platelet using M0–M9+ magnetic anomalies (Lovecchio *et al.* 2020; Reeves 2020a). The Pampean platelet (42) moves with respect to platelet 40. The platelet 43 (Patagonia) follows the movement of platelet 41. The overlap between plate 40 and 201 is here proposed based on the occurrence of the Torres syncline, a Cretaceous structure and magmatic domain (Paraná traps) that can be correlated as a piercing point with the Etendeka traps in Namibia (Fig. 3).

Shear zones of SW Gondwana

Below, we describe 57 crustal-scale Late Neoproterozoic–Cambrian shear zones of SW Gondwana, developed within the orogenic belts that surround the cratons, grouped within their respective continents, Africa (Afr) and South America (SAm) and located in their tectonic units (Fig. 1b). A continental scale geological map of SW Gondwana exhibits these structures and the terrane distribution classified by their ages (Fig. 3). All the compiled data are shown in Table 1. The location of each shear zone is shown on the structural map with their acronyms according to Table 1 and text below (Fig. 4). We also present a diagram with a compilation of the deformation ages plus the structural map with the cratons' contours, and their tectonic foliation traces are discriminated from the main fabric of the Pan African–Brasiliano orogens (Figs 5 & 6).

Pampia block (SAm)

Córdoba Fault (CRD). To the west of Río de La Plata, the Pampia cratonic block was affected by the Pampean orogeny, recorded by a north–south tectonic foliation, related to a convergent setting that prevailed during the Late Neoproterozoic until the Ordovician (Rapela *et al.* 2007; Casquet *et al.* 2018). In the Sierras de Córdoba sector, the boundary between the Pampia block and the Río de la Plata Craton is the Córdoba Fault (CRD), a dextral strike-slip fault that was active in the Cambrian during and after the Pampean orogeny (Casquet *et al.* 2018). The interpretation of this structure is based

R. da S. Schmitt *et al.***Table 1.** Compiled data from 57 SW Gondwana Ediacaran–Cambrian shear zones (South America and Africa)

Shear zone	Acronym	Width (km)	Length (km)	Tectonic domain	Continent	Crustal level	T (°C)	P (kbar)	Strike
Sierra de la Ventana Thrust Front	SLV		>100	Sierra de la Ventana Fold and Thrust Belt	SAm	middle–upper			NW–SE
Córdoba Fault/shear zone	CRD		>1000	Pampean Orogen, Argentina	SAm	upper			north–south
Isla de Patrualla	ISP		>100	Uruguay	SAm				north–south
Sarandí del Yí (a)	SY	2	200	Nico Pérez Terrane, Uruguay	SAm	middle–upper	650–600		NNW–SSE
Sarandí del Yí (b)	SY	2	200	Nico Pérez Terrane, Uruguay	SAm	middle–upper	550–450		NNW–SSE
Sierra Ballena	SB	5	>300	Cuchilla Dionisio Terrane, Uruguay	SAm	middle–upper	550–400		NNE–SSW
Tupambaé	TU		60	Nico Pérez Terrane, Uruguay	SAm		400–550		east–west
Sierra de Sosa	SS		>100	Nico Pérez Terrane, Uruguay	SAm		550–300		NE–SW
María Albina	MA		>100	Nico Pérez Terrane, Uruguay	SAm		550		NNE–SSW
Cordillera	CR		>100	Cuchilla Dionisio Terrane, Uruguay	SAm		<450		NE–SW
Laguna de Rocha	LR	2	100	Cuchilla Dionisio Terrane, Uruguay	SAm	middle–upper			NNE–SSW
Cerro Amaro	CA	<10	>100	Cuchilla Dionisio Terrane, Uruguay	SAm		450–550		NNE–SSW
Ayrosa Galvão–Arroio Grande	AG	8	>100	Dom Feliciano Belt	SAm		400–600		ENE–WSW
Dorsal de Canguçu	DG	2	200	Dom Feliciano Belt	SAm	middle–upper	650–450		NE–SW
Passo do Marinheirinho	PM		c. 100	Dom Feliciano Belt	SAm				NNE–SSW
Ibaré	IB	3	100	São Gabriel block	SAm	lower–middle	350–500		NW–SE
Major Gercino	MG	10	80	Dom Feliciano Belt	SAm	middle–upper	350–500	2.0–5.0	NE–SW
Itajaí–Perimbó	IP	15	80	Dom Feliciano Belt	SAm	middle–upper	350–500		NE–SW
Palmital	PAL		c. 85	Ribeira South	SAm	middle–upper	400–500		NW–SE
Alexandra	AX		c. 80	Ribeira South	SAm	middle–upper	400–500		NW–SE
Serrinha (Passarelli <i>et al.</i> 2011)	SE	>1	>150	Ribeira South	SAm	middle	650–740	5.7–9.0	NE–SW
Piên	PI		200	Ribeira South	SAm	middle–upper	300–450		NE–SW
Serra do Azeite	SA	2	c. 100	Ribeira South	SAm	middle–upper	400–500		NE–SW
Lancinha–Cubatão	LAN	15	c. 250	Ribeira South	SAm	middle–upper	400–500		ENE–WSW
Cubatão	CUB	1	c. 450	Ribeira South	SAm	middle–upper	460–520	4.5–9.5	ENE–WSW
Itariri	ITR	0.7	>35	Ribeira South	SAm	middle	670–730	5.4	east–west
Morro Agudo	MAG		c. 125	Ribeira South	SAm		250–280		NNE–SSW
Ribeira	RI	3	c. 100	Ribeira South	SAm	middle–upper	400–600	5.0–7.0	ENE–WSW
Itapirapuã	ITP		>150	Ribeira South	SAm		500–700	5.0–11.0	NE–SW
Agudos	AD		c. 100	Ribeira South	SAm				NE–SW
Taxaquara	TX	1	150	Ribeira South	SAm	middle–upper	420–530	2.0–5.0	NE–SW
Guararema	GR		c. 200	Ribeira South	SAm	middle–upper			NE–SW
Caucaia	CC		c. 200	Ribeira South	SAm		400–600		NE–SW
Central Tectonic Boundary	CTB	1	300	Ribeira Central	SAm	lower–middle			NE–SW

Transatlantic SW Gondwana crustal-scale shear zones

Kinematic	Cataclastic/ mylonitic	Age (Ma)	Method	Age (Ma)	Method	Terrane limit	References
Thrust	Mylonitic	275				No	Ramos (2008)
Dextral	Cataclastic	After 520				Yes	Rapela <i>et al.</i> (2007)
Sinistral	Mylonitic					No	Passarelli <i>et al.</i> (2011)
Dextral	Mylonitic	623–596	U–Pb	600	Ar–Ar	Yes	Oriolo <i>et al.</i> (2015, 2016a, b)
Sinistral	Mylonitic/ cataclastic	589–584	U–Pb	594–587	Ar–Ar	Yes	Oriolo <i>et al.</i> (2016a, b)
Sinistral	Mylonitic/ cataclastic	563–551	U–Pb SHRIMP zm	586–579	Ar–Ar Ms, hBL	Yes	Oyhantçabal <i>et al.</i> (2009, 2010, 2011a, b)
Dextral	Mylonitic	549	U–Pb LA-ICP- MS zm			No	Oriolo <i>et al.</i> (2016b)
Sinistral	Mylonitic	610–598	U–Pb zm			No	Oriolo <i>et al.</i> (2016b)
Sinistral	Mylonitic/ cataclastic			600	Ar–Ar muscovite	No	Oriolo <i>et al.</i> (2016b)
Sinistral	Mylonitic/ cataclastic			632	K–Ar Ms	No	Oriolo <i>et al.</i> (2016b); Oyhantçabal <i>et al.</i> (2010)
Sinistral	Mylonitic/ cataclastic			564	K–Ar Ms	No	Menezes Santos (2010); Silva Lara <i>et al.</i> (2021)
Sinistral	Mylonitic	628	U–Pb	615	K–Ar Ms	No	Oriolo <i>et al.</i> (2016b)
Dextral	Mylonitic	615–574	U–Pb			No	Klein <i>et al.</i> (2018); Vieira <i>et al.</i> (2019, 2020)
Dextral	Mylonitic/ cataclastic	658–540	U–Pb zm/ Rb–Sr WR	624–531	K–Ar/Ar–Ar (Bt/Ms)	Yes	Frantz <i>et al.</i> (2003); Koester <i>et al.</i> (1997, 2008); Oriolo <i>et al.</i> (2018a, b); Vieira <i>et al.</i> (2020)
Sinistral	Cataclastic	<595	U–Pb zm			No	Oriolo <i>et al.</i> (2018a, b)
Dextral	Mylonitic/ cataclastic			662–560	K–Ar Ms	Yes	Hueck <i>et al.</i> (2020); Oriolo <i>et al.</i> (2018a, b); Philipp <i>et al.</i> (2018)
Dextral	Mylonitic/ cataclastic	640–570	U–Pb	570	K–Ar	No	Bitencourt (1996); Chemale <i>et al.</i> (2003, 2012); Passarelli <i>et al.</i> (2010, 2011)
Dextral	Mylonitic/ cataclastic	600–540	U–Pb			No	Percival <i>et al.</i> (2021); Basei <i>et al.</i> (2011); Guadagnin <i>et al.</i> (2010); Schroeder (2006)
Sinistral	Mylonitic/ cataclastic			531–520	K–Ar	Yes	Patias <i>et al.</i> (2019); Cury (2009); Siga (1995)
Sinistral	Mylonitic/ cataclastic					Yes	Patias <i>et al.</i> (2019); Cury (2009); Siga (1995)
Top-to- NNW/ sinistral	Mylonitic	600–540	U–Pb	575–504	K–Ar	Yes	Cury (2009); Passarelli <i>et al.</i> (2011)
Oblique thrust/ dextral	Mylonitic/ cataclastic	615	U–Pb	644–595	K–Ar (Bt/ Amp)	Yes	Harara (1993)
Sinistral	Mylonitic	579	U–Pb	600–570	K–Ar	Yes	Faleiros <i>et al.</i> (2011)
Dextral	Mylonitic/ cataclastic					Yes	Cabrita <i>et al.</i> (2022); Faleiros <i>et al.</i> (2022); Castro <i>et al.</i> (2014); Passarelli <i>et al.</i> (2011)
Dextral	Mylonitic/ cataclastic	850–760/ 610–570	U–Pb, K–Ar, Ar–Ar			Yes	Cabrita <i>et al.</i> (2022); Faleiros <i>et al.</i> (2022); Castro <i>et al.</i> (2014); Passarelli <i>et al.</i> (2011)
Sinistral	Mylonitic	626–580	U–Pb zm	500	Ar–Ar	Yes	Passarelli <i>et al.</i> (2011, 2019)
Sinistral	Cataclastic					No	Faleiros <i>et al.</i> (2022)
Dextral	Mylonitic	623–579	U–Pb			No	Faleiros <i>et al.</i> (2011)
Dextral	Mylonitic	675–600	U–Pb			No	Faleiros <i>et al.</i> (2022)
Top-to-SE	Mylonitic					No	Faleiros <i>et al.</i> (2022)
Dextral	Mylonitic	560–535	U–Pb	550–536	Ar–Ar	Yes	Ribeiro <i>et al.</i> (2019, 2020)
Dextral	Mylonitic					Yes	Silva (2017); Ribeiro <i>et al.</i> (2019, 2020)
Dextral	Mylonitic					No	Meira <i>et al.</i> (2019); Cabrita <i>et al.</i> (2022); Faleiros <i>et al.</i> (2022)
Dextral/ top- down- to-NW	Mylonitic	600–550				Yes	Fontainha <i>et al.</i> (2021); Heilbron <i>et al.</i> (2008)

(Continued)

R. da S. Schmitt *et al.*Table 1. *Continued.*

Shear zone	Acronym	Width (km)	Length (km)	Tectonic domain	Continent	Crustal level	T (°C)	P (kbar)	Strike
Além Paraíba	AP	5	200	Ribeira Central	SAm	lower–middle	600–780		NE–SW
Cabo Frio Thrust Buquira	CFT BQ	1	300 >150	Ribeira Central Brasília South	SAm SAM	lower–middle	700–750	8.0	NE–SW ENE–WSW
São Bento do Sapucaí–Caxambu	SBC	3	220	Brasília South	SAm	middle–upper	450–650	1.5–3.0	NE–SW
Extrema	EX		130	Brasília South	SAm				NE–SW
Maria da Fé	MF	1.5	30	Brasília South	SAm		400–600		NNE–SSW
Três Corações	TC	>1	70	Brasília South	SAm		400–500		NE–SW
Campo do Meio	CM		>250	Brasília South	SAm				east–west
Poços de Calda	PC		170	Brasília South	SAm				NE–SW
Kwanza shear zone	KW	1–2	c. 80	Angola–West Congo Belt	Afr				east–west
Three Palms Mylonite Zone	TH	1–2	c. 390	Kaoko Belt, Namibia	Afr	middle–upper	545–555	4.0–4.8	NNW–SSE
Village Mylonite Zone	VMZ	1	63	Kaoko Belt, Namibia	Afr	middle–upper	634	4.0	north–south
Khumib Mylonite Zone	KHU	1	c. 138	Kaoko Belt, Namibia	Afr	middle–upper	704	5.2	north–south
Hartmann Mylonite Zone	HAR	1	c. 117	Kaoko Belt, Namibia	Afr	middle–upper			north–south
Purros Mylonite Zone	PMZ	5	>600	Kaoko Belt, Namibia	Afr	lower–middle	640	8.8	north–south
Ahub Mylonite Zone	AH	1	c. 140	Kaoko Belt, Namibia	Afr		>500–590		NE–SW
Ogden Mylonite Zone	OG	5	c. 15	Damara Belt, Namibia	Afr		500–465	4.0–5.0	NE–SW
Khan shear zone (low T)	KSZ		c. 40	Damara Belt, Namibia	Afr	lower–middle			
Khan shear zone (low T)	KSZ		c. 40	Damara Belt, Namibia	Afr	lower–middle			
Goantagab shear zone	GSZ	1–2	c. 84	Damara Belt, Namibia	Afr				NW–SE
Okahandja shear zone (high-T, main branch)	OSZ	10–300	c. 560	Damara Belt, Namibia	Afr	lower–middle	584 ± 9	4.75	NW–SE
Okahandja shear zone (medium-T, main branch)	OSZ			Damara Belt, Namibia	Afr				NW–SE
Okahandja shear zone (low-T)	OSZ			Damara Belt, Namibia	Afr				east–west
Okahandja shear zone (low-T)	OSZ			Damara Belt, Namibia	Afr				east–west
Tinkas shear zone (low-T)	TSZ	15	c. 10	Damara Belt, Namibia	Afr	middle–upper			east–west
Colenso Fault	CF	1	c. 150	Saldania Belt, South Africa	Afr				NW–SE
Colenso Fault	CF	1	c. 150	Saldania Belt, South Africa	Afr				NW–SE
Khorixas–Gaseneirob shear zone	KG	1	c. 560	Damara Belt, Namibia	Afr	upper	450		ENE–WSW
Kunene shear zone	KN	4	c. 166	Kaoko Belt, Namibia	Afr	middle	min. 450		north–south

Amp; amphibole; ap., apatite; Bt, biotite; hBL, hornblende; mnz., monazite; Ms, muscovite; ttn., titanite; zrn, zircon.

Transatlantic SW Gondwana crustal-scale shear zones

Kinematic	Cataclastic/ mylonitic	Age (Ma)	Method	Age (Ma)	Method	Terrane limit	References
Dextral	Mylonitic	580–530	U–Pb			No	Fontainha <i>et al.</i> (2021); Giraldo <i>et al.</i> (2019); Cavalcante <i>et al.</i> (2018)
Thrust	Mylonitic	530–490	U–Pb mnz.			Yes	Schmitt <i>et al.</i> (2004, 2016)
Dextral	Mylonitic					No	Duffles <i>et al.</i> (2016); Fontainha <i>et al.</i> (2021)
Dextral	Mylonitic	610–552	U–Pb			No	Fontainha <i>et al.</i> (2021); Vinagre <i>et al.</i> (2016, 2020)
Dextral	Mylonitic	573–563	U–Pb zrn			No	Fontainha <i>et al.</i> (2021)
Sinistral	Mylonitic	586 ± 8.7	U–Pb			No	Zuquim <i>et al.</i> (2011)
Dextral	Mylonitic					No	Fontainha <i>et al.</i> (2021)
Sinistral	Mylonitic					No	Ebert and Hasui (1998); Zanardo <i>et al.</i> (2006); Fontainha <i>et al.</i> (2021)
Dextral	Mylonitic					No	Fontainha <i>et al.</i> (2021)
Dextral		540–490	Relative dating (metamorphic peak)				Monié <i>et al.</i> (2012)
Sinistral	Mylonitic	580–550	U–Pb zrn and mnz.	524 ± 7	Ar–Ar muscovite	Yes	Oriolo <i>et al.</i> (2018 <i>a, b</i>); Konopásek <i>et al.</i> (2005); Gray <i>et al.</i> (2006); Goscombe <i>et al.</i> (2003 <i>a, b</i>); Goscombe and Gray (2008); Foster <i>et al.</i> (2009); Franz <i>et al.</i> (1999); Kröner <i>et al.</i> (2004)
Sinistral	Mylonitic						Goscombe <i>et al.</i> (2003 <i>b</i>); Goscombe and Gray (2008)
Sinistral	Mylonitic						Goscombe and Gray (2008); Foster <i>et al.</i> (2009)
Sinistral	Mylonitic						Foster <i>et al.</i> (2009); Oriolo <i>et al.</i> (2018 <i>a, b</i>)
Sinistral	Mylonitic	580–550	U–Pb	524 ± 6	Ar–Ar hornblende	Yes	Oriolo <i>et al.</i> (2018 <i>a, b</i>); Konopásek <i>et al.</i> (2005); Goscombe <i>et al.</i> (2003 <i>a, b</i> , 2017); Foster <i>et al.</i> (2009)
Sinistral	Mylonitic						Goscombe and Gray (2008)
Sinistral	Mylonitic						Foster <i>et al.</i> (2009)
Dextral	Mylonitic	500–495	U–Pb (LA-ICP- MS)				Goscombe <i>et al.</i> (2022)
Sinistral	Mylonitic	c. 485					Goscombe <i>et al.</i> (2022)
Sinistral	Mylonitic	Post 530	U–Pb zrn in Voetspor granite				Goscombe <i>et al.</i> (2017); Passchier <i>et al.</i> (2007, 2016); Schmitt <i>et al.</i> (2012)
Dextral	Mylonitic	525–521	U–Pb (LA-ICP- MS) ttn. and ap.				Goscombe <i>et al.</i> (2022)
Dextral	Mylonitic	515.9 ± 1.9	U–Pb (LA-ICP- MS) mnz.				Goscombe <i>et al.</i> (2022)
	Mylonitic						
	Mylonitic						
Sinistral normal	Mylonitic	485–513	Correlated with sinistral reactivation of OSZ and KSZ				Goscombe <i>et al.</i> (2022)
Sinistral	Mylonitic	550	U–Pb, zrn syntectonic granites				Kisters <i>et al.</i> (2002)
Dextral	Mylonitic/ cataclastic	540–510	U–Pb, zrn syntectonic granites				Kisters <i>et al.</i> (2002)
Dextral/ top-to- NNW	Mylonitic	590–510					Personal comm. with Schmitt; Miller (1983)
Sinistral	Mylonitic	Post 590	Relative dating				Goscombe <i>et al.</i> (2017)

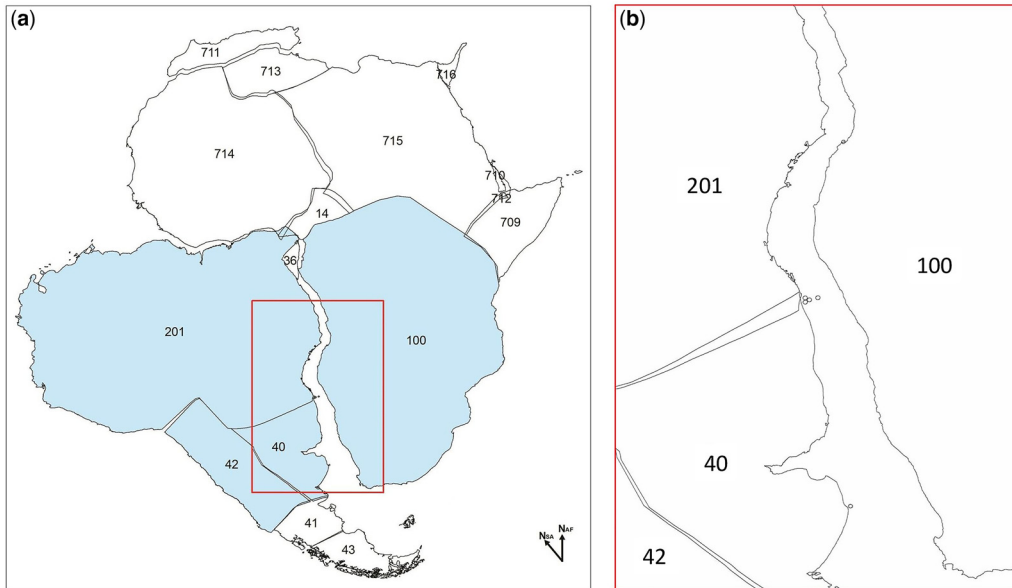


Fig. 2. (a) New reconstruction model for South America and Africa from the new geological map of Gondwana, built for the Jurassic Period (Schmitt *et al.* 2023). The rectangle indicates the studied area in SW Gondwana. (b) SW Gondwana study area of this paper, comprising four reconstructed platelets. Note also that dredged samples of continental crust obtained at the Rio Grande Rise, 1000 km offshore of the southern Brazilian coastline, were added to the model (Santos *et al.* 2019). This is where platelets 40 and 201 overlap. All the geological and structural maps from this paper are shown on this model. The parameters of rotation are shown in Table 2, modified from Richetti *et al.* (2018) and Heine *et al.* (2013).

mainly on geophysical data, and it is considered a tectonic suture, interpreted as post-520 Ma because it truncates the main fabric and metamorphic peak assemblage of the Pampean orogeny.

Dom Feliciano Belt (SAM)

Sarandí del Yí (SY). This roughly north–south transcurrent shear zone is a terrane limit separating the Río de la Plata Craton to the west from the Nico Pérez Terrane to the east, in the Uruguayan shield (Figs 1 & 4). The latter is an Archean block affected by the Neoproterozoic tectonic events, with magmatism and metamorphism (Fig. 3; Oyhantçabal *et al.* 2011a, b; Oriolo *et al.* 2018a, b). Its regional trend changes from north–south in the south to NNW–SSE in its northern part, grading from proto- to ultramylonite towards the east; it is c. 2 km in width and at least 200 km in length. The mylonitic foliation is subvertical with mean dip to the west, with the stretching lineation plunging shallowly to the south (Oriolo *et al.* 2015). Macro- to microstructural and geochronological data indicate two well constrained times of deformation (Oriolo *et al.* 2015, 2016a). The earliest deformation involved dextral shearing under upper to middle amphibolite facies conditions (600–650°C), giving rise to the reactivation of

Paleoproterozoic crustal fabrics in the easternmost Piedra Alta Terrane (Oriolo *et al.* 2015). The age of dextral shearing is constrained to c. 630–600 Ma by U–Pb data on zircon, Ar–Ar data on amphibole and U–Pb data on titanite from mylonites (Oriolo *et al.* 2016a, b). It underwent c. 584 Ma sinistral shearing with a pure-shear-dominant component, giving rise to contemporaneous magmatism under lower amphibolite to upper greenschist facies conditions (450–550°C) (Oriolo *et al.* 2015). The age of sinistral shearing is constrained by U–Pb data on zircon, Ar–Ar data on amphibole, Ar–Ar data on muscovite and U–Pb data on titanite (Oriolo *et al.* 2016a, b). The end of ductile deformation is constrained by the post-kinematic Cerro Caperuza granite, which yielded a 570.9 ± 11.0 Ma age obtained with U–Pb laser ablation inductively coupled plasma mass spectrometry (LA-ICP-MS) zircon age (Oriolo *et al.* 2016b).

Isla de Patrulla (ISP). This north–south sinistral shear zone is a conjugate fault (Fig. 4). It separates the Patrulla block (Arroyo del Soldado Group) from the China metamorphic Complex in the Nico Pérez Terrane (Gaucher *et al.* 2005; Rossello *et al.* 2007; Blanco 2010).

Transatlantic SW Gondwana crustal-scale shear zones

Table 2. Data for kinematic reconstruction of Gondwana, with plate ID and rotation parameters including rotation pole

Plate	Plate ID	Rotation parameters			Rotation pole	Comment
		Latitude	Longitude	Angle		
Amazonia	201	50.4400	-34.3800	53.4000	Fixed to West Africa (714)	Heine <i>et al.</i> (2013)
Tucano	36	-57.1900	-55.3100	0.3700	Fixed to Amazonia (201)	Heine <i>et al.</i> (2013)
Paraná/Río de la Plata	40	42.1009	-30.6974	57.7807	Fixed to Austral (100)	Reeves (2020a, b) and adjusted with the reduction of COB 50%
Valdes	41	44.0543	-31.2149	57.8819	Fixed to Austral (100)	Reeves (2020a, b), Lovecchio <i>et al.</i> (2020) and adjusted with the reduction of COB 70%
Pampean	42	-26.1819	-50.4750	-1.1045	Fixed to Paraná (040)	Moving with respect to plate 40
Patagonia	43	42.2676	-31.2110	57.7352	Fixed to Austral (100)	Moving with respect to plate 41 and adjusted by COB
Rio Grande Rise	50	9.1996	-40.1124	-17.3656	Fixed to Amazonia (201)	Modified from Graça <i>et al.</i> (2019)
West Africa	714	22.0700	-3.1700	2.8500	Fixed to Nubian (715)	Heine <i>et al.</i> (2013)
Nubian	715	-7.8000	32.3500	2.5000	Fixed to Austral (100)	Reeves (2020a, b)
Atlas Mountains	711	35.7890	-31.1085	1.4411	Fixed to Algeria (713)	New geological map of Gondwana (in prep.)
Algeria	713	30.3843	-3.5315	-3.9261	Fixed to West Africa (714)	New geological map of Gondwana (in prep.)
Benue	14	8.2500	6.9500	-1.7900	Fixed to Austral (100)	Heine <i>et al.</i> (2013)
Austral	100	90.0000	0.0000	0.0000	Fixed	Fixed to present-day position
Somalia	709	-3.8547	33.6444	5.4669	Fixed to Austral (100)	Modified from Collet <i>et al.</i> (2000)
Danakil	710	15.5000	40.0000	-23.0000	Fixed to Nubian (715)	Collet <i>et al.</i> (2000)
Aisha	712	59.5775	-9.6618	-2.0539	Fixed to Nubian (715)	New geological map of Gondwana (in prep.)
Sinai	716	-31.0900	-147.1800	7.5300	Fixed to Nubian (715)	New geological map of Gondwana (in prep.)

Parameters of rotation shown were modified from Richetti *et al.* (2018) and Heine *et al.* (2013). COB, continent-oceanic boundary.

Sierra de Sosa (SS). This NE-SW sinistral shear zone is part of the Nico Pérez Terrane transcurrent shear zone system, in which it separates the Paleoproterozoic Valentines-Rivera Granulitic Complex from the Archean La China Complex. The NE-SW mylonitic foliation dips 70° to the NW with a stretching lineation plunging 15° to the SW (Oriolo *et al.* 2016b). Microstructural data indicate that the main

deformation conditions are constrained at 300–400°C, although they started at a higher temperature, *c.* 550°C (Oriolo *et al.* 2016b). The timing of SS activity is constrained by U-Pb LA-ICP-MS on zircon from the magmatic protolith, of 598.1 ± 2.2 Ma, thus indicating that subsequent sinistral shearing occurred after emplacement. However, shearing could also have predated the obtained age,

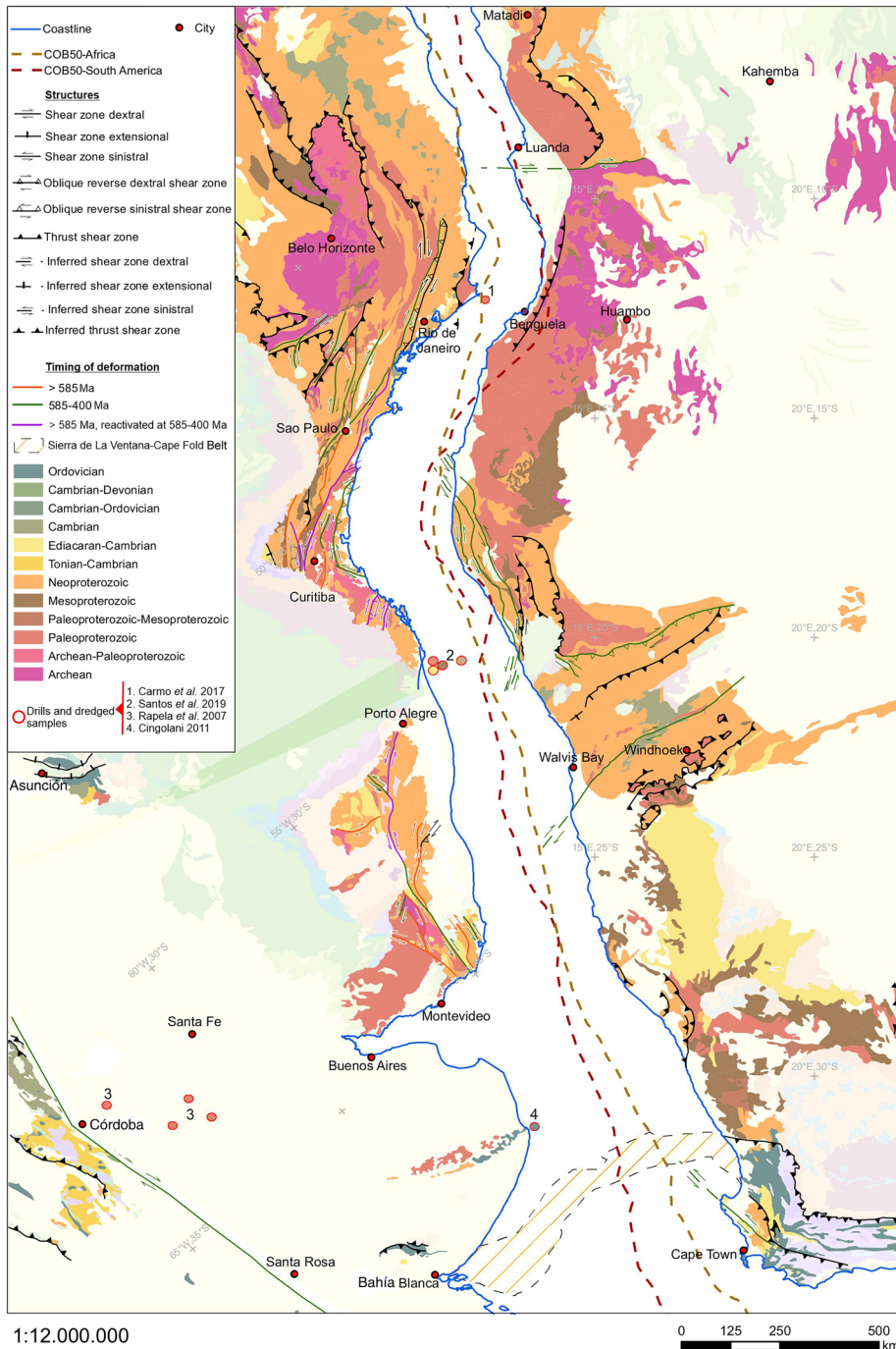


Fig. 3. Simplified geological map of SW Gondwana, reconstructed with the software GPlates, with geological units classified by age and crustal-scale structural features. African plate is fixed. South American platelets and their coordinates are rotated towards Africa. The 50% reduced continent-oceanic boundary lines from both continents are shown as dashed lines. The circles represent drills and dredged samples from continental crust that are dated. Source: modified from the new geological map of Gondwana built up at DCGG-UFRJ (Schmitt *et al.* 2023). 1, Carmo *et al.* (2017); 2, Santos *et al.* (2019); 3, Rapela *et al.* (2007); 4, Cingolani (2011).

Transatlantic SW Gondwana crustal-scale shear zones

despite not being recorded by geochronological data (Oriolo *et al.* 2016b). The SS likely continues northwards and correspond with the Caçapava Lineament within the Dom Feliciano Belt (Oyhantçabal *et al.* 2018).

María Albina (MA). To the east of the Sierra de Sosa shear zone, the María Albina shear zone is also part of the Nico Pérez Terrane transcurrent shear zone system, separating the Archean La China Complex from metasedimentary rocks of the Las Tetras Complex (Fig. 4). This sinistral NNE–SSW shear zone shows a mylonitic foliation dipping 50° to the east, with subhorizontal stretching lineation plunging to the NNE (Oriolo *et al.* 2016b). Microstructural data indicate that the shearing started at *c.* 550°C and continued to low-grade deformation conditions; there is evidence of cataclastic overprint deformation at the western margin of the shear zone (Oriolo *et al.* 2016b). Two Ar–Ar muscovite plateau ages, of 597.2 ± 3.2 and 596.8 ± 1.1 Ma, constrain the tectonic activity (Oriolo *et al.* 2016b), very similar to the Sierra de Sosa shear zone.

Tupambaé (TU). This shear zone affects the Valentines–Rivera Granulitic Complex in the northern Nico Pérez Terrane. It is oblique to most shear zones in the Uruguayan shield, displaying an ENE-striking mylonitic foliation and dextral kinematics (Oriolo *et al.* 2016b). Microstructures indicate deformation conditions of *c.* 400–550°C (Oriolo *et al.* 2016b). U–Pb LA-ICP-MS on zircon from a granite protolith yields an age of 549.0 ± 2.9 Ma, indicating crystallization age with subsequent shearing (Oriolo *et al.* 2016b, 2018a, b).

Sierra Ballena (SB). This crustal-scale shear zone is part of a high strain transcurrent system that divides the Neoproterozoic Dom Feliciano Belt of South America into two different domains in the Uruguayan shield: the Nico Pérez Terrane and schist belt of Dom Feliciano Belt to the west, and the Cuchilla Dionisio/Punta del Este Terrane and Aiguá Batholith to the east (Figs 1, 3 & 4; Bossi and Gaucher 2004; Oyhantçabal *et al.* 2009, 2010, 2011b; Basei *et al.* 2018). Its northern continuation is correlated with the Dorsal de Canguçú (DC) and Major Gercino (MG) shear zones of southern Brazil (Fernandes and Koester 1999; Oyhantçabal *et al.* 2009, 2011b; Passarelli *et al.* 2011). The NNE–SSW Sierra Ballena is *c.* 4 km wide, with an extension of over 250 km. Subvertical mylonitic foliation shows a strike-slip stretching lineation that plunges shallowly to the SSW, with sinistral kinematic indicators and an oblique reverse component and predominant pure-shear deformation (Oyhantçabal *et al.* 2009, 2011a). Microstructural data indicate deformation conditions at 400–550°C and

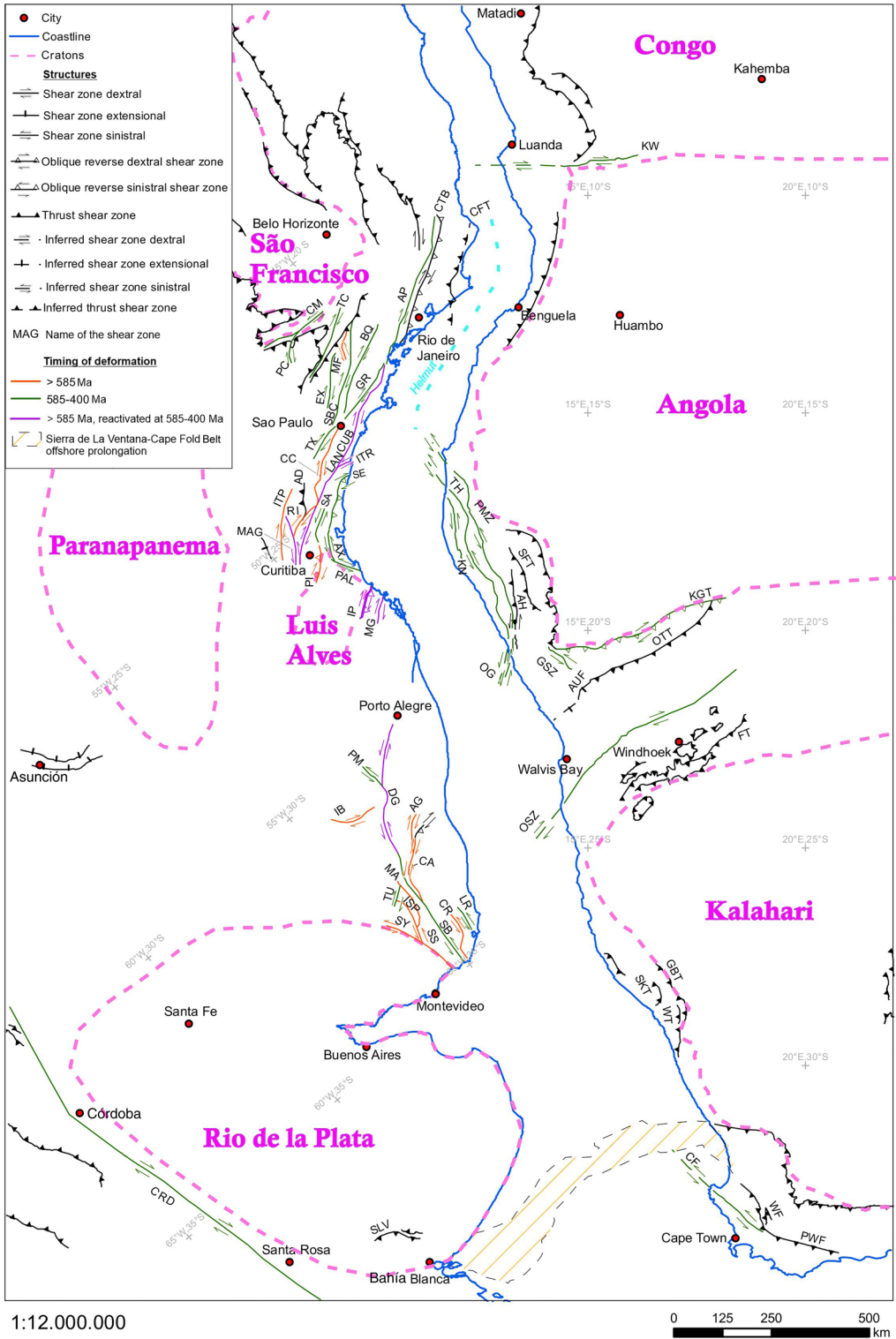
predominant pure-shear deformation (Oyhantçabal 2005; Oyhantçabal *et al.* 2009, 2011b). Based on geochronological and structural data, two main transpressional events are interpreted: at 658–600 Ma characterized by the nucleation and evolution of conjugate vertical shear zones, and at *c.* 580–560 Ma in which a sinistral reactivation of the north–south branches is recorded (Oyhantçabal *et al.* 2009, 2011b).

Cordillera (CR). This dextral NE–SW shear zone is considered as a conjugate fault to the Sierra Ballena shear zone, located to the east of it, and plays an important role in emplacement of large volumes of granitic magma in the Uruguayan sector (Oyhantçabal 2005; Oyhantçabal *et al.* 2011b). The convergence of both shear zones is likely the principal element that controls magma ascent accommodating the emplacement of huge volumes of granitic magmas (Oyhantçabal *et al.* 2009). The NE–SW mylonitic foliation dips steeply to the SE, with a stretching lineation plunging *c.* 20° to the SW. However, a relict lineation plunging moderately to the WNW is also observed (Oyhantçabal 2005; Oriolo *et al.* 2016b). Cataclasites locally overprint mylonitic features, also associated with phyllonites and ultramylonites (Oriolo *et al.* 2016b). Microstructures, as quartz dominantly recrystallized by bulging and subgrain rotation recrystallization and microfractured feldspars, suggest low temperature deformation conditions (below *c.* 450°C; Oyhantçabal 2005; Oriolo *et al.* 2016b). Most of the shear zones from the Uruguayan shield postdate the onset of regional deformation (after *c.* 600 Ma), but the CR deformation might have started before, based on K–Ar muscovite ages of 632.7 ± 6.1 Ma (Oriolo *et al.* 2016b).

Laguna de Rocha (LR). This sinistral NNE–SSW shear zone affects supracrustal rocks from the Punta del Este Terrane, being the tectonic contact between the Cerro Olivo Complex (Tonian orthogneisses) and the Rocha Formation (low-grade Ediacaran metasedimentary unit). This shear zone is composed of mylonitic to cataclastic features, and displays a subvertical foliation and deformation conditions within the greenschist facies (Menezes *et al.* 2010; Silva Lara *et al.* 2022). K–Ar muscovite from the shear zone yielded an age of 564 ± 6.1 Ma, which is interpreted as syn-kinematic crystallization age (Silva Lara *et al.* 2021). Furthermore, clay-sized white mica fractions yield K–Ar ages between 535 and 525 Ma, which are interpreted to represent the end of the ductile deformation within the shear zone (Silva Lara *et al.* 2021).

Cerro Amaro (CA). This shear zone crosscuts the Aiguá Batholith in the Uruguayan shield (Figs 3 &

R. da S. Schmitt *et al.*



1:12.000.000

0 125 250 500 km

Transatlantic SW Gondwana crustal-scale shear zones

4). It preserves a NE–SW mylonitic foliation steeply dipping to the west and a stretching lineation moderately plunging to the north, and sinistral sense of shear (Oriolo *et al.* 2016b). Microstructures indicate deformation conditions of *c.* 450–550°C and a large component of pure shear (Oriolo *et al.* 2016b). Based on K–Ar muscovite ages of 615.2 ± 6.6 Ma (Oriolo *et al.* 2016b), it is considered to have been active earlier before the onset of regional deformation (after *c.* 600 Ma), as the Cordillera shear zone was. The CA shear zone continues into southern Brazil, where it is named the Ayrosa Galvão–Arroio Grande shear zone (Vieira *et al.* 2021).

Ayrosa Galvão–Arroio Grande (AG). This shear zone system in the southeastern Dom Feliciano Belt (Figs 1b & 4) affects the metamorphic basement represented by orthogneisses, ultramafic–mafic–sedimentary rocks and pre- and syntectonic granitoids (Vieira *et al.* 2021). It preserves a subvertical NE–SW mylonitic foliation, a subhorizontal ENE-plunging stretching lineation and dominant dextral kinematics. Furthermore, the Arroio Grande branch displays an important east–west oriented foliation (Vieira *et al.* 2021). This shear zone system extends southwestwards into Uruguay, where it is named the Cerro Amaro shear zone (Vieira *et al.* 2019, 2021). U–Pb SHRIMP zircon ages between 609 and 560 Ma in syntectonic granite constrain the age of deformation. This time interval is similar to that of the Dorsal de Canguçu shear zone in the central domain of the Dom Feliciano Belt, and to that of the Cerro Amaro shear zone, its Uruguayan counterpart (Vieira *et al.* 2021).

Dorsal de Canguçu (DG). This NE–SW shear zone is the main feature of the Dom Feliciano Belt in southern Brazil and is *c.* 200 km in length. It forms the boundary between the granitic Pelotas Batholith and the metavolcanic–metasedimentary sequences of the Porongos Group (Philipp *et al.* 2016). Its southern continuation correlates with the Sierra Ballena shear zone (SB). It has a subvertical to NW-dipping mylonitic foliation, and subhorizontal stretching lineation plunging to both NE and SW.

Although a sinistral sense of shear is dominant, dextral indicators are observed in the northeastern segment (Fernandes and Koester 1999; Oriolo *et al.* 2018a, b). P–T deformation conditions are found in the upper greenschist facies, with transition from ductile to brittle regime, constraining temperature in the range of 450–500°C (Frantz *et al.* 2003). The main shear zone activity is synchronous with the magmatic activity in the Dom Feliciano Belt, suggesting more than 85 myr of deformation. This estimate is based on several U–Pb zircon data from syntectonic magmatic units with crystallization ages between 658 and 605 Ma (Frantz *et al.* 2003; Koester *et al.* 2008; Vieira *et al.* 2020). Another range of U–Pb zircon ages between 585 and 540 Ma is recorded, interpreted as crystallization ages affected by the influence of post-magmatic fluids during late shearing (Vieira *et al.* 2020). K–Ar data on biotite from syntectonic granitic suites yielded cooling ages between 600 and 575 Ma, whereas K–Ar data on muscovite yielded two ages of 624 ± 41 and 586 ± 11 Ma (Koester *et al.* 1997, 2001). Although interpreted as cooling ages, the muscovite might represent mixing ages related to neo-formed crystals during shearing (Koester *et al.* 1997). Furthermore, Ar–Ar data on biotite from mylonites yielded ages between 535 and 531 Ma, constraining the timing of late tectonic activity (Philipp *et al.* 2003).

Passo do Marinheirinho (PM). This shear zone is characteristic of a brittle fault zone that transects the Dorsal de Canguçu shear zone, affecting granitic suites (e.g. Pelotas Batholith), and is the contact between the Florianópolis Batholith and the Tijucas Terrane (Oriolo *et al.* 2018a, b). The PM is NNE-striking and has a subvertical cataclastic foliation and sinistral sense of shear. A U–Pb zircon crystallization age of *c.* 595 Ma from the Pelotas Batholith sets a maximum deformation age for the shear zone (Oriolo *et al.* 2018a, b and references therein).

Ibaré (IB). The NW–SE Ibaré shear zone limits the Taquarembó Terrane to the south and the São

Fig. 4. SW Gondwana with main thrust zones and shear zone names (as per Table 1). South America: AD, Agudos; AG, Ayrosa Galvão–Arroio Grande; AP, Além Paraíba; AX, Alexandra; BQ, Buquira; CA, Cerro Amaro; CC, Caucaia; CFT, Cabo Frio Thrust; CM, Campo do Meio; CR, Cordillera; CRD, Córdoba Fault; CTB, Central Tectonic Boundary; CUB, Cubatão; DG, Dorsal de Canguçu; EX, Extrema; GR, Guararema; IB, Ibaré; IP, Itajaí–Perimbo; ISP, Isla de Patullá; ITP, Itapirapuã; ITR, Itariri; LAN, Lancinha; LR, Laguna de Rocha; MA, María Albina; MAG, Morro Agudo; MF, Maria da Fé; MG, Major Gercino; PAL, Palmital; PC, Poços de Caldas; PI, Piên; PM, Passo do Marinheirinho; RI, Ribeira; SA, Serra do Azeite; SB, Sierra Ballena; SBC, São Bento do Sapucaí–Caxambu; SE, Serrinha; SLV, Sierra de la Ventana; SS, Sierra de Sosa; SY, Sarandí del Yí; TC, Três Corações; TU, Tupambaé; TX, Taxaquara. Africa: AH, Ahub; AUF, Autseib Fault; CF, Colenso Fault; FT, Frontal Thrust; GBT, Gembokvlei Thrust; GSZ, Goantagab shear zone; KGT, Khorixas–Gaseneirob Thrust; KN, Kunene; KW, Kwanza; OG, Ogden; OSZ, Okahandja shear zone; OTT, Otjohorong Thrust; PMZ, Purros Mylonite Zone; PWF, Piketberg–Wellington Fault; SFT, Sesfontien Thrust; SKT, Schakalsberge Thrust; TH, Three Palms; WF, Worcester Fault; WT, Wildperdrand Thrust.

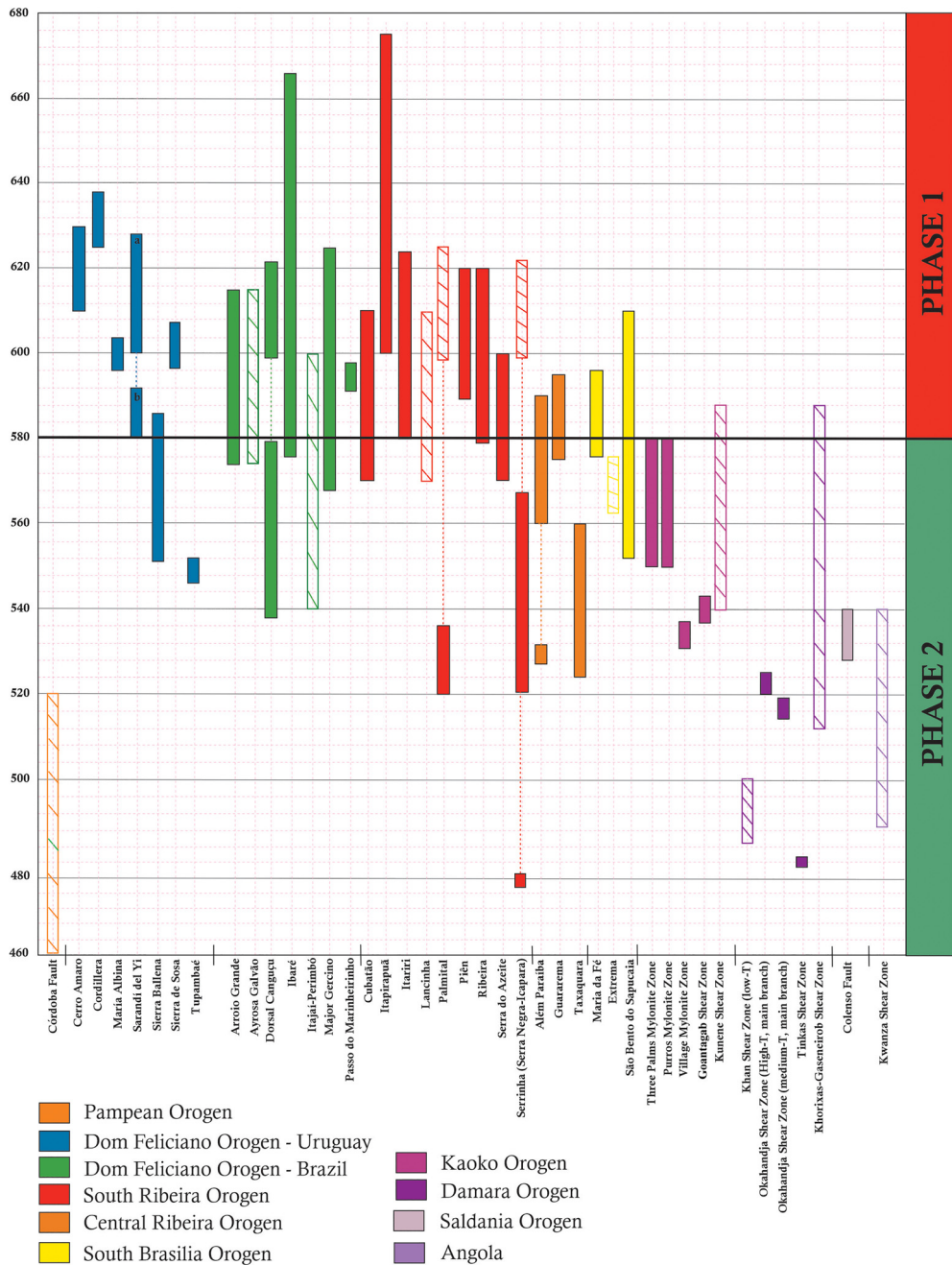


Fig. 5. Summary of geochronological data obtained from the crustal-scale shear zones in SW Gondwana. Diagram based on Table 1. The bars show the absolute ages of tectonic activity. The hashed bars refer to the relative age of the deformation, based on, for example, crosscutting relations. Source: phases 1 and 2 correspond to the Gondwana amalgamation orogenic phases from Schmitt *et al.* (2018).

Gabriel Terrane to the north. This *c.* 100 km-long structure is transverse to the main structural grain of the southeastern South American Platform

(Fig. 4; Philipp *et al.* 2018; Hueck *et al.* 2020). It is interpreted as an escape shear zone along a lateral ramp during the top-to-SW accretion between these

Transatlantic SW Gondwana crustal-scale shear zones

terrane (Philipp *et al.* 2018). It forms ultra- to mylonitic and phyllonite fabrics, with a NW–SE subvertical to steeply NE-dipping foliation and stretching lineations that are subhorizontal and gently plunging to the NW (Hueck *et al.* 2020). Shear sense indicators are scarce. Based on the deflection from east–west to NW–SE of the internal structural grain of the São Gabriel Terrane close to the shear zone, its kinematics are interpreted as dextral (Philipp *et al.* 2016, 2018; Hueck *et al.* 2020).

Major Gercino (MG). This ENE–WSW dextral shear zone separates a northwestern schist belt domain from a southeastern granitoid domain of the Dom Feliciano Belt (Fig. 4; Basei *et al.* 1992). The shear zone is at least 70 km in length and up to 10 km wide. The mylonitic foliation varies in strike from N 20° E to N 65° E and dips steeply to the NW, with a stretching lineation that varies from low-plunge to the NE to locally moderate plunge to the SW (Hueck *et al.* 2019). Strain partitioning, recorded by a progressive transition from early stages of thrust to transpressive tectonics, is constrained by the *c.* 615 to 585 Ma age of syntectonic granites (Passarelli *et al.* 2010; Chemale *et al.* 2012). This deformation phase is characterized by pure-shear-dominated strike-slip deformation (Passarelli *et al.* 2010; Hueck *et al.* 2019). K–Ar ages on synkinematic muscovite of 604–598 Ma corroborate the indication that the emplacement of the granitic magmatism was coeval with mylonitization (Hueck *et al.* 2019). K–Ar dating of biotite and muscovite from country rocks yields a 584–561 Ma age interval, interpreted to reflect post-collisional exhumation (Hueck *et al.* 2019) during the regional cooling stage (Passarelli *et al.* 2010). Late- to post-tectonic *c.* 550 Ma plutons and K–Ar mica ages from low-grade metamorphic mylonites ranging from 570 to 540 Ma (Passarelli *et al.* 2010) constrain the age of late activity along this shear zone (Chemale *et al.* 2012; Florisbal *et al.* 2012; Peruchi *et al.* 2018; Hueck *et al.* 2019).

Regional thrusting with NW-vergence at *c.* 650–635 Ma is observed only in the oldest rocks of the Florianópolis Batholith (Porto Belo Complex), with mylonites showing temperatures up to 700°C at 4.3 kbar, related to a top-to-NNW thrusting (De Toni *et al.* 2020a).

Itajaí–Perimó (IP). This ENE–WSW shear zone, along with the Major Gercino shear zone, constitutes one of the main tectonic features in the northern Dom Feliciano Belt, and is the boundary between the Western and Central Domains (Figs 3 & 4). This shear zone is the tectonic front of the Dom Feliciano Belt, deforming the southern border of the Itajaí foreland basin, deposited on top of the Luís Alves microplate, and is characterized by mylonitic rocks of the

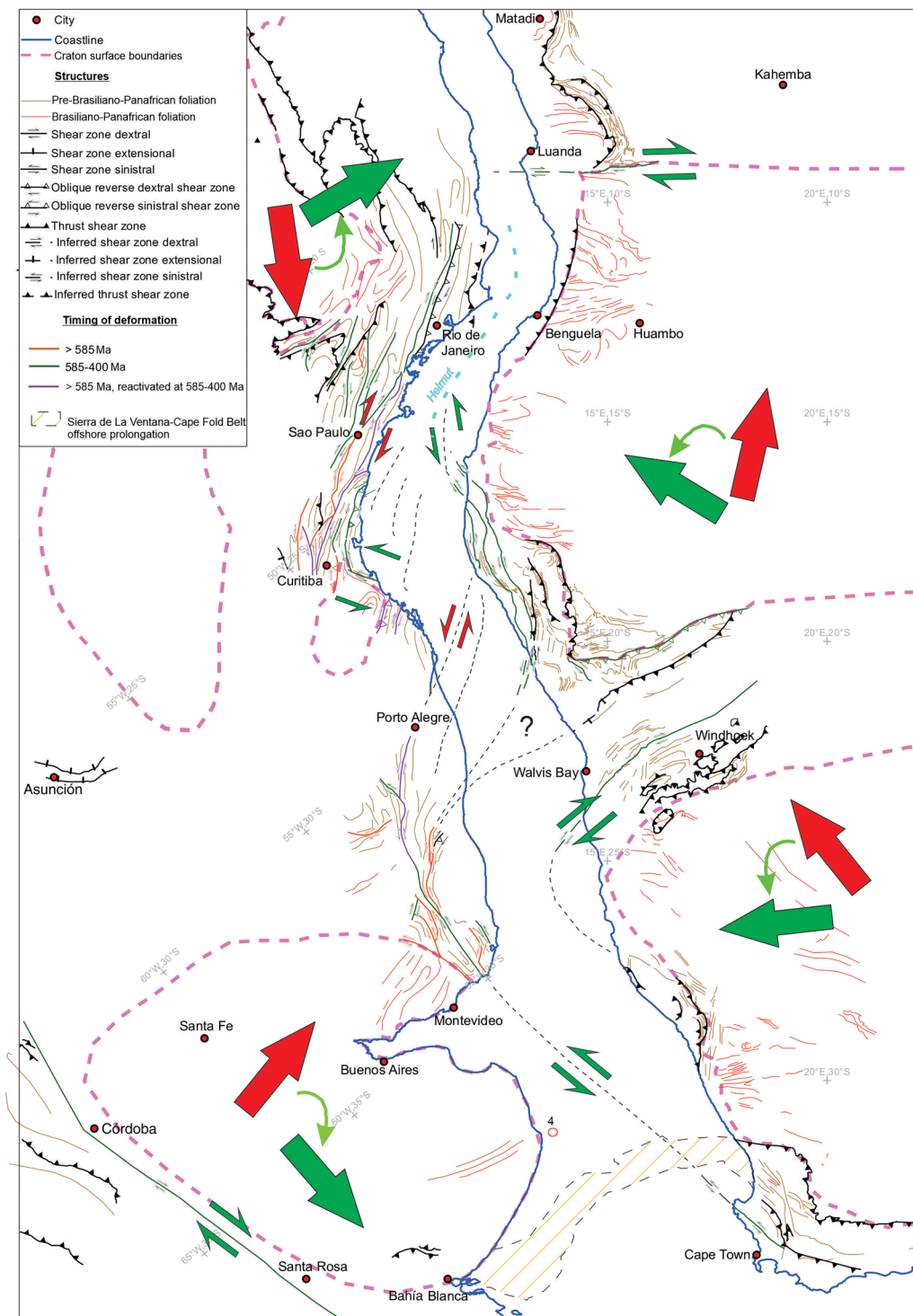
Brusque Group (volcano-sedimentary protoliths), Parapente Granite and the Paleoproterozoic gneisses of the São Miguel Complex. The orientation of the shear zone shifts from N 60° E/80° SE in the Gaspar–Blumenau area, which has a predominantly downdip stretching lineation with a sinistral component, to N 40° E/70° NW in the Gravata–Penha area, with predominant sinistral strike-slip kinematics. Basei *et al.* (2008) consider the age of 843 ± 12 Ma of the Parapente Granite as the maximum age for the development of the IP in ductile conditions at higher temperatures. However, this shear zone may have originated around 600 Ma (Basei *et al.* 2011) when the Brusque Group was thrust over the Itajaí Basin. After the deposition in the Itajaí Basin (Guadagnin *et al.* 2010), the mineralization of Ribeirão da Prata occurred possibly around 532 Ma (Rocha *et al.* 2005), with a geometry constrained by the transcurrent character of the IP, which suggests the IP was active both during basin deposition and thrusting (Guadagnin *et al.* 2010; Percival *et al.* 2021).

Southern Ribeira Belt (SAM)

Palmital–Serrinha shear system. The Palmital–Serrinha shear system, in the southern Ribeira Belt, separates the Paranaguá Terrane from the Curitiba Terrane and Luís Alves Craton to the west (Fig. 4; Cury 2009; Passarelli *et al.* 2011). Several authors consider the Paranaguá Terrane to be genetically linked to the Dom Feliciano Belt to the south, implying that the shear zone system would be late-orogenic (e.g. Basei *et al.* 1992; Patias *et al.* 2019). On the other hand, some authors consider the basement of this terrane (São Francisco do Sul Complex) to be associated with the Angola Craton in Africa (e.g. Passarelli *et al.* 2019).

The Serra Negra and Serrinha shear zones represent a collisional front to the north, with main north–NW vergence and oblique components (strike-slip and downdip lineations; Passarelli *et al.* 2011, 2019). Cury (2009) and Patias *et al.* (2019) consider the Icapara shear zone to be contiguous with the Serra Negra shear zone and so the limit of these terranes. The transcurrent Palmital (PAL) and Alexandra (AX) shear zones represent the southern continuation of this system, with main sinistral kinematics and oblique components characterized by coexistence of strike-slip and downdip lineations. Therefore, this system delineates a tectonic transpressive wedge along the Paranaguá Terrane, with both sinistral and dextral kinematics with lateral ramp characteristics to preferential westward thrust. The shear zones would represent the partition of the main strain associated with the collision of the Paranaguá Terrane, with the western domains related to the Neoproterozoic amalgamation of

R. da S. Schmitt *et al.*



1:12.000.000

After 585 Ma

Transatlantic SW Gondwana crustal-scale shear zones

southwestern Gondwana (Cury 2009; Passarelli *et al.* 2011, 2019).

Palmital (PAL). The sinistral NNW–SSE Palmital shear zone, at least 85 km in length, is the southern part of the shear system that separates the Paranaçuá Terrane from the Luís Alves Craton (Fig. 4). It displays an ultra- to protomylonitic NNW–SSE foliation, but also brecciated granites and cataclasites (Cury 2009; Patias *et al.* 2019). The steep mylonitic foliation shows a predominantly low-plunging strike-slip lineation. PAL is interpreted as the lateral ramp of the ESE–WNW frontal thrust of the Paranaçuá Terrane (Cury 2009; Patias *et al.* 2019). Microstructures in mylonitic granites indicate deformation conditions of 400–500°C, with quartz dynamically recrystallized by bulging and subgrain rotation (Cury 2009). PAL activity is constrained between 600 and 520 Ma by the age of a syntectonic granite from the Morro Ingles Suite. U–Pb zircon ages of 581 ± 19 and 601 ± 7 Ma are interpreted as crystallization ages, while biotite K–Ar ages between 531 and 520 Ma are interpreted as cooling ages (Cury 2009). Alternatively, we consider that the Cambrian ages are related to the sinistral kinematics of the Palmital shear zone. The shear zone truncates almost orthogonally the NNE–SSW tectonic fabric of the Paranaçuá Terrane (Fig. 4), implying that it postdates the main orogenic peak.

Alexandra (AX). The Alexandra shear zone forms the northwestern contact between the Paranaçuá Terrane and the Luís Alves Craton (Fig. 4). It is a NNE–SSW striking sinistral transpressional shear zone, characterized by the coexistence of strike-slip and downdip stretching lineations, in a transposed steeply dipping mylonitic foliation (Cury 2009; Patias *et al.* 2019). Like the Palmital shear zone, it probably represents a lateral ramp during the collision of the Paranaçuá Terrane with the Luís Alves Craton (Cury 2009). Geochronological data are scarce, but AX is considered to correlate with the Palmital shear zone, implying that it was active *c.* 600–520 Ma (Cury 2009).

Serrinha (SE). The dextral 2.5 km thick Serrinha shear zone (Passarelli 2001) represents the northern part of the 400 km long shear system that is the

contact between the Curitiba and Paranaçuá terranes (Fig. 4). The SE consists of gneissic–granite rocks imbricated with metasedimentary mylonitic rocks. It is located north of the Icapara shear zone, which allows the assignment of the low-grade metasedimentary sequences and the post-collisional A-type Graciosa granites (Cordeiro and Mandira–Itapitanguí stocks) to the Paranaçuá Terrane. The SE records a transition from a dextral lateral ramp NW-striking shear zone with a gently dipping mylonite foliation that predominates in its eastern portion to a frontal ramp with downdip lineations in its western portion. The Serrinha mylonites were formed at *c.* 575 ± 5 Ma (Passarelli *et al.* 2008, 2011) under amphibolite facies peak metamorphic conditions of *c.* 650–740°C and 5.7–9.0 kbar (Passarelli 2008).

Piên (PI). The Piên shear zone or Piên suture zone forms the boundary between the Curitiba Terrane and the Luís Alves Craton, characterized by deformed arc-related calc-alkaline granitoids with associated mafic and ultramafic rocks (Harara 1993, 2001; Passarelli *et al.* 2018). It displays a moderate to steeply NW-dipping NE–SW ultra- to mylonitic foliation. Metamorphic conditions are constrained by the mineralogy typical of greenschist to lower amphibolite facies transition. In addition, deformation under brittle conditions is also observed (Harara 1993). The granites were deformed and the mafic–ultramafic rocks obducted between 605 and 595 Ma (Harara 1993, 2001; Passarelli *et al.* 2018). According to these authors, the shear zone's origin reflects the progressive oceanic crust consumption and subsequent terrane collision between the Luís Alves Craton and the Piên Suite (Curitiba Terrane), with associated dextral and thrust kinematic indicators.

Serra do Azeite (SA). The ENE–WSW sinistral Serra do Azeite shear zone forms the tectonic contact between the Curitiba and Luís Alves terranes (Faleiros *et al.* 2011). It is 1–2 km wide, with a subvertical mylonitic foliation and a subhorizontal, ENE-plunging stretching lineation (Faleiros *et al.* 2016). The mylonitic paragenesis is developed under greenschist facies. The opposite sense of movement of the Cubatão and Serra do Azeite

Fig. 6. Structural contour map of cratons and belts from SW Gondwana. It includes cratons' surface boundaries (dashed pink line), shear zones and thrust zones with kinematic sense and the tectonic fabric from the crustal terranes (foliation trace). Shear zones in orange were active before 585 Ma (Phase 1); shear zones in green were active in the interval 585–400 Ma (Phase 2); shear zones generated in Phase 1 and reactivated in Phase 2 are in purple; shear zones without geochronological data are shown in black. In this transatlantic correlation of shear zones from Africa and South America, the large arrows represent the kinematics of the cratonic blocks after 585 Ma in two steps. The red arrow is the first movement, and the green arrow indicates the younger movement of the cratonic block, based on the age and kinematics of the shear zones here compiled and correlated. The rotation from the red arrow to the green arrow is also indicated. The Río de La Plata Craton is the only craton with a clockwise rotation after 585 Ma. Source: map based on Schmitt *et al.* (2018) and new Gondwana geological database.

shear zones suggests that these faults could have acted as lateral ramps for the west-directed thrusting in the Curitiba Terrane (Faleiros *et al.* 2011). An alternative model of local transtensional deformation in this shear zone was presented by Dehler *et al.* (2007) for the Cajati area, which also has 600–570 Ma Ar–Ar ages interpreted to constrain the timing of deformation (Machado *et al.* 2007). An age of *c.* 580 Ma (monazite rims) is interpreted as the minimum age for the juxtaposition of these units in the Curitiba Terrane (Faleiros *et al.* 2011).

Lancinha–Cubatão (LAN–CUB). The Lancinha–Cubatão shear system is one of the major NE–SW structures with ductile to ductile–brittle characteristics that are parallel to the SE Brazilian coast (Fig. 4; Passarelli *et al.* 2011; Cabrita *et al.* 2022). This transpressional shear system separates the Embu and the Apiaí supracrustal terranes from the SE granitic–gneiss–migmatitic Curitiba Terrane. The N 70° E–N 75° E steep foliation has a shallowly plunging oblique lineation developed under upper greenschist conditions (Passarelli *et al.* 2011) at medium temperature of 460–520°C and at 4.5–9.5 kbar (Cabrita *et al.* 2022). U–Pb ages of metamorphic epidote (*c.* 598 Ma) are related to the deformation during the juxtaposition of the Embu and Curitiba terranes (Passarelli *et al.* 2008, 2011). Additionally, ages of *c.* 610–570 Ma, obtained in igneous apatite within the mylonites, are interpreted as reset ages due to ductile deformation (Cabrita *et al.* 2022). The northeastern continuation of this shear system is interpreted as a suture zone, named the Central Tectonic Limit (Almeida *et al.* 1998; Heilbron *et al.* 2008). The correlation between the Cubatão and Além Paraíba shear zones is ruled out by Passarelli *et al.* (2011).

Itariri (ITR). The sinistral Itariri shear zone, defined in the state of São Paulo (Silva *et al.* 1978), separates the Curitiba Terrane from the Coastal Terrane (Mongaguá Complex; Passarelli and Verma 2020). It displays a steeply NE-dipping WNW–ESE foliation, is 400 to 700 m in width and is composed mostly of granite–gneiss mylonites, with local mylonitic paragneiss (Passarelli *et al.* 2008). This transpressional ductile shear zone is characterized by westerly-directed transport at *c.* 700°C and 5.4 kbar under amphibolite grade conditions (Passarelli 2008). The *c.* 580 Ma age of the deformation, which generated the wedge formed by the Itariri and Cubatão shear zones, is supported by concordant U–Pb zircon ages from mylonites from the Itariri and north branch of the Cubatão shear zones (Passarelli *et al.* 2008). The sinistral Itariri shear zone has been interpreted to displace the Coastal Terrane (Mongaguá Complex) to the NE, creating the wedge configuration

between the Embu and Curitiba terranes (Passarelli *et al.* 2019).

Morro Agudo (MAG). This NNE–SSW shear zone, with subvertical mylonitic foliation, deforms the granitoids of the Três Córregos suite in the Apiaí Terrane (Fig. 4). MAG displays deflection of the regional foliation deflection, mesoscale S–C fabric structures and foliation orientation indicative of a sinistral shear sense (Faleiros *et al.* 2022). Related rocks are dominated by brittle features (breccia and ultra- to cataclase), indicating deformation conditions below 280°C (Faleiros *et al.* 2022).

Ribeira (RI). The Ribeira shear zone, within the Apiaí Terrane, crosscuts mainly Mesoproterozoic metasedimentary rocks and Ediacaran granitic intrusions (Faleiros *et al.* 2022). RI is an ENE–WSW dextral strike-slip shear zone, with subvertical mylonitic foliation and a predominant subhorizontal stretching lineation. Macro- to microscopic indicators show a dextral kinematic shear sense. Nevertheless, RI also displays an oblique- to downdip stretching lineation at the interference zone with ENE-striking shear zones (e.g. Agudos shear zone, AD), where reverse shear sense criteria are observed with top-to-ESE kinematics (Faleiros *et al.* 2022). The deformation conditions are constrained between 300 and 600°C due to variation in the evolution of recrystallization mechanisms, from bulging to grain boundary migration in quartz. Available geothermobarometric data support this evidence, indicating deformation conditions of 300–630°C and 5–7 kbar (Faleiros *et al.* 2022). Along the Ribeira shear zone, deformation activity is recorded by ages of 580 ± 8 Ma in monazite U–Pb (Faleiros *et al.* 2022) and 612 ± 3 Ma in zircon U–Pb (Salaazar *et al.* 2013).

Itapirapuã (ITP). The Itapirapuã shear zone, within the Apiaí Terrane, is the boundary between Calymnian (Água Clara Formation) and early Tonian (Itaiacoca Group) metasedimentary rocks. ITP is considered an old suture zone reactivated in the Neoproterozoic (Faleiros *et al.* 2022). It displays a subvertical NE–SW mylonitic fabric with a subhorizontal to NE-plunging stretching lineation. The kinematic indicators show mainly a dextral sense of shear, with a local NNE-striking sinistral kinematics near its northern termination (Faleiros *et al.* 2022). Monazite U–Pb data in mylonitic paragneiss yield a core age of 829 ± 18 Ma and a younger rim age of 675 ± 7 Ma. Also, mylonitic granitic rocks affected by the shear zone yield a U–Pb crystallization age of 600 ± 6 Ma. Therefore, the available geochronological data suggest an origin of the shear zone in the Tonian as a suture zone, which

Transatlantic SW Gondwana crustal-scale shear zones

was reactivated during the Brasiliano tectonic event at *c.* 650–600 Ma (Faleiros *et al.* 2022).

Agudos (AD). The Agudos shear zone is essentially an intra-terrane structure with a steeply NW-dipping NE–SW striking foliation, with a downdip stretching lineation indicative of top-to-SE kinematics. Adjacent to other strike-slip shear zones (e.g. Ribeira SZ), however, AD shows a subhorizontal lineation (Faleiros *et al.* 2022). According to Faleiros *et al.* (2022), field relationships indicate that intra-terrane shear zones, such as AD, in the Apiaí Terrane were active before the intrusion of the 612 ± 3 Ma age, crosscutting the Itaoca Granite. On the other hand, AD affected metaconglomerates containing granitic pebbles that yield a zircon U–Pb age of 593 ± 15 Ma, and volcanic rocks from the Iporanga Formation with a U–Pb zircon age of 579 ± 34 Ma. Thus, the maximum deformation age is uncertain; however, a long period of shearing is suggested.

Taxaquara–Guararema (TX–GR). The Taxaquara shear zone displays a NE–SE striking mylonitic foliation and ENE- to WSW-stretching lineation with variable plunge and dextral kinematic indicators. TX–GR crosscuts granitic rocks, forming ultra- to mylonites in the southern Ribeira Belt. Microstructures and geothermobarometric data indicate that deformation occurred at metamorphic conditions 420–530°C and *c.* 3.9–4.4 kbar (Ribeiro *et al.* 2019). Zircon and titanite from mylonites yielded U–Pb ages of 606 ± 4 and 604 ± 8 Ma, respectively, and are interpreted as the age of protolith crystallization. Apatite U–Pb ages from mylonites of 558–542 Ma and muscovite Ar–Ar plateau ages of 540–536 Ma are interpreted as cooling ages during shearing. Therefore, the activity of TX–GR, constrained between 560 and 536 Ma, suggests it post-dates the collisional phase of deformation in the Ribeira Belt (Ribeiro *et al.* 2020).

Generally, the Guararema shear zone (GR) is considered to be the continuation of the Taxaquara shear zone to the east of the São Paulo Basin (Silva 2017; Ribeiro *et al.* 2019 and references therein; Archanjo *et al.* 2021). In this study, we have adopted this proposed connection between the Taxaquara and Guararema shear zones.

Caucaia (CC). The Caucaia shear zone displays a subvertical NE–SW to east–west mylonitic foliation, with a shallowly NE-plunging stretching lineation and dextral kinematic indicators (Sartori 2012). CC affects mainly mica-schists and granitoids in the southern Ribeira Belt. The deformation occurred under greenschist to amphibolite facies metamorphic conditions, *c.* 400–600°C, in a pure-shear-dominant component (Sartori 2012).

Central Ribeira Belt (SAM)

Central Tectonic Boundary (CTB). The Central Tectonic Boundary (CTB) separates two tectonic terranes: occidental and oriental. The former is interpreted as a stack of thrust sheets formed by Paleoproterozoic gneisses interleaved with Neoproterozoic supracrustal units (Heilbron *et al.* 2008). CTB is interpreted as a suture zone, which dips at moderate to high angles to the NW and has an oblique stretching lineation plunging to the north. The dextral kinematic sense is recorded by several indicators, suggesting a top-to-NW extensional component (Almeida *et al.* 1998). The significance of this extension is not well understood, since this 300 km-long high strain zone is related to the collision between these two terranes (Heilbron *et al.* 2008).

Além Paraíba (AP). The ENE–WSW Além Paraíba shear zone is an intra-terrane shear zone in the Central Ribeira Orogen (Giraldo *et al.* 2019), and is more than 200 km in length and up to 5 km wide. AP is characterized by a subvertical high-grade mylonitic foliation (715°C and 4.3–7.1 kbar), with a subhorizontal stretching lineation and dextral displacement kinematic indicators (Giraldo *et al.* 2019). The adjacent rocks reached granulite facies conditions (850°C and 8 kbar) at about 593 Ma, and deformation occurred at 562 Ma (Giraldo *et al.* 2019), shortly after the metamorphic peak. Zircon ages of 583 and 591 Ma in the shear zone and monazite ages of 611 to 553 Ma (Giraldo *et al.* 2019) led to the interpretation that motion along the shear zone occurred in the interval of 585–560 Ma, due to oblique collision in the Ribeira Orogen. A 530 Ma granite cross-cut the shear zone but was also deformed, indicating a Cambrian reactivation.

Cabo Frio Thrust (CFT) and associated dextral shear zones. This NE–SW high strain zone, up to 1 km wide and at least 120 km in length, marks the contact between two contrasting terranes in the SE Ribeira Belt: the Neoproterozoic Oriental Terrane (locus of 700–450 Ma magmatic units intruding supracrustal units; Tupinambá *et al.* 2012) and the Paleoproterozoic Cabo Frio Tectonic Domain (with *c.* 1.9 Ga orthogneisses, tectonically interleaved with Neoproterozoic supracrustal units; Schmitt *et al.* 2016). The shearing is interpreted to be related to D1–D2 progressive ductile phases, dated at 530–515 Ma (Schmitt *et al.* 2012, 2016; Vieira *et al.* 2022). Ophiolite relicts and high-pressure metamorphic rocks were thrust over the Cabo Frio Tectonic Domain, which is interpreted as the lower plate of an ancient subduction zone (Martins *et al.* 2016, 2021; Capistrano *et al.* 2020; Vieira *et al.* 2022). Although it is folded by a reclined crustal-scale structure, a downdip K-feldspar–quartz stretching

lineation indicates that it is a thrust zone with top-to-east–SE vergence (Schmitt *et al.* 2016). The geometry of the reclined fold plus the deep high magnetic anomaly signature (Stanton *et al.* 2010) indicate that this shear zone/suture has a subvertical envelope and not a SE-dipping envelope (De Freitas *et al.* 2021). In addition, D3 ductile NW–SE dextral shear zones occur in both terranes. Although they are seen in outcrop scale, these *c.* 520 Ma shear zones are common, suggesting there could be a larger shear zone along the Brazilian continental margin that might correlate in the reconstruction with major east–west structures in Africa, e.g. the Malange deformation zone (Heilbron *et al.* 2008; Schmitt *et al.* 2008, 2016; Monié *et al.* 2012). The Cabo Frio is the only thrust zone detailed in this paper due to the timing of this late collisional event, the Cambrian Buzios orogeny (Schmitt *et al.* 2016), that, as the Damara and Pampean collision zones, occurred during the last adjustments between the converging palaeocontinents during Gondwana consolidation.

Southern Brasília Belt (SAM)

Buquira (BQ). The Buquira shear zone separates the Embu Complex from the Socorro–Guaxupé Nappe (Fontainha *et al.* 2021). BQ is more than 150 km long and is composed mainly of an anastomosing network of mylonites and ultramylonites. The ENE–WSW mylonitic foliation is steep and south–southeasterly dipping (Duffles *et al.* 2016; Fontainha *et al.* 2021). The deformation occurred under greenschist to lower amphibolite facies (Fontainha *et al.* 2021). Kinematic indicators associated with lineation display a dextral shear sense, but a reverse component can also be observed (Duffles *et al.* 2016).

São Bento do Sapucaí–Caxambu (SBC). The São Bento do Sapucaí–Caxambu shear system branches in two segments: the Caxambu shear zone (Trouw *et al.* 2007), deforming the supracrustal units of the Andrelândia Group and their basement in the southern Brasília Belt, and the São Bento do Sapucaí shear zone (Vinagre *et al.* 2016, 2020), deforming granitic units from the Socorro–Guaxupé Nappe of the southern Brasília and Ribeira belts (Fontainha *et al.* 2021). SBC is a NE–SW shear zone system about 220 km in length and 1–3 km in width. The mylonitic foliation dips steeply to both SE and NW, with a low–moderate angle stretching lineation plunging to NE, locally to SW (Trouw *et al.* 2007; Vinagre *et al.* 2020). Kinematic indicators show oblique dextral sense of shear, with locally a top-to-SE component. Sinistral displacement is also locally described (Vinagre *et al.* 2020). Microstructural features suggest that dynamic recrystallization occurred at temperatures between 450 and 650°C, and geothermobarometric data

suggest pressures of 1–3 kbar (Trouw *et al.* 2007; Vinagre *et al.* 2020). LA-ICP-MS data from the São Bento do Sapucaí shear zone yield U–Pb ages of *c.* 613 Ma on metamorphic rims of detrital zircon grains from paragneisses and a U–Pb age of *c.* 610 Ma from a deformed gabbro–norite (Vinagre *et al.* 2020). A late tectonic pegmatitic leucogranite, which crosscuts the shear zone, yields zircon U–Pb ages between 656 and 611 Ma, interpreted as inheritance ages, and a monazite crystal yields a crystallization age of 552 Ma. Therefore, the age of the shear zone’s activity is constrained between 610 and 552 Ma (Vinagre *et al.* 2020).

Extrema (EX). The Extrema shear zone is parallel to the São Bento do Sapucaí–Caxambu shear zone system, at a distance of *c.* 130 km to the north of it. The NE–SW mylonitic foliation, which dips steeply to both SE and NW and contains a shallowly WSW-plunging stretching lineation, is developed at low metamorphic grade (Novo *et al.* 2014; Fontainha *et al.* 2021). Kinematic indicators show a predominant dextral sense of shear, but it is also possible to observe juxtaposed structures with opposite kinematics along the southern and northern limits of this shear zone (Faleiros *et al.* 2022). A syntectonic granite partially affected by the Conceição das Pedras shear zone, considered the northern extension of the Extrema shear zone, constrains the age of shearing to between 563 and 573 Ma (Peternel *et al.* 2005; Fontainha *et al.* 2021).

Maria da Fé (MF). The Maria da Fé shear zone, 40 km in length and 2.5 km wide, occurs at the interference zone between the Southern Brasília and Central Ribeira orogens. This NNE–SSW sinistral shear zone is an exception in this region because most shearing zones are dextral. The timing of sinistral shearing was determined by dating zircon crystals of a 587 ± 8 Ma pegmatite vein that crosscuts the zone, but it is also offset by it (Zuquim *et al.* 2011). Mylonitic fabric is indicative of temperatures in the order of 450–600°C (Zuquim *et al.* 2011). The zone is interpreted to be the consequence of NW–SE compression at 590–560 Ma, related to collisional tectonics that formed the Central Ribeira Orogen (Zuquim *et al.* 2011; Trouw *et al.* 2013; Fontainha *et al.* 2021).

Três Corações (TC). The NE–SW Três Corações dextral shear zone is a narrow subvertical zone of only a few tens of metres thick, but more than 100 km in length. TC is comprised of low-grade mylonites and locally fault breccias. No data constraining the age of shearing are available, but in the general geological context, the age of shearing is thought to range from 590 to 550 Ma (Trouw *et al.* 2013; Fontainha *et al.* 2021).

Transatlantic SW Gondwana crustal-scale shear zones

Poços de Caldas (PC). The Poços de Caldas shear zone is a curved structure, with a NE–SW strike in the western segment and an east–west strike in the eastern segment (Fig. 4). PC is *c.* 170 km in length, with a subvertical mylonitic foliation and local cataclasites. The deformation occurred at greenschist to lower amphibolite facies conditions (Fontainha *et al.* 2021). Kinematic indicators show a dextral shear sense. However, the rotation of the geological contacts, as shown in map view, suggests sinistral movement. This ambiguity is probably due to the result of a dextral reactivation of older sinistral activity that accompanied the initial formation of PC (Fontainha *et al.* 2021).

Campo do Meio (CM). The Campo do Meio shear zone, north of the Poços de Caldas shear zone, *c.* 25 km wide and *c.* 250 km in length, is considered the northern limit of the Socorro–Guaxupé Nappe (Fig. 4). CM displays ductile-to-brittle deformation characteristics, a sinistral shear sense and an east–west striking subvertical foliation. The shear zone crosscuts and overprints older thrust structures. Deformation occurred under low metamorphic grade, greenschist to lower amphibolite facies (Ebert and Hasui 1998; Zanardo *et al.* 2006; Fontainha *et al.* 2021).

Angola Craton and West Congo Belt (Afr)

The north–south Kaoko Belt is exposed along the coast and continues offshore northwards from the Kunene mouth at the border between Angola and Namibia (Fig. 1b). The few publications on the Angola shield do not describe shear zones related to Pan-African–Brasiliano overprint along the southwestern Angolan coast. Regional geological maps and satellite images show spectacular exposures of metamorphic and magmatic Paleoproterozoic–Mesoproterozoic geological units, enhancing also east–west trace of tectonic foliation in the desert, within the Angola Craton (Fig. 4). This structural grain is attributed as Paleoproterozoic fabric by recent papers (Lehmann *et al.* 2020; Rey-Moral *et al.* 2022). The geological map shows a discontinuity along an east–west lineament, immediately south of Luanda, separating the Archean–Paleoproterozoic shield to the south from the Neoproterozoic West Congo Belt to the north (Fig. 3). This region is described as the Malange uplift, a Mesozoic tectonic structure bordering the inner Cretaceous Kwanza Basin (Hudek and Jackson 2002). Some authors interpret that the kilometre-scale dextral drag of this Neoproterozoic belt is related to this lineament, which would represent a major shear zone from the Neoproterozoic (Heilbron *et al.* 2008; de Wit and Linol 2015; Schmitt *et al.* 2016). Other authors consider that this is a recent structure and that the

bending of the orogen would be related to orogenic folding (Fossen *et al.* 2021). Here, we name this structure as the dextral Kwanza shear zone, developed during the tectonic emplacement of the Neoproterozoic–Paleoproterozoic crystalline nappes during the Cambrian (Monié *et al.* 2012).

Kaoko Belt (Afr)

The Kaoko Belt is one of the Pan-African belts in Africa and constitutes a part of the Damara Orogen in NW Namibia. Initially, it was divided into Eastern, Central, Western and Southern Kaoko zones (Miller 1983), in which most of the boundaries are lineaments, thrusts, faults or mylonite zones (Miller 2008). More recently, a new proposal divides this belt into three domains separated by major shear zones: Western, Central and Eastern Kaoko (Goscombe *et al.* 2003b; Oriolo *et al.* 2018a, b), with the alternative names of ‘Escape Zone’ and ‘Foreland’ for the Central and Eastern Kaoko zones, respectively. The main boundaries between these domains are the Purros and Three Palms mylonite zones, which are evident in the aeromagnetic data. Goscombe and Gray (2008) subdivide the Kaoko Belt into three domains, which are, from west to east: Coastal Terrane (CT), Orogen Core (OC) and Escape Zone (ES). The CT exhibits rocks that differ in various aspects, metamorphism and structural style when related to the rest of the Kaoko Belt, showing different lithostratigraphy and provenance source as well as high temperature of metamorphism and igneous rocks. The Coastal Terrane is interpreted as an outboard continental margin arc that was obducted and incorporated with the rest of the Kaoko Belt during the transpressional orogenesis (Goscombe and Gray 2008). The OC is described as a central region in the Kaoko Belt, between the Coastal Terrane and the Escape Zone, with the Damara Sequence metamorphosed at amphibolite to granulite facies, Pan-African intrusions and basement slivers (Foster *et al.* 2009). This region is composed of three domains, from north to south: Hartmann, Khumib and Hoarusib domains, which have a lenticular shape, are different from each other and have tectono-metamorphic characteristics.

Three Palms Mylonite Zone (TH). This high strain zone is about 1–2 km wide and about 390 km in length, dividing the Western Kaoko Zone into the Coastal Terrane and the Orogen Core. This shear zone is connected with the Purros Mylonite Zone through several discrete anastomosing shear zones between the Khumib and Hoarusib rivers that resemble a horsetail structure, named the Hartmann Mylonite Zone (HMZ), the Khumib Mylonite Zone (KMZ) and the Village Mylonite Zone (VMZ).

Their strike varies from north to NW, and they dip moderately to steeply to the west (60–90°). A north–NE orientation predominates in the central–northern area with a moderate dip to the east, whereas a north orientation predominates in the southern region with shallow to moderate dips to the west (Goscombe and Gray 2007, 2008; Foster *et al.* 2009; Oriolo *et al.* 2018a, b). The sinistral strike-slip movement is based on many kinematic indicators and subhorizontal to gently south–SE plunging stretching lineations (Goscombe and Gray 2008; Oriolo *et al.* 2018a, b). According to Foster *et al.* (2009), the main phase of mylonitization in the TH was related to ductile recrystallization that produced a coarse biotite–muscovite schistosity with quartz aggregate ribbons and plagioclase sub-grain pressure shadows. The age for the main sinistral shearing is provided by U–Pb data on zircon and monazite from granites and orthogneisses, suggesting the metamorphism (transpressional orogenesis) peaked *c.* 580–550 Ma (Gray *et al.* 2006). Muscovite Ar–Ar ages in mylonitic orthogneiss of $c. 481 \pm 3$ and 492 ± 3 Ma are interpreted to reflect isotopic resetting during further early Proterozoic deformation (Gray *et al.* 2006), and Ulrich *et al.* (2011) indicated that one sinistral shearing event occurred after 550 Ma (Oriolo *et al.* 2018a, b and references therein).

Purros Mylonite Zone (PMZ). The PMZ represents a well-exposed example of a crustal-scale transcurrent shear zone and, for many researchers, is one of the most remarkable structural features in the central part of the Kaoko Belt (Konopásek *et al.* 2005 and references therein). It is more than 600 km in length and about 5 km wide. According to Goscombe *et al.* (2003b), the PMZ is possibly the boundary between Paleoproterozoic and Mesoproterozoic basements, defining the boundary between the Central and Western zones. The NNW–SSE PMZ displays a WNW to WSW steeply dipping mylonitic foliation in the northern region. By contrast, in the south, the foliation dips moderately to the WSW (Goscombe *et al.* 2003b; Goscombe and Gray 2008). Sinistral rotation of mantled feldspar porphyroblasts and dynamic recrystallization of quartz and feldspar suggest maximum of upper amphibolite facies deformation conditions (Oriolo *et al.* 2018a, b). Ar–Ar whole rock age of 467 ± 3 Ma from a mylonitic schist near the PMZ was interpreted to be the result of K–Ar resetting during the late stages of shearing (Gray *et al.* 2006).

Village Mylonite Zone (VMZ). Goscombe *et al.* (2003b) defined this high strain zone, visible on satellite images. The VMZ is one of the four crustal-scale shear zones in the Orogen Core, and can be described as a secondary anastomosed branch

of the TH, located between the KMZ and the TH. Several authors report that this zone diverges into two branches that merge with the TH and with the PMZ (Goscombe and Gray 2008; Foster *et al.* 2009). Brittle deformation of feldspars and ductile behaviour of quartz in S3 foliation suggest deformation at low-temperature conditions (greenschist facies). Sinistral shear sense is interpreted based on rotated K-feldspar porphyroclasts and other microstructures.

Ahub Mylonite Zone (AH). The AH is located in the southern area of the Escape Zone (EZ), sub-parallel to the PMZ. The EZ is an alternative term for the Central Kaoko Zone, and is characterized by deep basin and slope facies of the Damara Sequence, ranging from lower greenschist facies in the east to upper amphibolite facies in the west (Foster *et al.* 2009; Oriolo *et al.* 2018a, b). This north–south trending mylonite to protomylonite zone is 1 km wide, and it is connected to the thrust-bound basement slivers inclined to the west (Goscombe and Gray 2008). According to the same authors, the AH, unlike the other shear zones from the Kaoko Belt, is a strike-slip shear zone with a high flattening component. The kinematic indicators are shear bands and mantled porphyroclasts exhibiting sinistral sense of shear. In the southern sector, foliation dips steeply to the east, and the mineral stretching lineation plunges shallowly to the north. Moreover, the AH has an important lateral shear regime evidenced by vertical down-dip boudin neck axes, and there is a high proportion of symmetrical mantled porphyroclasts stretched equally, suggesting a moderate flattening component across this zone (Goscombe and Gray 2008).

Damara Belt (Afr)

Khan shear zone (KSZ). The Khan shear zone is located north of the Damara Core Complex (DCC) and has a throw of 2.8 km. According to Goscombe *et al.* (2022), KSZ was the first low-T retrograde shear zone to overprint the core complex during exhumation. This zone affects marble from the Karibib Formation, and it has a dextral sense of displacement. The age of this shear zone was obtained through *in situ* LA-ICP-MS dating of apatite and titanite within carbonate mylonite, providing an age of 500.3 ± 3 for apatite and 495.0 ± 6.4 Ma for titanite. Furthermore, the KSZ was reactivated with a sinistral–normal sense (Goscombe *et al.* 2022).

Okahandja shear zone (OSZ). Along with the Omaruru Lineament–Waterberg Thrust and the Autseib Fault–Otjohorong Thrust, the OSZ is an important NE–SW shear zone in Central Namibia, with more than 300 km in length and interpreted as the

Transatlantic SW Gondwana crustal-scale shear zones

continuation of the Precambrian transcontinental Mwembeshi shear zone (Granath *et al.* 2022 and references therein). In accordance with Downing and Coward (1981), the OSZ is considered to be the southern margin of a magmatic arc generated by the northerly subduction of the Damaran Ocean crust between 750 and 520 Ma. Between 675 and 575 Ma, syn-orogenic strata and granitoid units, generated via subduction and crustal melting, underwent shear deformation in a low angle sinistral shear zone (Clemens and Kisters 2021; Granath *et al.* 2022).

The OSZ is a complex and composite structure located along the boundary between the South Central Zone and the Tinkas Belt, and commonly demarcates the southern limit of the Proterozoic basement and basal Damaran stratigraphy of the Nosib Group (Miller 1979; Goscombe *et al.* 2022). It is at least 130 km in length, is a sub-vertical zone and was reactivated six times during the evolution of the Damara Orogen. The main branch of the predominant shear zone is related to the later stages of the main phase of the orogen, displaying a sub-vertical foliation that was overprinted by two episodes of dextral–normal shear zones (Median and South Branches). Moreover, the main branch displays protomylonite, mylonite and rare ultramylonite fabrics, with medium-grained fabrics developed under upper amphibolite facies and a stretching lineation that plunges moderately to the SW. In addition, in the main branch, the NE–SW subvertical mylonitic foliations display dextral–normal sense kinematics. The estimated P–T conditions, calculated using mineral cores from mylonite assemblage, give $594 \pm 10^\circ\text{C}$ and $4.5\text{--}5.0 \pm 0.4$ kbar. Deformation age in the main branch was dated with *in situ* U–Pb LA-ICP-MS analysis on apatite, yielding an age of 520.7 ± 5.3 Ma from a mylonitized greywacke and a $^{206}\text{Pb}/^{238}\text{U}$ titanite lower intercept age of 524.5 ± 7.4 Ma from the same sample.

The median branch also shows dextral–normal sense, with NE–SW striking mylonitic fabrics with a SWW shallowly plunging stretching lineation. P–T conditions were estimated at $585 \pm 17^\circ\text{C}$ and 4.1 ± 0.4 kbar. The estimated age for this segment of OSZ is *c.* 519.9 ± 1.9 Ma, as indicated by *in situ* LA-ICP-MS dating monazite from metapelitic mylonite. There is another age of *in situ* LA-ICP-MS dating of apatite from the same sample, 485.2 ± 3.5 Ma, interpreted as reactivation because this age postdates mylonitization by 30 myr and is identical (within error) to U–Pb apatite and monazite cooling ages from the hanging wall of the KSZ, which experienced sinistral–normal reactivation at this time (Goscombe *et al.* 2022).

The southern branch can be divided into eastern and western sectors, with NNE–SSW oriented low-T mylonites and NE–SW oriented medium-T

mylonites in basement rocks. Other differences between these sectors are: (1) the eastern sector is a narrow (7–67 m wide) shear zone, steeply dipping to the ESE; the stretching lineation plunges shallowly to the SSW; and kinematic indicators show a dextral–normal shear sense; and (2) the western sector displays mylonite to protomylonite fabrics, with aggregate ribbons of quartz and feldspar that indicate higher temperatures of deformation ($>480^\circ\text{C}$; Passchier and Trouw 2005). The age for the southern branch was obtained by *in situ* LA-ICP-MS dating of titanite in a mylonitic greywacke, providing an uncorrected $^{206}\text{Pb}/^{238}\text{U}$ lower intercept age of 490 ± 10 Ma. Another age was calculated using *in situ* LA-ICP-MS dating of apatite in metapelite from the Tinkas Formation, providing a ^{207}Pb corrected weighted average $^{206}\text{Pb}/^{238}\text{U}$ age of 492.5 ± 2.7 Ma (Goscombe *et al.* 2022).

Tinkas shear zone (TSZ). According to Goscombe *et al.* (2022), the TSZ is a sub-vertical greenschist facies sinistral–normal shear zone, restricted to a 12–15 m wide zone demarcating the abrupt boundary between the Tinkas Belt and the Okahandja Zone (Fig. 4). The maximum age for mylonitization in TSZ was interpreted indirectly through the dating of post-kinematic, discordant, tabular muscovite-bearing pegmatite dykes and muscovite leucogranite sheets that provide U–Pb monazite ages of 513–512 Ma (Clemens *et al.* 2017a, b). Moreover, the sinistral movement of TSZ is correlated with reactivations of the OSZ and the KSZ that have ages around 485–482 Ma from U–Pb apatite and monazite data. The TSZ displays S–C fabrics and mylonite to protomylonite texture, with a NE–SW sub-vertical foliation. All kinematic indicators point to sinistral–normal slip along mineral aggregate lineations that, on average, plunge shallowly to the NE, and there is no evidence of dextral shear. However, this zone also experienced different episodes of brittle deformation that overprinted the mylonitic fabric (Goscombe *et al.* 2022).

Goantagab shear zone (GSZ). This is a high strain domain east of the Vrede–Doros–Brandberg line, where highly strained passive margin carbonates preserve pre-Kaokoan isoclinal folds and L–S fabrics in what may constitute an early crustal-scale shear zone (Goscombe *et al.* 2004, 2017; Passchier *et al.* 2016).

The Vrede–Doros–Brandberg (VDB) line is a tectonic boundary (Passchier *et al.* 2016) that we correlate with the Goantagab shear zone (Goscombe *et al.* 2017). The sinistral rotation of the Voetspoor pluton can be used as a kinematic indicator of this high strain zone. According to Passchier *et al.* (2007), the pluton was emplaced syn-D1/2 and rotated during D2 and D3 deformational phases.

Considering that the emplacement age of the pluton is 530 Ma (Schmitt *et al.* 2012), the shear zone movement should be at least in part younger. The reactivation would have occurred during the Cambrian.

Gariiep Belt (Afr)

The NNW–SSE Gariiep Belt (GB) is parallel to the Namibia–South Africa western coast and orthogonal to the Damara Belt. It is constituted mainly by thrust shear zones with minor transcurrent component. Frimmel (2018) reports that the GB is an important geological feature in southwestern Namibia, and can be mapped inland from the coast to around 80 km. Halbach and Alchin (1995) considered the Gariiep Belt as a southerly extension of the Damara Orogen and subdivided it into an eastern para-autochthonous or external and continental ‘Port Nolloth Zone’ and an allochthonous or internal oceanic ‘Marmora Terrane’, with the boundary defined by Schakalsberg thrust zone. The para-autochthonous, external zone is located on the western side of the Kalahari Craton, and the allochthonous, internal zone represents an obducted oceanic slab. Frimmel (1995, 2018) describes the GB as part of the larger network of Pan-African–Brasiliano orogenic belts in SW Gondwana, where these zones surround the composite Kalahari–Kaapvaal–Zimbabwe Craton and occur in the north Zambezi Belt, in the NW Damara Belt, Saldania in the south and GB in the west. Davies and Coward (1982) and other authors interpreted the GB as a sinistral transpressional orogen.

There are some geodynamic models proposed for the formation of these coast-parallel branches, relating them to the suture between South America and Africa during the Neoproterozoic. In this context, one model involves the existence and consumption of the large Adamastor Ocean, and an alternative model involves a methodology based on zircon provenance and isotopic geochemical data from strata in which the possible suture between South America and Africa would be inland of Uruguay and Brazil and not located along the modern South Atlantic coastline as proposed in the first model (Frimmel 2018 and references therein).

Saldania Belt (Afr)

Towards the south, entering South Africa, the east–west foliated Kalahari Craton units are widespread and continue into the offshore region. Further south, Paleozoic strata of the Cape Fold and Thrust Belt show spectacular folds in a thin-skinned deformation style related to the Permian–Triassic Gondwanide Orogen. Its crystalline basement is represented by the Neoproterozoic Saldania Belt. According to Frimmel and Frank (1998), similar to

the Gariiep Belt, the Saldania Belt shows only very low-grade metamorphic rocks, in contrast to the high-grade units of the Damara Belt. The most prominent Late Neoproterozoic–Early Paleozoic shear zone from the Saldania Belt is described below.

Colenso Fault (CF). According to Kisters *et al.* (2002), the Colenso Fault (CF) is a major NW–SE trending fault zone in the Pan-African Saldania Belt of the Western Cape Province in South Africa, and is closely associated with the *c.* 550 to 510 Ma Cape Granite Suite granitoids. The same authors describe this fault zone as characterized by intensely mylonitized and brecciated rocks that can be mapped for at least 150 km. The emplacement of the Darling Batholith, at 547 ± 6 Ma, records the sinistral strike-slip movement and suggests an intrusion of the pluton occurred during the main Pan-African collisional event in the Saldania Belt. The age of dextral strike-slip movement can be obtained from the emplacement age of the 520 Ma Trekoskraal granite, which intrudes syn-kinematically into the fault. The reversion of the motion in CF at *c.* 540 Ma coincides with the uplift in rocks from the Saldania Belt and is related to the change in regional-scale plate motions (Kisters *et al.* 2002 and references therein). The mylonitic structures suggest deformation at temperatures of *c.* 400–450°C, evidenced by partial dynamic recrystallization of feldspar (brittle–ductile behaviour) and by the local substitution of biotite by chlorite.

Discussion

Age and tectonic framework of the shear zone systems

In order to discuss the kinematic and tectonic scenarios of the final amalgamation and consolidation of the SW Gondwana continental crust, we require precise geochronological and P–T conditions constraints for the major shear zones. The formation and reactivation ages of some shear zone systems are precisely constrained based on sophisticated and distinct geochronological methods that track the timing of their evolution with changing P–T conditions (e.g. southern Ribeira Belt; Conte *et al.* 2020; Ribeiro *et al.* 2020; Faleiros *et al.* 2022; Cabrita *et al.* 2022). But these well-constrained data are not homogeneously distributed.

Based on the compiled database, all dated Pan African–Brasiliano shear zones show predominant activity between 640 and 540 Ma (Fig. 5). In order to analyse the kinematics and geodynamics of SW Gondwana, the shear zones are grouped within the major orogenic time intervals determined in Schmitt *et al.* (2018): Phase 1, older than 590–580 Ma; Phase 2, younger than 590–580 Ma. In Figure 6, the shear

Transatlantic SW Gondwana crustal-scale shear zones

zones are coloured according to their timing. We classify Phase 1 and Phase 2 shear zones plus a group of shear zones that were generated during the Phase 1 interval and were reactivated during Phase 2, especially the ones from SE Brazil (Central and South Ribeira Belt).

The African shear zones, bordering the Kalahari and Angola cratons, are predominantly from Phase 2. The South American shear zones were active mostly between 670 and 520 Ma, so they include both orogenic phases and some of them were reactivated in the Cambrian (Fig. 5).

Transatlantic correlation

To discuss the kinematic and tectonic scenarios of the final amalgamation and consolidation of the SW Gondwana continental crust, we need to extrapolate and correlate the structures exposed on land with those offshore. By integrating the structural and geological data with the plate reconstruction model for the SW Gondwana crust, it is possible to propose a more precise transatlantic correlation (de Wit *et al.* 2008). These authors concluded that it would be difficult to identify the respective ‘partners’ of the subvertical Pan-African–Brasiliano shear zones on either side of the South Atlantic, especially strike-oblique ones, with a low angle to the present coastlines and with similar ages.

Here, we discuss the possible correlation between individual shear zones and/or shear systems, emphasizing the timing of deformation, kinematics and whether they are terrane-bounding or intra-terrane structures. The new kinematic reconstruction model provides a tighter fit between the South American and African continents (Figs 2 & 3). The two continental masses are not only closer than the previous schematic reconstructions (e.g. Konopásek *et al.* 2016; Basei *et al.* 2018; Will *et al.* 2019), but they are also reconstructed using oceanic crust as well as continental margin data allied with continental intraplate deformation zones (Fig. 2).

From south to north, the first piercing point highlighted is the Permian–Triassic Sierra de la Ventana–Cape Fold and Thrust Belt in both the Argentinian and South African sides (Figs 3 & 6). This orogen is a product of the collision of the Patagonia continental block with the southern Gondwana margin at the end of the Paleozoic, characterized as the tectonic front of the Gondwanide Orogen that is now truncated at high angle across the South Atlantic margins (de Wit *et al.* 2008). Correlations between these belts on stratigraphical, structural and geochronological data are robust (e.g. Keidel 1916; Du Toit 1927, 1937). De Wit *et al.* (2008) point out that the extreme western section of the Cape Fold Belt bifurcates into north–south and NW-striking tectonic branches, flanking the easternmost outcrops of the

Saldanian basement of the Western Cape (Fig. 3), and they conclude that it would be hard to determine which branch correlates directly with the Sierra de la Ventana Fold and Thrust Belt. Pángaro and Ramos (2012) propose the continuation offshore of the NW branch, using the interpretation of seismic sections that show deformed Paleozoic sediments in a fold and thrust belt (Fig. 4).

Our kinematic reconstruction for the SW Gondwana crust is built on a unique African plate interacting with two South American platelets (Fig. 2). The South American plate is discontinued exactly at the Cretaceous Torres syncline feature, where the southern platelet (plate 40, southern Brazil) is rotated anticlockwise to be proximate to the South African plate (201), generating a sinistral east–west movement overlapping with platelet 201 in the South American continent (Fig. 2). This specific anticlockwise rotation of platelet 40 approximates the southern Brazilian shield rotation relative to the African continental crust, even though the COB lines, reduced to 50%, from Africa and South America do not fit, leaving a gap of at least 100 km (Fig. 3). This indicates that there is either missing continental crust or that there is magma addition to this sector of the margin. The second hypothesis is feasible considering that the Pelotas Basin, in Brazil, is a magma-rich margin with abundant seaward-dipping reflectors (SDRs; Stica *et al.* 2014) that represent thick packages of lavas and are diagnostic features of volcanic passive margins (McDermott *et al.* 2018). This analysis implies there is some space for extra approximation of these platelets.

The direct consequence of this reconstruction model is that it offsets the previously proposed correlations between the Brazilian shear zones (Fig. 4). The Dorsal de Canguçu–Sierra Ballena sinistral shear zone was previously correlated with the Major Gercino dextral shear zone (Figs 4 & 6; Passarelli *et al.* 2011; Konopásek *et al.* 2016; Philipp *et al.* 2016). Although they have a similar age of tectonic activity, with recurrent deformation from 630 to 550 Ma, the kinematic indicators are opposite. In our new reconstruction, they do not match. The Dorsal de Canguçu–Sierra Ballena shear zones would continue oceanwards, correlating with the Purros–Three Palms sinistral shear system in Namibia, more specifically, with the Kunene shear zone (Fig. 6). This correlation would be geologically more plausible, as the shear zones have similar age and kinematics.

Another piercing point that could arise from this new reconstruction is the correlation between the NW–SE Colenso sinistral shear zone developed in the Saldania Belt (South Africa) and the NE–SW Sierra Ballena sinistral shear zone in the southern Dom Feliciano Belt in Uruguay (Figs 4 & 6). This correlation is positioned where the piercing point

number 10 from de Wit *et al.* (2008; Fig. 1a) is located. These authors propose that NW-striking terrane boundary faults within the Saldania Belt (Western Cape, South Africa) connect with the southernmost extremity of the Alferes–Cordillera–Punta del Este shear zone (ACPESZ), south of the Río de la Plata Craton (e.g. Rozendaal *et al.* 1999). These faults are more than 800 km apart and could have been affected by the Late Paleozoic orogeny of the Sierra de la Ventana–Cape Fold Belt, but this younger deformation affects mainly the upper crust. Granites and gneisses from the basement blocks expose reverse faults and fractures, attesting to thick-skinned tectonics (Tomezzoli and Cristallini 2004; Ramos 2008; López-Gamundí *et al.* 2013). The Paleozoic sedimentary strata are folded and thrust, constituting a belt that is interpreted as an intracontinental orogenic zone. Therefore, there is no suture zone within SW Gondwana younger than the Brasiliano–Pan African events. Because these fold belts are both constructed upon a similar Neoproterozoic basement close to the Atlantic margin, their correct structural correlations have a direct bearing on the correlation of ‘piercing points’ in their surrounding basements (de Wit *et al.* 2008).

One of the controversial connections is the orthogonal match between the east–west Damara structures in Africa and the NE–SW Dom Feliciano Belt structures in southern Brazil and Uruguay (Fig. 6). The mafic–ultramafic rocks in northern Uruguay (Paso del Dragón; Peel *et al.* 2018) and in south Brazil (Arroio Grande Complex) are deformed by the dextral Ayrosa Galvão–Arroio Grande shear zone (AG; Ramos *et al.* 2018). The Arroio Grande branch of the system is oriented east–west. After reconstruction, its continuation matches with Damara Belt fabrics in Namibia. The Matchless Amphibolite, interpreted as an ophiolitic suture in the southern Damara Orogen (Meneghini *et al.* 2017), is parallel to this structure and is exposed around Namibia’s capital (Windhoek; Fig. 3). In our reconstruction model, this ophiolite suture does not fit perfectly the Arroio Grande Ophiolite in southern Brazil, but unknown shear zones offshore might account for this offset (Fig. 6). The correlation between the AG shear zone and the Damara Orogen structures requires further investigation. Alternatively, we propose also that the AG shear zone might correlate with the Ogden and Purros shear zones, but the kinematics is opposite, the Namibian shear zones are sinistral (Fig. 4).

The potential correlation between the sinistral Purros–Three Palms shear zone systems in the Kaoko Belt and the dextral Lancinha–Cubatão shear zone systems in the southern Ribeira Belt is difficult to evaluate since these systems are subparallel to the coast of the conjugate passive margins (Figs 3 & 4). These systems intersect at an acute angle of c.

30–40°, signalling that they could have been active during the same event, as indicated by the overlap between their geochronological ages (Fig. 5).

To the north, the dextral Kuanza shear zone could be correlated with shear zones in the South American plate, even though the former does not extend to the onshore SE Brazil area (Figs 3 & 6). The Cabo Frio Tectonic Domain (100 km east of Rio de Janeiro, in red near borehole 1 in Fig. 3) continues offshore to the northern Campos Basin (Strugale *et al.* 2021) and is correlated with the southern West Congo Belt (100 km north of Luanda, in red in Fig. 3). Both terranes have Cambrian metamorphic ages combined with ductile structures that interleave with Neoproterozoic metasedimentary units and with the Paleoproterozoic magmatic/metamorphic basement (Monié *et al.* 2012; Schmitt *et al.* 2016). Motion along the Kuanza shear zone, in relation to the dextral drag of the southern tip of the West Congo Belt, occurred in the 540–510 Ma interval that coincides with latest metamorphic events that amalgamated SW Gondwana (Schmitt *et al.* 2018). Therefore, this dextral structure that truncates (almost orthogonally) most of the Brazilian orogenic belts may be directly related to the indentation and final amalgamation of the cratonic blocks, as we discuss below.

Kinematics of SW Gondwana amalgamation

The timing and transatlantic correlation of these Ediacaran–Cambrian steep shear zones along with their kinematics allow us to discuss the tectonic scenario for the final amalgamation and consolidation of the SW Gondwana continental crust (Fig. 6). The lack of substantial geochronological data from some shear zones hinders a detailed kinematic model for the SW Gondwana amalgamation models. However, some authors have tried to construct this framework (e.g. Passarelli *et al.* 2011; Oriolo *et al.* 2018a, b; Faleiros *et al.* 2022; Goscombe *et al.* 2022). The upgrade here is the reconstruction of SW Gondwana developed according to the kinematic models for reconstructing the South Atlantic oceanic crust, and the best-fit methodology using plate kinematic software (Figs 2 & 3). Therefore, the correlation of the structures is better constrained than previous correlations.

Here, we present a simplified kinematic map for the time interval after 585 Ma, Phase 2 of the Gondwana amalgamation process (Schmitt *et al.* 2018) that spans most of the shear zones’ activity, including the reactivation of shear zones older than 585 Ma (Fig. 5). Hence, our reconstruction considers the shear zones active in the Late Ediacaran–Cambrian time plus the older ones reactivated during this time. Analysing the map with these specific structures, their correlation in the offshore, including

Transatlantic SW Gondwana crustal-scale shear zones

the superficial boundaries of the cratons, and the younger thrust zones, it is possible to construct a kinematic scenario (Fig. 6).

The morphology of the cratons and the timing of the collision between them control mostly the geometry, kinematics and tectonic regime of these late collisional shear zones within the surrounding belts. Although only the limits of surficial cratons are shown, the surrounding belts approximately follow these limits (Fig. 6). The subsurface geometry of the cratonic blocks remains to be added/discussed in forthcoming research. For now, four craton promontories are highlighted in this kinematic map for SW Gondwana, all could be correlated with the African margin of the South Atlantic (Fig. 6). The first promontory is marked by the foreland fold and thrust belt represented by the Vanrhynsdorp Group (Gresse 1995) that crops out along the coast of South Africa, between the Saldania and Gariep belts. This Kalahari promontory displays an east–west basement fabric, partially structurally overlain by these two NW–SE and north–south Late Neoproterozoic nappes, respectively. On the South American side, the Río de la Plata Craton exposes the same pre-Neoproterozoic cratonic fabric in the Tandilla system (Cingolani 2011). Along the coast of Mar del Plata, a drill core with Ordovician low-grade metasedimentary units is correlated with the orthogonal Cambrian Pampean Orogen (Punta Mogotes; Cingolani and Bonhomme 1982). Therefore, in the South Atlantic continental margins, in between South Africa and northern Argentina, a Brasiliano–Pan-African belt is located offshore (Fig. 6).

The second Kalahari promontory is located in southern Namibia, between the NW–SE Gariep and the ENE–WSW Damara belts. The latter exposes dextral Cambrian shear zones (e.g. Okahandja shear zone, OK) that are conjugate with respect to the sinistral Laguna de Rocha (LR) and Sierra Ballena (SB) shear zones in Uruguay. The absence of transcurrent shear zones in the Gariep Belt reinforces the interpretation that the late indentation of the Kalahari Craton was accommodated by the conjugate dextral Okahandja shear zone and the sinistral Colenso–Sierra Ballena shear zones (Figs 4 & 6). Therefore, as the Kalahari Craton collided with the southern Angola Craton between 590 and 530 Ma in a frontal collision (Lehmann *et al.* 2016), the Kalahari Craton rotated anticlockwise, closing Ediacaran–Cambrian basins in Uruguay, SE Brazil and others (e.g. Bossi and Gaucher 2004; Schmitt *et al.* 2016). Casquet *et al.* (2018) interpret the Cambro-Ordovician belt in between the Kalahari and Río de la Plata cratons, partially preserved as the Saldania Belt, was contiguous with the Pampean orogeny (Fig. 1b). The sinistral NW–SE Colenso shear zone and its continuity into South America (Sierra Ballena shear zone; Figs 4 & 6) would be coeval with the

dextral Córdoba Fault (Fig. 4), implying late movement of the Río de la Plata Craton to the south, disrupting the Saldania and Pampean belts and locking the internal Gondwana orogens (Fig. 6). Therefore, from 585 until 500 Ma, the relative movement of the Río de la Plata Craton is clockwise in relation to the Kalahari Craton.

The interaction and convergence between the cratons to the north are more difficult to envisage considering that (a) the Paranapanema Craton and Luís Alves microplate correlations are speculative, mostly covered by the Phanerozoic Parana Basin (Fig. 1) and (b) Tonian tectonic events and geological units are recorded in the São Gabriel, Apiaí and Ribeira terranes (Heilbron *et al.* 2008; Campanha *et al.* 2016; De Toni *et al.* 2020b). Irrespective of these uncertainties, two promontories of the Angola Craton give important hints on this internal SW Gondwana amalgamation (Fig. 6).

The Kamanjab inlier is located in the SW corner of the Angola Craton that crops out in northern Namibia (Figs 3 & 6). The activity of the Purros–Three Palms sinistral shear zone system, coeval with the Okahandja dextral shear zone, resulted in a north–NE movement of the Angola Craton in relation to the collision of the Kalahari Craton to the south. This northward displacement might be responsible for the Buzios collisional orogeny that amalgamated the Ribeira Belt, suturing the Angola and São Francisco cratons in SE Brazil (Schmitt *et al.* 2016, 2018). The second Angola Craton promontory, between the northern termination of the Kaoko Belt and the Kuanza shear zone in the north, continues towards offshore Angola and could be related to a well-known feature in the offshore Santos Basin in Brazil, the Helmut shear zone that separates two distinct continental domains within this Atlantic marginal basin (Fig. 4; Dehler *et al.* 2016). To the east of the Helmut shear zone, there is a resistant continental block that represents an external Cretaceous high in this marginal basin. It is interpreted as a rheologically competent continental crust block that could be part of the Angola Craton (Schmitt *et al.* 2016). The northwards movement of the Angola Craton evolves to an anticlockwise rotation, expressed by the dextral east–west Kwanza shear zone. Within the Cabo Frio Tectonic Domain, *c.* 515 Ma NW–SE dextral shear zones are widespread along with the Kwanza shear zone, and they represent conjugate movement with respect to the Three Palms–Purros sinistral shear system in Namibia that shows younger activity in the Cambrian (Fig. 5).

Considering that the transpressional dextral SE Brazilian shear system, Lancinha Cubatão and CTB–Além Paraíba (Passarelli *et al.* 2011; Faleiros *et al.* 2022), has older ages for deformation (Fig. 5), we interpret this movement as the accommodation of the São Francisco Craton during the

main collision of the Ribeira Belt. This later dextral system also reflects the anticlockwise rotation of the São Francisco Craton in Brazil relative to the Angola Craton.

Conclusion

The final amalgamation and consolidation of the SW Gondwana continental crust were attained by anticlockwise rotation of three cratons (Kalahari, Angola and São Francisco) in relation to the clockwise rotation of the Río de la Plata Craton in the Gondwana margin, accommodating the initiation of a long-term active margin starting with the Pampean orogeny and ending with the Gondwanide orogeny. These relative movements were accommodated by transcurrent shear zones active from 585 to 500 Ma within the Pan-African–Brasiliano belts that surround these cratons. The precision of this kinematic model supercedes previous models because it is based on a new kinematic reconstruction of the South Atlantic that provided a better fit between the South American and Africa plates. With a better correlation offshore of these subvertical late collisional shear zones, the final amalgamation of SW Gondwana as well as the initiation of its long-lived Paleozoic active margin are here presented. As pointed out by *de Wit et al. (2008)*, there is no other way to realize a Pan-African–Brasiliano tectonic evolution for the belts separated by the South Atlantic than to understand and unravel the Cretaceous tectonic evolution:

One way to realize this is to re-join Neoproterozoic ‘piercing points’ on the conjugate margin of continental blocks that are well-dated and otherwise geophysically and geologically characterized. We have argued that for South America and Africa this might be achievable in the case of at least ten well-defined Neoproterozoic ties around the margins of the South Atlantic Ocean, and we presented a detailed map of the Brasiliano/Pan-African structures of Gondwana to facilitate the planning of such experiments. Playing back the continental motions whilst simultaneously pinning these original ties together, should result in a more robust and accurate fit from which to re-track interactive mantle–lithosphere break-up mechanisms and help quantify internal Gondwana strains that led to the break-up and separation in the first place. Involving a greater degree of such geological and geophysical control to reconstruct the Gondwana break-up history will help to correct for early Trans-Atlantic rift distortions and thus to better reconstruct the evolution of continental margins of the South Atlantic; and this in turn will improve our general understanding of the evolution of continents

(*de Wit et al. 2008*, p. 408).

Acknowledgements This paper is a contribution to the IGCP-628 ‘The Gondwana Geological Map and the Tectonic Evolution of Gondwana’. The GIS database

from the Gondwana Digital Centre of Geoprocessing (GDCG) at UFRJ was built up through the Gondwana project, a cooperation between Petrobras/CENPES and UFRJ. The authors thank the reviews from Dr Victor Ramos and an anonymous reviewer, and also thank the Editor, Dr Brendan Murphy, for carefully handling this paper.

Competing interests The authors declare that they have no known competing financial interests or personal relationships that could have appeared to influence the work reported in this paper.

Author contributions **RDSS**: conceptualization (equal), data curation (lead), formal analysis (lead), funding acquisition (lead), investigation (lead), methodology (equal), project administration (lead), resources (lead), supervision (lead), validation (lead), visualization (lead), writing – original draft (lead), writing – review & editing (supporting); **RAJT**: conceptualization (equal), formal analysis (equal), investigation (equal), methodology (supporting), supervision (equal), validation (equal), visualization (equal), writing – original draft (equal), writing – review & editing (equal); **EADS**: data curation (equal), formal analysis (supporting), investigation (equal), methodology (equal), software (lead), supervision (equal), validation (equal), visualization (equal), writing – original draft (supporting), writing – review & editing (supporting); **JVMDJ**: data curation (equal), investigation (equal), methodology (equal), software (equal), validation (equal), visualization (equal), writing – original draft (supporting), writing – review & editing (supporting); **LFMDC**: data curation (supporting), investigation (equal), methodology (equal), software (equal), validation (equal), visualization (supporting), writing – original draft (supporting), writing – review & editing (supporting); **CRP**: conceptualization (supporting), formal analysis (supporting), investigation (equal), methodology (equal), validation (equal), writing – original draft (supporting), writing – review & editing (supporting).

Funding RDSS acknowledges financial support from CNPq research grant no. 311748/2018-0; from FAPERJ through grant no. E-26/200.995/2021; and from Petrobras through grants ID0E0FBG4360 and ID0EQBAI4362.

Data availability All data generated or analysed during this study are included in this published article.

References

- Affonso, G.M.P.C., Rocha, M.P. *et al.* 2021. Lithospheric architecture of the Paranapanema block and adjacent nuclei using multiple-frequency P-wave seismic tomography. *Journal of Geophysical Research: Solid Earth*, **126**, article e2020JB021183, <https://doi.org/10.1029/2020JB021183>
- Almeida, J.C.H.D., Tupinambá, M., Heilbron, M. and Trouw, R. 1998. Geometric and kinematic analysis at the Central Tectonic Boundary of the Ribeira belt, southeastern Brazil. *XL Congresso Brasileiro de Geologia EXPOGEO 98*, 11–16 October 1998,

Transatlantic SW Gondwana crustal-scale shear zones

- Belo Horizonte, Brazil. Sociedade Brasileira de Geologia, 32.
- Archanjo, C.J., Salazar, C.A., Caltabellota, F.P. and Rodrigues, S.W.O. 2021. The onset of the right-lateral strike-slip setting recorded in magnetic fabrics of A-type granite plutons of the Ribeira belt (SE Brazil). *Precambrian Research*, **366**, article 106417, <https://doi.org/10.1016/j.precamres.2021.106417>
- Basei, M.A.S., Siga Júnior, O., Machiavelli, A. and Mancini, F. 1992. Evolução tectônica dos terrenos entre os Cinturões Ribeira e Dom Feliciano (PR-SC). *Revista Brasileira de Geociências*, **22**, 216–221, <https://doi.org/10.25249/0375-7536.1992216221>
- Basei, M.A.S., Frimmel, H.E., Nutman, A.P., Preciozzi, F. and Jacob, J. 2005. A connection between the Neoproterozoic Dom Feliciano (Brazil/Uruguay) and Gariep (Namibia/South Africa) orogenic belts – evidence from a reconnaissance provenance study. *Precambrian Research*, **139**, 195–221, <https://doi.org/10.1016/j.precamres.2005.06.005>
- Basei, M.A.S., Grasso, C., Vlach, S.R.F., Nutman, A.P., Siga, O., Jr and Osako, L.S. 2008. A-type rift-related granite and the Lower Cryogenian age for the beginning of the Brusque Belt basin. *VI South American Symposium on Isotope Geology*, 13–17 April, San Carlos de Bariloche, Argentina, Abstracts CD, <https://repositorio.usp.br/directbitstream/632b997e-9175-4d00-a4d5-9cb8341ddb7f/1717917.pdf>
- Basei, M.A.S., Nutman, A., Siga, O., Jr, Passarelli, C.R. and Drukas, C.O. 2009. The evolution and tectonic setting of the Luís Alves Microplate of southeastern Brazil: an exotic terrane during the assembly of Western Gondwana. *Developments in Precambrian Geology*, **16**, 273–291, [https://doi.org/10.1016/S0166-2635\(09\)01620-X](https://doi.org/10.1016/S0166-2635(09)01620-X)
- Basei, M.A.S., Campos Neto, M.C. *et al.* 2011. Tectonic evolution of the Brusque Group, Dom Feliciano belt, Santa Catarina, southern Brazil. *Journal of South American Earth Science*, **32**, 324–350, <https://doi.org/10.1016/j.jsames.2011.03.016>
- Basei, M.A.S., Frimmel, H.E., Campos Neto, M.C., Ganade de Araujo, C.E., Castro, N.A. and Passarelli, C.R. 2018. The tectonic history of the southern Adamastor Ocean based on correlation of the Kaoko and Dom Feliciano belts. In: Siegesmund, S., Basei, M.A.S., Oyhantçabal, P. and Oriolo, S. (eds) *Geology of Southwest Gondwana*. Springer, Cham, 63–85.
- Battisti, M.A., Bitencourt, M.F. *et al.* 2022. Reconstruction of a volcano-sedimentary environment shared by the Porongos and Várzea do Capivarita complexes at 790 Ma, Dom Feliciano Belt, southern Brazil. *Precambrian Research*, **378**, article 106774, <https://doi.org/10.1016/j.precamres.2022.106774>
- Becker, T., Garoeb, H., Ledru, P. and Milesi, J.P. 2005. The Mesoproterozoic event within the Rehoboth Basement Inlier of Namibia: review and new aspects of stratigraphy, geochemistry structure and plate tectonic setting. *South African Journal of Geology*, **108**, 465–492, <https://doi.org/10.2113/108.4.465>
- Bitencourt, M.F. 1996. *Granitoides Sintectônicos da Região de Porto Belo-SC: uma Abordagem Petroológica e Estrutural do Magmatismo em Zonas de Cisalhamento*. PhD thesis, Universidade Federal do Rio Grande do Sul.
- Blanco, G. 2010. Provenance of the Ediacaran–Early Palaeozoic Arroyo del Soldado Group (Uruguay) and the Nama Group (Namibia): geodynamic implications for the SW-Gondwana amalgamation. *Serie Correlación Geológica*, **26**, 9–26, <https://www.insugeo.org.ar/publicaciones/docs/scg-26-0-01.pdf>
- Bossi, J. and Gaucher, C. 2004. The Cuchilla Dionisio Terrane, Uruguay: an allochthonous block accreted in the Cambrian to SW-Gondwana. *Gondwana Research*, **7**, 661–674, [https://doi.org/10.1016/S1342-937X\(05\)71054-6](https://doi.org/10.1016/S1342-937X(05)71054-6)
- Cabrita, D.I.G., Faleiros, F.M., Ribeiro, B.V., Menegon, L., Cawood, P.A. and Campanha, G.A.C. 2022. Deformation, thermochronology and tectonic significance of the crustal-scale Cubatão Shear Zone, Ribeira Belt, Brazil. *Tectonophysics*, **828**, 229278, <https://doi.org/10.1016/j.tecto.2022.229278>
- Campanha, G.A.C., Basei, M.S., Faleiros, F.M. and Nutman, A.P. 2016. The Mesoproterozoic to early Neoproterozoic passive margin Lajeado Group and Apiaí Gabbro. *Southeastern Brazil Geoscience Frontiers*, **7**, 683–694, <https://doi.org/10.1016/j.gsf.2015.08.004>
- Capistrano, G.G., Schmitt, R.S., Medeiros, S.R. and Vieira, T.A.T. 2020. Ediacaran ophiolite relics in the SE Brazilian coast: field, geochemical and geochronological evidence from metabasites and paragneisses. *Journal of South American Earth Sciences*, **105**, article 103040, <https://doi.org/10.1016/j.jsames.2020.103040>
- Carmo, I.O., Schmitt, R., Araujo, M.N.C. and Romeiro, M.A.T. 2017. Evidence for the Paleoproterozoic/Cambrian Angolan belt in the Brazilian margins – new data from offshore basement drill core. *5th Conjugate Margins Conference*, 22–25 August 2017, Pernambuco, Brazil, Abstracts.
- Casquet, C., Dahlquist, J.A. *et al.* 2018. Review of the Cambrian Pampean orogeny of Argentina; a displaced orogen formerly attached to the Saldania Belt of South Africa? *Earth-Science Reviews*, **177**, 209–225, <https://doi.org/10.1016/j.earscirev.2017.11.013>
- Castro, L.G., Ferreira, F.J.F., Cury, L.F., Fiori, A.P., Soares, P.C., Lopes, A.P. and Oliveira, M.J. 2014. Qualitative and semiquantitative interpretation of aeromagnetic data over the Lancinha Shear Zone, southern Ribeira Belt, in Paraná State, Southern Brazil. *Geologia USP, Série Científica*, **14**, 3–18, <https://doi.org/10.5327/Z1519-874X201400040001> [in Portuguese]
- Cavalcante, C., Lagoeiro, L., Fossen, H., Egydio-Silva, M., Morales, L.F.G., Ferreira, F. and Conte, F.T. 2018. Temperature constraints on microfabric patterns in quartzofeldspathic mylonites, Ribeira belt (SE Brazil). *Journal of Structural Geology*, **115**, 243–262, <https://doi.org/10.1016/j.jsg.2018.07.013>
- Chemale, F., Jr, Mallmann, G., Bitencourt, M.F. and Kawashita, K. 2003. Isotope geology of syntectonic magmatism along the Major Gercino Shear Zone, southern Brazil: implications for the timing of deformation events. *IV South American Symposium on Isotope Geology*, 24–27 August 2003, Salvador, Brazil. Geological Society of Chile, 516–519.
- Chemale, F., Jr, Mallmann, G., Bitencourt, M.F. and Kawashita, K. 2012. Time constraints on magmatism along the Major Gercino Shear Zone, southern Brazil: implications for West Gondwana reconstruction. *Gondwana*

- Research*, **22**, 184–199, <https://doi.org/10.1016/j.jgr.2011.08.018>
- Cingolani, C.A. 2011. The Tandilia System of Argentina as a southern extension of the Río de la Plata craton: an overview. *International Journal of Earth Sciences*, **100**, 221–242, <https://doi.org/10.1007/s00531-010-0611-5>
- Cingolani, C.A. and Bonhomme, M.G. 1982. Geochronology of the Upper Proterozoic sedimentary rocks, Argentina. *Precambrian Research*, **18**, 119–122 and 125–132, [https://doi.org/10.1016/0301-9268\(82\)90040-7](https://doi.org/10.1016/0301-9268(82)90040-7)
- Clemens, J.D. and Kisters, A.F.M. 2021. Magmatic indicators of subduction initiation: the bimodal Goas Intrusive Suite in the Pan-African Damara Belt of Namibia. *Precambrian Research*, **362**, article 106309, <https://doi.org/10.1016/j.precamres.2021.106309>
- Clemens, J.D., Buick, I.S. and Kisters, A.F.M. 2017a. The Donkerhuk batholith, Namibia: a giant S-type granite emplaced in the mid crust, in a fore-arc setting. *Journal of the Geological Society, London*, **174**, 157–169, <https://doi.org/10.1144/jgs2016-028>
- Clemens, J.D., Buick, I.S., Kisters, A.F.M. and Frei, D. 2017b. Petrogenesis of the granitic Donkerhuk batholith in the Damara Belt of Namibia: protracted, syntectonic, short-range, crustal magma transfer. *Contributions to Mineralogy and Petrology*, **172**, 1–23, <https://doi.org/10.1007/s00410-017-1370-0>
- Collet, B., Taud, H., Parrot, J.F., Bonavia, F. and Chorowicz, J. 2000. A new kinematic approach for the Danakil block using a digital elevation model representation. *Tectonophysics*, **316**, 343–357, [https://doi.org/10.1016/S0040-1951\(99\)00263-2](https://doi.org/10.1016/S0040-1951(99)00263-2)
- Conte, T., Cavalcante, C., Lagoeiro, L.E., Fossen, H. and Silveira, C.S. 2020. Quartz textural analysis from an anastomosing shear zone system: implications for the tectonic evolution of the Ribeira belt, Brazil. *Journal of South American Earth Sciences*, **103**, article 102750, <https://doi.org/10.1016/j.jsames.2020.102750>
- Cury, L.F. 2009. *Geologia do Terreno Paranaguá*. PhD thesis, Universidade de São Paulo.
- Davies, C.J. and Coward, M.P. 1982. The structural evolution of the Gariep arc in southern Namibia (south-west Africa). *Precambrian Research*, **17**, 173–198, [https://doi.org/10.1016/0301-9268\(82\)90023-7](https://doi.org/10.1016/0301-9268(82)90023-7)
- De Freitas, N.C., Almeida, J., Heilbron, M., Cutts, K. and Dussin, I. 2021. The Cabo Frio Thrust: a folded suture zone, Ribeira belt, SE Brazil. *Journal of Structural Geology*, **149**, article 104379, <https://doi.org/10.1016/j.jsg.2021.104379>
- Dehler, N.M., Machado, R. and Fassbinder, E. 2007. Shear structures in the Serra do Azeite Shear Zone, southeastern Brazil: transtensional deformation during regional transpression in the central Mantiqueira province (Ribeira belt). *Journal of South American Earth Sciences*, **23**, 176–192, <https://doi.org/10.1016/j.jsames.2006.09.017>
- Dehler, N.M., Magnavita, L.P., Correa Gomes, L., Rigoti, C.A., Oliveira, J.A.B., Sant'Anna, M.V. and Da Costa, L.D. 2016. The 'Helmut' geophysical anomaly: a regional left-lateral transtensional shear zone system connecting Santos and Campos basins, southeastern Brazil. *Marine and Petroleum Geology*, **72**, 412–422, <https://doi.org/10.1016/j.marpetgeo.2016.01.012>
- De Toni, G.B., Bitencourt, M.F., Konopásek, J., Martini, A., Andrade, P.H.S., Florisbal, L.M. and Campos, R.S. 2020a. Transpressive strain partitioning between the Major Gercino Shear Zone and the Tijucas Fold Belt, Dom Feliciano Belt, Santa Catarina, southern Brazil. *Journal of Structural Geology*, **136**, article 104058, <https://doi.org/10.1016/j.jsg.2020.104058>
- De Toni, G.B., Bitencourt, M.F., Nardi, L.V.S., Florisbal, L.M., Almeida, B.S. and Geraldes, M. 2020b. Dom Feliciano Belt orogenic cycle tracked by its pre-collisional magmatism: the Tonian (*ca.* 800 Ma) Porto Belo Complex and its correlations in southern Brazil and Uruguay. *Precambrian Research*, **342**, article 105702, <https://doi.org/10.1016/j.precamres.2020.105702>
- de Wit, M.J. and Linol, B. 2015. Precambrian basement of the Congo Basin and its flanking terrains. In: de Wit, M.J., Guillocheau, F. and de Wit, M.C.J. (eds) *Geology and Resource Potential of the Congo Basin*. Springer, 19–37, <https://doi.org/10.1007/978-3-642-29482-2>
- de Wit, M.J., Bowring, A.S., Ashwal, D.L., Randrianasolo, G.L., Morel, V.P.I. and Rambeloson, A.R. 2001. Age and tectonic evolution of Neoproterozoic ductile shear zones in southwestern Madagascar, with implications for Gondwana studies. *Tectonics*, **20**, 1–45, <https://doi.org/10.1029/2000TC900026>
- de Wit, M.J., Stankiewicz, J. and Reeves, C. 2008. Restoring Pan-African–Brazilian connections: more Gondwana control, less Trans-Atlantic corruption. *Geological Society, London, Special Publications*, **294**, 399–412, <https://doi.org/10.1144/SP294.20>
- Downing, K.N. and Coward, M.P. 1981. The Okahandja Lineament and its significance for Damaran tectonics in Namibia. *Geologische Rundschau*, **70**, 972–1000, <https://doi.org/10.1007/BF01820175>
- Duffles, P., Trouw, R.A.J., Mendes, J.C., Gerdes, A. and Vinagre, R. 2016. U–Pb age of detrital zircon from the Embu sequence, Ribeira belt, SE Brazil. *Precambrian Research*, **278**, 69–86, <https://doi.org/10.1016/j.precamres.2016.03.007>
- Du Toit, A.L. 1927. *A Geological Comparison of South America with South Africa*. The Carnegie Institution, Washington, 381.
- Du Toit, A.L. 1937. *Our Wandering Continents*. Oliver and Boyd, Edinburgh.
- Ebert, H.D. and Hasui, Y. 1998. Transpressional tectonics and strain partitioning during oblique collision between three plates in the Precambrian of southeast Brazil. *Geological Society, London, Special Publications*, **135**, 231–252, <https://doi.org/10.1144/GSL.SP.1998.135.01.15>
- Faleiros, F.M., Campanha, G.A.C., Martins, L., Vlach, S.R.F. and Vasconcelos, P.M. 2011. Ediacaran high-pressure collision metamorphism and tectonics of the southern Ribeira Belt (SE Brazil): evidence for terrane accretion and dispersion during Gondwana assembly. *Precambrian Research*, **189**, 263–291, <https://doi.org/10.1016/j.precamres.2011.07.013>
- Faleiros, F.M., Moraes, R., Pavan, M. and Campanha, G.A.C. 2016. A new empirical calibration of the quartz c-axis fabric opening-angle deformation thermometer. *Tectonophysics*, **671**, 173–182, <https://doi.org/10.1016/j.tecto.2016.01.014>
- Faleiros, F.M., Ribeiro, B.V. *et al.* 2022. Strain partitioning along terrane bounding and intraterrane shear

Transatlantic SW Gondwana crustal-scale shear zones

- zones: constraints from a long-lived transpressional system in West Gondwana (Ribeira Belt, Brazil). *Lithosphere*, **2022**, article 2103213, <https://doi.org/10.2113/2022/2103213>
- Fernandes, L.A.D. and Koester, E. 1999. The Neoproterozoic Dorsal de Canguçu strike-slip shear zone: its nature and role in the tectonic evolution of southern Brazil. *Journal of African Earth Sciences*, **29**, 3–24, [https://doi.org/10.1016/S0899-5362\(99\)00076-7](https://doi.org/10.1016/S0899-5362(99)00076-7)
- Floribal, L.M., Janasi, V.A., Bitencourt, M.F. and Heaman, L.M. 2012. Space–time relation of post-collisional granitic magmatism in Santa Catarina, southern Brazil: U–Pb LA-MC-ICP-MS zircon geochronology of coeval mafic–felsic magmatism related to the Major Gercino Shear Zone. *Precambrian Research*, **216–219**, 132–151, <https://doi.org/10.1016/j.precamres.2012.06.015>
- Fontainha, M.V.F., Trouw, R.A.J., Dantas, E.L., Polo, H.J.O., Serafim, I.C.C.O., Furtado, P.C. and Negrão, A.P. 2021. Reactivated shear zones: a case study in a tectonic superposition zone between the Southern Brasília and Ribeira orogens, southeastern Brazil. *Journal of South American Earth Sciences*, **112**, article 103537, <https://doi.org/10.1016/j.jsames.2021.103537>
- Fossen, H. 2016. *Structural Geology*. Cambridge University Press.
- Fossen, H., Meira, V.T., Cavalcante, C., Konopásek, J. and Janoušek, V. 2021. Comment to ‘Neoproterozoic magmatic arc systems of the central Ribeira belt, SE-Brazil, in the context of the West-Gondwana pre-collisional history: A review’. *Journal of South American Earth Sciences*, **107**, 103052, <https://doi.org/10.1016/j.jsames.2020.103052>
- Foster, D.A., Goscombe, B.D. and Gray, D.R. 2009. Rapid exhumation of deep crust in an obliquely convergent orogen: the Kaoko Belt of the Damara Orogen. *Tectonics*, **28**, <https://doi.org/10.1029/2008TC002317>
- Franke, D., Ladage, S. et al. 2010. Birth of a volcanic margin off Argentina, South Atlantic. *Geochemistry, Geophysics, Geosystems*, **11**, 1–20, <https://doi.org/10.1029/2009GC002715>
- Frantz, J.C., McNaughton, N.J., Marques, J.C., Hartmann, I.A., Botelho, N.F. and Caravaca, G. 2003. SHRIMP U–Pb zircon ages of granitoids from southernmost Brazil: constraints on the temporal evolution of the Dorsal de Canguçu transcurrent shear zone and the eastern Dom Feliciano Belt. *IV South American Symposium on Isotope Geology*, 24–27 August, Salvador, Brazil. Geological Society of Chile, 174–177.
- Franz, L., Romer, R.L. and Dingeldey, D.P. 1999. Diachronous Pan-African granulite-facies metamorphism (650 Ma and 550 Ma) in the Kaoko belt, NW Namibia. *European Journal of Mineralogy*, **11**, 167–180, https://www.researchgate.net/publication/279582528_Diachronous_Pan-African_granulite-facies_metamorphism_650_Ma_and_550_Ma_in_the_Kaoko_belt_NW_Namibia
- Frimmel, H.E. 1995. Metamorphic evolution of the Gariep Belt. *South African Journal of Geology*, **98**, 176–190.
- Frimmel, H.E. 2018. The Gariep Belt. In: Siegesmund, S., Basei, M.A.S., Oyhantçabal, P. and Oriolo, S. (eds) *Geology of Southwest Gondwana*. Springer, Cham, 353–386.
- Frimmel, H.E. and Frank, W. 1998. Neoproterozoic tectono-thermal evolution of the Gariep Belt and its basement, Namibia and South Africa. *Precambrian Research*, **90**, 1–28, [https://doi.org/10.1016/S0301-9268\(98\)00029-1](https://doi.org/10.1016/S0301-9268(98)00029-1)
- Gaina, C., Torsvik, T.H., van Hinsbergen, D.J., Medvedev, S., Werner, S.C. and Labails, C. 2013. The African plate: a history of oceanic crust accretion and subduction since the Jurassic. *Tectonophysics*, **604**, 4–25, <https://doi.org/10.1016/j.tecto.2013.05.037>
- Ganade de Araujo, C.E., Rubatto, D., Hermann, J., Cordani, U.G., Cabry, R. and Basei, M.A.S. 2014. Ediacaran 2500-km-long synchronous deep continental subduction in the West Gondwana Orogen. *Nature Communications*, **5**, article 5198, <https://doi.org/10.1038/ncomms6198>
- Gaucher, C., Poire, D.G., Gomez Peral, L. and Chigliano, L. 2005. Litoestratigrafía, bioestratigrafía y correlaciones de las sucesiones sedimentarias del Neoproterozoico–Cámbrico del Craton del Río de la Plata (Uruguay y Argentina). *Latin American Journal of Sedimentology and Basin Analysis*, **12**, 145–160, <http://www.scielo.org.ar/pdf/lajsba/v12n2/v12n2a06.pdf>
- Giraldo, S.J., Trouw, R.A.J., Duffes, P., da Costa, R.V., Mejia, M.I. and Marimón, R.S. 2019. Structural analysis combined with new geothermobarometric and geochronological results of the Além Paraíba shear zone, between Três Rios and Bananal, Ribeira Orogen, SE Brazil. *Journal of South American Earth Sciences*, **90**, 118–136, <https://doi.org/10.1016/j.jsames.2018.11.018>
- Goscombe, B. and Gray, D.R. 2007. The Coastal Terrane of the Kaoko Belt, Namibia: outboard arc-terrane and tectonic significance. *Precambrian Research*, **155**, 139–158, <https://doi.org/10.1016/j.precamres.2007.01.008>
- Goscombe, B.D. and Gray, D.R. 2008. Structure and strain variation at mid-crustal levels in a transpressional orogen: a review of Kaoko Belt structure and the character of West Gondwana amalgamation and dispersal. *Gondwana Research*, **13**, 45–85, <https://doi.org/10.1016/j.gr.2007.07.002>
- Goscombe, B., Hand, M. and Gray, D. 2003a. Structure of the Kaoko Belt, Namibia: progressive evolution of a classic transpressional orogen. *Journal of Structural Geology*, **25**, 1049–1081, [https://doi.org/10.1016/S0191-8141\(02\)00150-5](https://doi.org/10.1016/S0191-8141(02)00150-5)
- Goscombe, B., Hand, M., Gray, D. and Mawby, J. 2003b. The metamorphic architecture of a transpressional orogen: the Kaoko Belt, Namibia. *Journal of Petrology*, **44**, 679–711, <https://doi.org/10.1093/ptrology/44.4.679>
- Goscombe, B., Gray, D. and Hand, M. 2004. Variation in metamorphic style along the northern margin of the Damara Orogen, Namibia. *Journal of Petrology*, **45**, 1261–1295, <https://doi.org/10.1093/ptrology/egh013>
- Goscombe, B., Foster, D.A., Gray, D., Wade, B., Marsellos, A. and Titus, J. 2017. Deformation correlations, stress field switches and evolution of an orogenic intersection: the Pan-African Kaoko–Damara orogenic junction. *Namibia Geoscience Frontiers*, **8**, 1187–1232, <https://doi.org/10.1016/j.gsf.2017.05.001>
- Goscombe, B., Foster, D.A. et al. 2022. Episodic intra-continental reactivation during collapse of a collisional orogen: the Damara Belt, Namibia. *Gondwana Research*, **109**, 285–375, <https://doi.org/10.1016/j.gr.2022.05.003>

- Graça, M.C., Kusznir, N. and Stanton, N.S.G. 2019. Crustal thickness mapping of the central South Atlantic and the geodynamic development of the Rio Grande Rise and Walvis Ridge. *Marine and Petroleum Geology*, **101**, 230–242, <https://doi.org/10.1016/j.marpetgeo.2018.12.011>
- Granath, J., Wanke, A. and Stollhofen, H. 2022. Synkinematic inversion in an intracontinental extensional field? A structural analysis of the Waterberg Thrust, northern Namibia. *Journal of Structural Geology*, **161**, article 104660, <https://doi.org/10.1016/j.jsg.2022.104660>
- Gray, D.R., Foster, D.A., Goscombe, B., Passchier, C.W. and Trouw, R.A.J. 2006. $^{40}\text{Ar}/^{39}\text{Ar}$ thermochronology of the Pan-African Damara Orogen, Namibia, with implications for tectonothermal and geodynamic evolution. *Precambrian Research*, **150**, 49–72, <https://doi.org/10.1016/j.precamres.2006.07.003>
- Gresse, P.G. 1995. Transpression and transection in the late Pan-African Vanrhynsdorp foreland thrust–fold belt, South Africa. *Journal of African Earth Sciences*, **21**, 91–105, [https://doi.org/10.1016/0899-5362\(95\)00089-C](https://doi.org/10.1016/0899-5362(95)00089-C)
- Guadagnin, F., Chemale, F. *et al.* 2010. Depositional age and provenance of the Itajaí Basin, Santa Catarina State, Brazil: implications for SW Gondwana correlation. *Precambrian Research*, **180**, 156–182, <https://doi.org/10.1016/j.precamres.2010.04.002>
- Halbich, I.W. and Alchin, D.J. 1995. The Gariep belt: stratigraphic–structural evidence for obliquely transformed grabens and back-folded thrust stacks in a combined thick-skin thin-skin structural setting. *Journal of African Earth Sciences*, **21**, 9–33, [https://doi.org/10.1016/0899-5362\(95\)00080-D](https://doi.org/10.1016/0899-5362(95)00080-D)
- Harara, O.M. 1993. *Análise Estrutural, Petrográfica e Geocronológica dos Litotipos da Região de Piên (PR) e Adjacências*. Master's dissertation, Universidade de São Paulo.
- Harara, O.M.M. 2001. *Mapeamento e Investigação Petrográfica e Geocronológica dos Litotipos da Região do Alto Rio Negro (PR-SC): um Exemplo de Sucessivas e Distintas Atividades Magmáticas Durante o Neoproterozóico III*. PhD thesis, University of São Paulo, <https://doi.org/10.11606/T.44.2001.tde-17112015-091642>
- Heilbron, M., Valeriano, C.M., Tassinari, C.C.G., Almeida, J., Tupinambá, M., Siga, J. and Trouw, R. 2008. Correlation of Neoproterozoic terranes between the Ribeira Belt, SE Brazil and its African counterpart: comparative tectonic evolution and open questions. *Geological Society, London, Special Publications*, **294**, 211–237, <https://doi.org/10.1144/SP294.12>
- Heine, C., Zoethout, J. and Müller, R.D. 2013. Kinematics of the South Atlantic rift. *Solid Earth*, **4**, 215–253, <https://doi.org/10.5194/se-4-215-2013>
- Heller, B.M., Hueck, M., Passarelli, C.R. and Basei, M.A.S. 2021. Zircon U–Pb geochronology and Hf isotopes of the Luís Alves Terrane: Archean to Paleoproterozoic evolution and Neoproterozoic overprint. *Journal of South American Earth Sciences*, **106**, 103008, <https://doi.org/10.1016/j.jsames.2020.103008>
- Hudek, M.R. and Jackson, M.P.A. 2002. Structural segmentation, inversion and salt tectonics on a passive margin: evolution of the Inner Kwanza Basin, Angola. *GSA Bulletin*, **114**, 1222–1244, [https://doi.org/10.1130/0016-7606\(2002\)114<1222:SSIAST>2.0.CO;2](https://doi.org/10.1130/0016-7606(2002)114<1222:SSIAST>2.0.CO;2)
- Hueck, M., Basei, M.A.S., Wemmer, K., Oriolo, S., Heidelberg, F. and Siegesmund, S. 2019. Evolution of the Major Hercino Shear Zone in the Dom Feliciano Belt, South Brazil, and implications for the assembly of southwestern Gondwana. *International Journal of Earth Sciences*, **108**, 403–425, <https://doi.org/10.1007/s00531-018-1660-4>
- Hueck, M., Wemmer, K. *et al.* 2020. Dating recurrent shear zone activity and the transition from ductile to brittle deformation: white mica geochronology applied to the Neoproterozoic Dom Feliciano Belt in South Brazil. *Journal of Structural Geology*, **141**, 104199, <https://doi.org/10.1016/j.jsg.2020.104199>
- Jacobs, J., Pisarevsky, S., Thomas, R.J. and Becker, T. 2008. The Kalahari Craton during the assembly and dispersal of Rodinia. *Precambrian Research*, **160**, 142–158, <https://doi.org/10.1016/j.precamres.2007.04.022>
- Jelsma, H.A., McCourt, S. *et al.* 2018. The geology and evolution of the Angolan Shield, Congo Craton. In: Siegesmund, S., Basei, M.A.S., Oyhantçal, P. and Oriolo, S. (eds) *Geology of Southwest Gondwana*. Springer, Cham, 217–239.
- Jung, S. and Mezger, K. 2003. Petrology of basement-dominated terranes: I. Regional metamorphic $T-t$ path from U–Pb monazite and Sm–Nd garnet geochronology (Central Damara orogen, Namibia). *Chemical Geology*, **198**, 223–247, [https://doi.org/10.1016/S0009-2541\(03\)00037-8](https://doi.org/10.1016/S0009-2541(03)00037-8)
- Karner, G.D. and Driscoll, N.W. 1999. Tectonic and stratigraphic development of the West African and eastern Brazilian margins: insights from quantitative basin modelling. *Geology Society, London, Special Publications*, **153**, 11–40, <https://doi.org/10.1144/GSL.SP.1999.153.01.02>
- Keidel, J. 1916. La geología de las sierras de la Provincia de Buenos Aires y sus relaciones con las montañas de Sudáfrica y los Andes. *Anales del Ministerio de Agricultura de la Nación, Sección Geología, Mineralogía y Minería, Buenos Aires*, **3**, 1–78.
- Kisters, A.F.M., Belcher, R.W., Scheepers, R., Rozendaal, A., Jordaan, L.S. and Armstrong, R.A. 2002. Timing and kinematics of the Colenso Fault: the Early Paleozoic shift from collisional to extensional tectonics in the Pan-African Saldania Belt, South Africa. *South African Journal of Geology*, **105**, 257–270, <https://doi.org/10.2113/1050257>
- Klein, F.G., Koester, E., Vieira, D.T., Ramos, R.C., Porcher, C.C. and Philipp, R.P. 2018. Geologia do Granito Três Figueiras: magmatismo peraluminoso de 585 Ma no sudeste do Cinturão Dom Feliciano. *Pesquisas em Geociências*, **46**, article e0665, <https://doi.org/10.22456/1807-9806.88646>
- Koester, E., Soliani, J.E., Fernandes, L.A.D., Kraemer, G. and Tommasi, A. 1997. Geocronologia Rb/Sr e K/Ar dos granitoides sintectônicos à Zona de Cisalhamento Transcorrente Dorsal de Canguçu na região de Encruzilhada do Sul (RS). *Pesquisas em Geociências*, **24**, 67, <https://doi.org/10.22456/1807-9806.21185>
- Koester, E., Roisenberg, A., Fernandes, L.A.D., Soliani, J.E., Nardi, L.V.S. and Kraemer, G. 2001. Petrologia dos granitoides sintectônicos à Zona de Cisalhamento

Transatlantic SW Gondwana crustal-scale shear zones

- Transcorrente Dorsal de Canguçu, Encruzilhada do Sul, RS. *Revista Brasileira de Geociências*, **31**, 131–140, <https://doi.org/10.25249/0375-7536.2001312131140>
- Koester, E., Chemale Junior, F., Porcher, C.C., Bertotti, A.L. and Fernandes, L.A.D. 2008. U–Pb ages of granitoids from eastern Sul-Riograndense Shield. *VI South American Symposium on Isotope Geology*, 13–17 April, San Carlos de Bariloche, Argentina.
- Konopásek, J., Kröner, S., Kitt, S.L., Passchier, C.W. and Kröner, A. 2005. Oblique collision and evolution of large-scale transient shear zones in the Kaoko belt, NW Namibia. *Precambrian Research*, **136**, 139–157, <https://doi.org/10.1016/j.precamres.2004.10.005>
- Konopásek, J., Sláma, J. and Košler, J. 2016. Linking the basement geology along the Africa–South America coasts in the South Atlantic. *Precambrian Research*, **280**, 221–230, <https://doi.org/10.1016/j.precamres.2016.05.011>
- Kröner, S., Konopásek, J., Kröner, A., Passchier, C.W., Poller, U., Wingate, M.T.D. and Hofmann, L.H. 2004. U–Pb and Pb–Pb zircon ages for metamorphic rocks in the Kaoko Belt of Northwestern Namibia: a Palaeo- to Mesoproterozoic basement reworked during the Pan-African orogeny. *South African Journal of Geology*, **107**, 455–476, <https://doi.org/10.2113/107.3.455>
- Kumar, N., Danforth, A., Nuttall, P., Hellwig, J., Bird, D.E. and Venkatraman, S. 2013. From oceanic crust to exhumed mantle: a 40 year (1970–2010) perspective on the nature of crust under the Santos Basin, SE Brazil. *Geological Society, London, Special Publications*, **369**, 147–165, <https://doi.org/10.1144/SP369.16>
- Lehmann, J., Saalman, K. *et al.* 2016. Structural and geochronological constraints on the Pan-African tectonic evolution of the northern Damara Belt, Namibia. *Tectonics*, **35**, 103–135, <https://doi.org/10.1002/2015TC003899>
- Lehmann, J., Bybee, G.M., Hayes, B., Owen-Smith, T.M. and Belyanin, G. 2020. Emplacement of the giant Kunene AMCG complex into a contractional ductile shear zone and implications for the Mesoproterozoic tectonic evolution of SW Angola. *International Journal of Earth Sciences*, **109**, 1463–1485, <https://doi.org/10.1007/s00531-020-01837-5>
- López-Gamundí, O., Fildani, A., Weislogel, A. and Rossello, E. 2013. The age of the Tunas Formation in the Sauce Grande basin–Ventana foldbelt (Argentina): implications for the Permian evolution of the southwestern margin of Gondwana. *Journal of South American Earth Sciences*, **45**, 250–258, <https://doi.org/10.1016/j.jsames.2013.03.011>
- Lovecchio, J.P., Rohais, S., Joseph, P., Bolatti, N.D. and Ramos, V.A. 2020. Mesozoic rifting evolution of SW Gondwana: a poly-phased, subduction-related, extensional history responsible for basin formation along the Argentinean Atlantic margin. *Earth-Science Reviews*, **203**, article 103138, <https://doi.org/10.1016/j.earscirev.2020.103138>
- Machado, R., Dehler, N.M. and Vasconcelos, P. 2007. ⁴⁰Ar/³⁹Ar ages (600–570 Ma) of the Serra do Azeite transtensional shear zone: evidence for syncontractional extension in the Cajati area, southern Ribeira belt. *Anais da Academia Brasileira de Ciências*, **79**, 713–723, <https://doi.org/10.1590/S0001-3765200700400011>
- Mantovani, M.S.M. and Brito Neves, B.B. 2009. The Parapanema lithospheric block: its nature and role in the accretion of Gondwana. *Developments in Precambrian Geology*, **16**, 257–272, [https://doi.org/10.1016/S0166-2635\(09\)01619-3](https://doi.org/10.1016/S0166-2635(09)01619-3)
- Martino, R.D., Guerreschi, A.B. and Anzil, P.A. 2010. Metamorphic and tectonic evolution at 31°36' S across a deep crustal zone from the Sierra Chica de Córdoba, Sierras Pampeanas, Argentina. *Journal of South American Earth Sciences*, **30**, 12–28, <https://doi.org/10.1016/j.jsames.2010.07.008>
- Martins, G.G., Mendes, J.C., Schmitt, R.S., Armstrong, R. and Valeriano, C.M. 2016. 550–490 Ma pre- to post-collisional shoshonitic rocks in the Ribeira Belt (SE Brazil) and their tectonic significance. *Precambrian Research*, **286**, 352–369, <https://doi.org/10.1016/j.precamres.2016.10.010>
- Martins, G.G., Mendes, J.C., Schmitt, R.S. and Armstrong, R. 2021. Unravelling source and tectonic environment of an Ediacaran magmatic province from southeast Brazil: insights from geochemistry and isotopic investigation. *Lithos*, **404–405**, article 106428, <https://doi.org/10.1016/j.lithos.2021.106428>
- McDermott, C., Lonergan, L., Collier, J.S., McDermott, K.G. and Bellingham, P. 2018. Characterization of seaward-dipping reflectors along the South American Atlantic margin and implications for continental breakup. *Tectonics*, **37**, 3303–3327, <https://doi.org/10.1029/2017TC004923>
- Meert, J.G. 2003. A synopsis of events related to the assembly of the eastern Gondwana. *Tectonophysics*, **362**, 1–40, [https://doi.org/10.1016/S0040-1951\(02\)00629-7](https://doi.org/10.1016/S0040-1951(02)00629-7)
- Meira, V.T., Garcia-Casco, A., Hyppolito, T., Juliani, C. and Schorscher, J.H.D. 2019. Tectono-metamorphic evolution of the Central Ribeira Belt, Brazil: a case of late Neoproterozoic intracontinental orogeny and flow of partially molten deep crust during the assembly of West Gondwana. *Tectonics*, **38**, 3182–3209, <https://doi.org/10.1029/2018TC004959>
- Meneghini, F., Fagereng, Å. and Kisters, A. 2017. The Matchless Amphibolite of the Damara Belt, Namibia: unique preservation of a Late Neoproterozoic ophiolitic suture. *Ofoliti*, **42**, 129–145, <https://doi.org/10.4454/ofoliti.v42i2.488>
- Menezes, M., Schmitt, R.S., Ribeiro, A., Nummer, A., Cabrera, J., Bossi, J. and Gaucher, C. 2010. Geologia estrutural e estratigrafia da Formação Rocha, SE do Uruguai. *VI Congresso Uruguayo de Geología*, 10 May 2010, San Francisco de las Sierras, Uruguay, Abstracts CD, https://inis.iaea.org/collection/NCLCollectionStore/_Public/45/054/45054829.pdf
- Menezes Santos, M. 2010. *Geologia estrutural e estratigrafia da formação Rocha na região de La Paloma e Rocha, Uruguai*. Dissertação de Mestrado, Universidade do Estado do Rio de Janeiro [Master's Thesis, State University of Rio de Janeiro].
- Miller, R.M. 1979. The Okahandja Lineament, a fundamental tectonic boundary in the Damara Orogen of South West Africa/Namibia. *Transactions of the Geological Society of South Africa*, **82**, 349–361.
- Miller, R.M. 1983. Evolution of the Damara Orogen of South West Africa/Namibia. *Geological Society of South Africa Special Publications*, **11**.
- Miller, R.M. 2008. *The Geology of Namibia*. Ministry of Mines and Energy, Geological Survey, **1**.

- Monié, P., Bosch, D., Bruguier, O., Vauchez, A., Rolland, Y., Nsungani, P. and Buta Neto, A. 2012. The Late Neoproterozoic/Early Palaeozoic evolution of the West Congo Belt of NW Angola: geochronological (U–Pb and Ar–Ar) and petrostructural constraints. *Terra Nova*, **24**, 238–247, <https://doi.org/10.1111/j.1365-3121.2012.01060.x>
- Müller, R.D., Cannon, J. *et al.* 2018. GPlates: building a virtual Earth through deep time. *Geochemistry, Geophysics, Geosystems*, **19**, 2243–2261, <https://doi.org/10.1029/2018GC007584>
- Novo, T., Rezende, C., Prosdocimi, G., Martins, L. and Peixoto, E. 2014. *Programa Mapeamento Geológico do Estado de Minas Gerais – Projeto Fronteiras de Minas Gerais. Folha Extrema (SF-23-Y-B-IV) Escala 1:100.000*. Codemig, UFMG, CPMTC.
- Oriolo, S., Oyhantçabal, P., Heidelbach, F., Wemmer, K. and Siegesmund, S. 2015. Structural evolution of the Sarandí del Yí Shear Zone, Uruguay: kinematics, deformation conditions and tectonic significance. *International Earth Science*, **104**, 1759–1777, <https://doi.org/10.1007/s00531-015-1166-2>
- Oriolo, S., Oyhantçabal, P. *et al.* 2016a. Timing of deformation in the Sarandí del Yí Shear Zone, Uruguay: implications for the amalgamation of western Gondwana during the Neoproterozoic Brasiliano–Pan-African Orogeny. *Tectonics*, **35**, 754–771, <https://doi.org/10.1002/2015TC004052>
- Oriolo, S., Oyhantçabal, P. *et al.* 2016b. Shear zone evolution and timing of deformation in the Neoproterozoic transpressional Dom Feliciano Belt, Uruguay. *Journal of Structural Geology*, **92**, 59–78, <https://doi.org/10.1016/j.jsg.2016.09.010>
- Oriolo, S., Becker, T. *et al.* 2018a. The Kalahari Craton, southern Africa: from Archean crustal evolution to Gondwana amalgamation. In: Siegesmund, S., Basei, M.A.S., Oyhantçabal, P. and Oriolo, S. (eds) *Geology of Southwest Gondwana*. Springer, Cham, 133–159.
- Oriolo, S., Hueck, M., Oyhantçabal, P., Goscombe, B., Wemmer, K. and Siegesmund, S. 2018b. Shear zones in Brasiliano–Pan-African belts and their role in amalgamation and break-up of southwest Gondwana. In: Siegesmund, S., Basei, M.A.S., Oyhantçabal, P. and Oriolo, S. (eds) *Geology of Southwest Gondwana*. Springer, Cham, https://doi.org/10.1007/978-3-319-68920-3_22
- Oyhantçabal, P. 2005. *The Sierra Ballena Shear Zone: Kinematics, Timing and Its Significance for the Geotectonic Evolution of Southeast Uruguay*. PhD dissertation, Universität zu Göttingen, http://webdoc.sub.gwdg.de/diss/2005/oyhantcabal_cironi/oyhantcabal_cironi.pdf
- Oyhantçabal, P., Siegesmund, S., Wemmer, K., Presnyakov, S. and Layer, P. 2009. Geochronological constraints on the evolution of the southern Dom Feliciano Belt (Uruguay). *Journal of the Geological Society, London*, **166**, 1075–1084, <https://doi.org/10.1144/0016-76492008-122>
- Oyhantçabal, P., Siegesmund, S., Wemmer, K. and Layer, P. 2010. The Sierra Ballena Shear Zone in the southernmost Dom Feliciano Belt (Uruguay): evolution, kinematics, and deformation conditions. *International Journal of Earth Sciences*, **99**, 1227–1246, <https://doi.org/10.1007/s00531-009-0453-1>
- Oyhantçabal, P., Siegesmund, S. and Wemmer, K. 2011a. The Río de la Plata Craton: a review of units, boundaries, ages and isotopic signature. *International Journal of Earth Sciences*, **100**, 201–220, <https://doi.org/10.1007/s00531-010-0580-8>
- Oyhantçabal, P., Siegesmund, S., Wemmer, K. and Passchier, C.W. 2011b. The transpressional connection between Dom Feliciano and Kaoko belts at 580–550 Ma. *International Journal of Earth Sciences*, **100**, 379–390, <https://doi.org/10.1007/s00531-010-0577-3>
- Oyhantçabal, P., Oriolo, S., Philipp, R.P., Wemmer, K. and Siegesmund, S. 2018. The Nico Pérez Terrane of Uruguay and southeastern Brazil. In: Siegesmund, S., Basei, M.A.S., Oyhantçabal, P. and Oriolo, S. (eds) *Geology of Southwest Gondwana*. Springer, Cham, https://doi.org/10.1007/978-3-319-68920-3_22
- Pángaro, F. and Ramos, V.A. 2012. Paleozoic crustal blocks of onshore and offshore central Argentina: new pieces of the southwestern Gondwana collage and their role in the accretion of Patagonia and the evolution of Mesozoic South Atlantic sedimentary basins. *Marine and Petroleum Geology*, **37**, 162–183, <https://doi.org/10.1016/j.marpetgeo.2012.05.010>
- Pángaro, F., Ramos, V.A. and Pazos, P.J. 2016. The Hesperides basin: a continental-scale upper Palaeozoic to Triassic basin in southern Gondwana. *Basin Research*, **28**, 685–711, <https://doi.org/10.1111/bre.12126>
- Passarelli, C.R. 2001. *Caracterização Estrutural e Geocronológica dos Domínios Tectônicos da Porção Sul-oriental do Estado de São Paulo*. PhD thesis, Universidade de São Paulo, <http://www.teses.usp.br/teses/disponiveis/44/44134/tde-03022014-155518/pt-br.php>
- Passarelli, C.R. 2008. *História tectono-termal e cinemática do Sistema de Cisalhamento Cubatão-Itariri e Serrinha*. FAPESP 04/07837-4 Research Report.
- Passarelli, C.R. and Verma, S.K. 2020. Evidence of mingling between contrasting magmas in the Ribeirão do Óleo Pluton, Coastal Terrane and the tectonic implications on the Ribeira Belt, Brazil. *International Journal of Earth Sciences*, **109**, 317–344, <https://doi.org/10.1007/s00531-019-01804-9>
- Passarelli, C.R., Wemmer, K., Siga, O., Jr, Siegesmund, S. and Basei, M.A.S. 2008. Tectonothermal evolution of the SE São Paulo State Precambrian terranes. *VI South American Symposium on Isotope Geology*, 13–17 April, San Carlos de Bariloche, Argentina, Abstracts, 150, <https://repositorio.usp.br/directbitstream/96fa25ce-dbe6-45bc-9e46-a1446fefcf94/1717792.pdf>
- Passarelli, C.R., Basei, M.A.S., Siga, O., Jr, Reath, I.M. and Campos, C. 2010. Deformation and geochronology of syntectonic granitoids emplaced in the Major Gercino Shear Zone, southeastern South America. *Gondwana Research*, **17**, 688–703, <https://doi.org/10.1016/j.gr.2009.09.013>
- Passarelli, C.R., Basei, M.A.S., Wemmer, K., Siga, O., Jr and Oyhantçabal, P. 2011. Major shear zones of southern Brazil and Uruguay: escape tectonics in the eastern border of Río de la Plata and Paranapanema cratons during the western Gondwana amalgamation. *International Journal of Earth Sciences*, **100**, 391–414, <https://doi.org/10.1007/s00531-010-0594-2>

Transatlantic SW Gondwana crustal-scale shear zones

- Passarelli, C.R., Basei, M.A.S., Siga, O. and Harara, O.M.M. 2018. The Luís Alves and Curitiba terranes: continental fragments in the Adamastor Ocean. In: Siegesmund, S., Basei, M., Oyhantçabal, P. and Oriolo, S. (eds) *Geology of Southwest Gondwana*. Springer, Cham, https://doi.org/10.1007/978-3-319-68920-3_8
- Passarelli, C.R., Verma, S.K., McReath, I., Basei, M.A.S. and Siga, O., Jr 2019. Tracing the history from Rodinia break-up to the Gondwana amalgamation in the Embu Terrane, southern Ribeira Belt, Brazil. *Lithos*, **342–343**, 1–17, <https://doi.org/10.1016/j.lithos.2019.05.024>
- Passchier, C.W. and Trouw, R.A. 2005. *Microtectonics*. Springer Science and Business Media.
- Passchier, C.W., Trouw, R.A.J., Goscombe, B., Gray, D. and Kröner, A. 2007. Intrusion mechanisms in a turbidite sequence: the Voetspoor and Doros plutons in NW Namibia. *Journal of Structural Geology*, **29**, 481–496, <https://doi.org/10.1016/j.jsg.2006.09.007>
- Passchier, C., Trouw, R.A. and Schmitt, R.S. 2016. How to make a transverse triple junction – new evidence for the assemblage of Gondwana along the Kaoko–Damara belts, Namibia. *Geology*, **44**, 843–846, <https://doi.org/10.1130/G38015.1>
- Patias, D., Cury, L.F. and Siga, O., Jr 2019. Transpressional deformation during Ediacaran accretion of the Paranaquá Terrane, southernmost Ribeira Belt, Western Gondwana. *Journal of South American Earth Sciences*, **96**, article 102374, <https://doi.org/10.1016/j.jsames.2019.102374>
- Peel, E., Sánchez Bettucci, L. and Basei, M.A.S. 2018. Geology and geochronology of Paso del Dragón Complex (northeastern Uruguay): implications on the evolution of the Dom Feliciano Belt (Western Gondwana). *Journal of South American Earth Sciences*, **85**, 250–262, <https://doi.org/10.1016/j.jsames.2018.05.009>
- Percival, J.J., Konopásek, J., Eiesland, R., Sláma, J., de Campos, R.S., Battisti, M.A. and Bitencourt, M.F. 2021. Pre-orogenic connection of the foreland domains of the Kaoko–Dom Feliciano–Garipe orogenic system. *Precambrian Research*, **354**, article 106060, <https://doi.org/10.1016/j.precamres.2020.106060>
- Peruchi, F.M., Florisbal, L.M., Bitencourt, M.F., Padilha, D.F. and Nardi, L.V.S. 2018. Ediacaran post-collisional K-rich granitic magmatism within the Major Gercino Shear Zone, southern Brazil: an example of prolonged magmatism and differentiation under active transcurrent tectonism. *Lithos*, **402–403**, article 106341, <https://doi.org/10.1016/j.lithos.2021.106341>
- Peterneel, R., Trouw, R.A.J. and Schmitt, R.S. 2005. Interferência entre duas faixas móveis neoproterozóicas: o caso das faixas Brasília e Ribeira no sudeste do Brasil. *Revista Brasileira de Geociências*, **35**, 297–310, <https://doi.org/10.25249/0375-7536.2005353297310>
- Philipp, R.P., Machado, R. and Chemale, F., Jr 2003. Reavaliação e novos dados geocronológicos (Ar/Ar, Rb/Sr e Sm/Nd) do Batólito Pelotas no Rio Grande do Sul: implicações petrogenéticas e idade de reativação das conas de cisalhamento. *Geologia USP Série Científica*, **3**, 71–84, <https://doi.org/10.5327/S1519-874X2003000100006>
- Philipp, R.P., Pimentel, M.M. and Chemale, F. 2016. Tectonic evolution of the Dom Feliciano Belt in southern Brazil: geological relationships and U–Pb geochronology. *Brazilian Journal of Geology*, **46**, 83–104, <https://doi.org/10.1590/2317-4889201620150016>
- Philipp, R.P., Pimentel, M.M. and Basei, M.A.S. 2018. The tectonic evolution of the São Gabriel Terrane, Dom Feliciano Belt, southern Brazil: the closure of the Charrua Ocean. In: Siegesmund, S., Oyhantçabal, P., Basei, M.A.S. and Oriolo, S. (eds) *Geology of Southwest Gondwana*. Springer, Cham, 243–265.
- Pinto, M.L. and Vidotti, R.M. 2019. Tectonic framework of the Paraná Basin unveiled from gravity and magnetic data. *Journal of South American Earth Sciences*, **90**, 216–232, <https://doi.org/10.1016/j.jsames.2018.12.006>
- Ramos, R.C., Koester, E., Vieira, D.T., Porcher, C.C., Gezatt, J.N. and Silveira, R.L. 2018. Insights on the evolution of the Arroio Grande Ophiolite (Dom Feliciano Belt, Brazil) from Rb–Sr and SHRIMP U–Pb isotopic geochemistry. *Journal of South American Earth Sciences*, **86**, 38–53, <https://doi.org/10.1016/j.jsames.2018.06.004>
- Ramos, V.A. 2008. Patagonia: a Paleozoic continent adrift? *Journal of South American Earth Sciences*, **26**, 235–251, <https://doi.org/10.1016/j.jsames.2008.06.002>
- Ramos, V.A., Vujovich, G., Martino, R. and Otamendi, J. 2010. Pampia: a large cratonic block missing in the Rodinia supercontinent. *Journal of Geodynamics*, **50**, 243–255, <https://doi.org/10.1016/j.jog.2010.01.019>
- Rapela, C.W., Pankhurst, R.J. et al. 2007. The Río de la Plata craton and the assembly of SW Gondwana. *Earth-Science Reviews*, **83**, 49–82, <https://doi.org/10.1016/j.earscirev.2007.03.004>
- Reeves, C.V. 2020a. African geology, the Bouvet mantle plume and the early opening of the Gondwana margins. Poster presented at the Netherlands Earth Science Congress, 12–13 March, Utrecht, <https://doi.org/10.13140/RG.2.2.16620.72327>
- Reeves, C.V. 2020b. *Finite Euler Rotation Poles for Gondwana Reassembly*. Earthworks Research Update No. 14, <https://www.reeves.nl/upload/ResearchUpdateNo14.pdf>
- Rey-Moral, C., Mochales, T. et al. 2022. Recording the largest gabbro-anorthositic complex worldwide: the Kunene Complex (KC), SW Angola. *Precambrian Research*, **379**, article 106790, <https://doi.org/10.1016/j.precamres.2022.106790>
- Ribeiro, B.V., Faleiros, F.M., Campanha, G.A.C., Lagoeiro, L., Weinberg, R.F. and Hunter, N.J.R. 2019. Kinematics, deformational conditions and tectonic setting of the Taxaquara Shear Zone, a major transpressional zone of the Ribeira Belt (SE Brazil). *Tectonophysics*, **751**, 83–108, <https://doi.org/10.1016/j.tecto.2018.12.025>
- Ribeiro, B.V., Mulder, J.A. et al. 2020. Using apatite to resolve the age and protoliths of mid-crustal shear zones: a case study from the Taxaquara Shear Zone, SE Brazil. *Lithos*, **378–379**, article 105817, <https://doi.org/10.1016/j.lithos.2020.105817>
- Richetti, P.C., Schmitt, R.S. and Reeves, C. 2018. Dividing the South American continent to fit a Gondwana reconstruction: a model based on continental geology. *Tectonophysics*, **747–748**, 79–98, <https://doi.org/10.1016/j.tecto.2018.09.011>
- Rocha, F.F.N., Bastos Neto, A.C., Remus, M.V.D. and Pereira, V.P. 2005. A fonte dos metais da Mina de Ouro do

- Schramm, Santa Catarina: evidências de dados de isótopos de Pb e elementos terras raras. *Pesquisas em Geociências*, **32**, 51–61, <https://doi.org/10.22456/1807-9806.19538>
- Rossello, E.A., Veroslavsky, G., Masquelin, H. and De Santa Ana, H. 2007. El corredor tectónico Juro-Cretácico Santa Lucía–Aiguá–Merín (Uruguay): evidencias cinemáticas transcurrentes dextrales y controles estructurales preexistentes. *Revista de la Asociación Geológica Argentina*, **62**, 92–104.
- Rozendaal, A., Gresse, P.G., Scheepers, R. and Le Roux, J.P. 1999. Neoproterozoic to early Cambrian crustal evolution of the Pan-African Saldania Belt, South Africa. *Precambrian Research*, **97**, 303–323, [https://doi.org/10.1016/S0301-9268\(99\)00036-4](https://doi.org/10.1016/S0301-9268(99)00036-4)
- Salazar, C.A., Archanjo, C.J., Rodrigues, S.W.O., Hollanda, M.H.B.M. and Liu, D. 2013. Age and magnetic fabric of the Três Córregos granite batholith: evidence for Ediacaran transtension in the Ribeira Belt (SE Brazil). *International Journal of Earth Sciences*, **102**, 1563–1581, <https://doi.org/10.1007/s00531-013-0908-2>
- Santos, R.V., Ganade, C.E. *et al.* 2019. Dating Gondwanan continental crust at the Rio Grande Rise, South Atlantic. *Terra Nova*, **31**, 424–429, <https://doi.org/10.1111/ter.12405>
- Sartori, J.E. 2012. *Análise de Vorticidade e Microestruturas da Zona de Cisalhamento Caucaia (SP)*. Master's dissertation, University of São Paulo, <https://doi.org/10.11606/D.44.2012.tde-22012015-142136>
- Schmitt, R.S., Trouw, R.A.J., van Schmus, W.R. and Pimentel, M.M. 2004. Late amalgamation in the central part of West Gondwana: new geochronological data and the characterization of a Cambrian collisional orogeny in the Ribeira Belt (SE Brazil). *Precambrian Research*, **133**, 29–61, <https://doi.org/10.1016/j.precamres.2004.03.010>
- Schmitt, R.S., Trouw, R.A.J., van Schmus, W.R. and Passchier, C.W. 2008. Cambrian orogeny in the Ribeira Belt (SE Brazil) and correlations within West Gondwana: ties that bind underwater. *Geological Society, London, Special Publications*, **294**, 279–296, <https://doi.org/10.1144/SP294.15>
- Schmitt, R.S., Trouw, R.A.J., Passchier, C.W., Medeiros, S.R. and Armstrong, R. 2012. 530 Ma syntectonic syenites and granites in NW Namibia – their relation with collision along the junction of the Damara and Kaoko belts. *Gondwana Research*, **21**, 362–377, <https://doi.org/10.1016/j.gr.2011.08.006>
- Schmitt, R.S., Trouw, R., van Schmus, W.R., Armstrong, R. and Stanton, N.S.G. 2016. The tectonic significance of the Cabo Frio Tectonic Domain in the SE Brazilian margin: a Paleoproterozoic through Cretaceous saga of a reworked continental margin. *Brazilian Journal of Geology*, **46**, 37–66, <https://doi.org/10.1590/2317-4889201620150025>
- Schmitt, R.S., de Fragoso, R.A. and Collins, A.S. 2018. Suturing Gondwana in the Cambrian: the orogenic events of the final amalgamation. In: Siegesmund, S., Basei, M.A.S., Oyhançabal, P. and Oriolo, S. (eds) *Geology of Southwest Gondwana*. Springer, Cham, 411–432.
- Schmitt, R.S., Silva, E.A., Gomes, I.V. and Benedek, M.R. 2023. Greater India and the New Gondwana Geological Map (IGCP-628). *Journal of the Geological Society of India*, **99**, 443–448, <https://doi.org/10.1007/s12594-023-2330-0>
- Schroeder, G.S. 2006. *Análise Tectônica da Bacia do Itajaí*. Master's dissertation, Universidade do Rio Grande do Sul, <http://hdl.handle.net/10183/13536>
- Siga, O., Jr 1995. *Domínios Tectônicos do Sudeste do Paraná e Nordeste de Santa Catarina: Geocronologia e Evolução Crustal*. PhD thesis, Universidade de São Paulo.
- Silva, A.T.S.F., Chiodi Filho, C., Chiodi, D.K. and Algarte, J.P. 1978. Geologia integrada das folhas Iguape e Cananéia. *XXX Congresso Brasileiro de Geologia*, Recife, Brazil, Abstracts, **1**, 208–221.
- Silva, B.Y.B. 2017. *Evolução Tectônica da Porção Central do Terreno Embu ao Norte da Zona de Cisalhamento Taxaquara–Guararema*. Master's dissertation, University of São Paulo, <https://doi.org/10.11606/D.44.2017.tde-22082017-084753>
- Silva Lara, H., Siegesmund, S., Wemmer, K., Hueck, M., Basei, M.A.S. and Oyhançabal, P. 2021. The Sierra de Aguirre Formation, Uruguay: post-collisional Ediacaran volcanism in the southernmost Dom Feliciano Belt. *Journal of South American Earth Sciences*, **107**, 103118, <https://doi.org/10.1016/j.jsames.2020.103118>
- Silva Lara, H., Siegesmund, S., Oriolo, S., Hueck, M., Wemmer, K., Basei, M.A. and Oyhançabal, P. 2022. Reassessing the polyphase Neoproterozoic evolution of the Punta del Este Terrane, Dom Feliciano Belt, Uruguay. *International Journal of Earth Sciences*, **111**, 2283–2316, <https://doi.org/10.1007/s00531-022-02230-0>
- Soto, M., Morales, E., Veroslavsky, G., de Santa Ana, H., Ucha, N. and Rodríguez, P. 2011. The continental margin of Uruguay: crustal architecture and segmentation. *Marine and Petroleum Geology*, **28**, 1676–1689, <https://doi.org/10.1016/j.marpetgeo.2011.07.001>
- Stanton, N., Schmitt, R.S., Galdeano, A., Maia, M. and Mane, M. 2010. Crustal structure of the southeastern Brazilian margin, Campos Basin, from aeromagnetic data: new kinematic constraints. *Tectonophysics*, **490**, 15–27, <https://doi.org/10.1016/j.tecto.2010.04.008>
- Stica, J.M., Zalán, P.V. and Ferrari, A.L. 2014. The evolution of rifting on the volcanic margin of the Pelotas Basin and the contextualization of the Paraná–Etendeka LIP in the separation of Gondwana in the South Atlantic. *Marine and Petroleum Geology*, **50**, 1–21, <https://doi.org/10.1016/j.marpetgeo.2013.10.015>
- Strugale, M., Schmitt, R.S. and Cartwright, J. 2021. Basement geology and its controls on the nucleation and growth of rift faults in the northern Campos Basin, offshore Brazil. *Basin Research*, **33**, 1906–1933, <https://doi.org/10.1111/BRE.12540>
- Tedeschi, M., Pedrosa-Soares, A. *et al.* 2018. Protracted zircon geochronological record of UHT garnet-free granulites in the southern Brasília orogen (SE Brazil): petrochronological constraints on magmatism and metamorphism. *Precambrian Research*, **316**, 103–126, <https://doi.org/10.1016/j.precamres.2018.07.023>
- Tomezzoli, R. and Cristallini, E. 2004. Secciones estructurales de Las Sierras Australes de la provincia de Buenos Aires: repetición de la secuencia estratigráfica a partir de fallas inversas? *Revista de la Asociación Geológica Argentina*, **59**, 1–11.

Transatlantic SW Gondwana crustal-scale shear zones

- Torsvik, T.H., Rousse, S., Labails, C. and Smethurst, M.A. 2009. A new scheme for the opening of the South Atlantic Ocean and the dissection of an Aptian salt basin. *Geophysical Journal International*, **177**, 1315–1333, <https://doi.org/10.1111/j.1365-246X.2009.04137.x>
- Trouw, C.C., de Medeiros, F.F.F. and Trouw, R.A.J. 2007. Evolução tectônica da Zona de Cisalhamento Caxambu. *MG Revista Brasileira de Geociências*, **37**, 767–776, <https://doi.org/10.25249/0375-7536.2007374767776>
- Trouw, R.A.J. and de Wit, M.J. 1999. Relation between the Gondwanide Orogen and contemporaneous intracratonic deformation. *Journal of African Earth Sciences*, **28**, 203–213, [https://doi.org/10.1016/S0899-5362\(99\)00024-X](https://doi.org/10.1016/S0899-5362(99)00024-X)
- Trouw, R.A.J., Peternel, R. *et al.* 2013. A new interpretation for the interference zone between the southern Brasília belt and the central Ribeira belt, SE Brazil. *Journal of South American Earth Sciences*, **48**, 43–57, <https://doi.org/10.1016/j.jsames.2013.07.012>
- Tupinambá, M., Heilbron, M. *et al.* 2012. Juvenile contribution of the Neoproterozoic Rio Negro Magmatic Arc (Ribeira Belt, Brazil): implications for Western Gondwana amalgamation. *Gondwana Research*, **21**, 422–438, <https://doi.org/10.1016/j.gr.2011.05.012>
- Ulrich, S., Konopásek, J., Jeřábek, P. and Tajčmanová, L. 2011. Transposition of structures in the Neoproterozoic Kaoko Belt (NW Namibia) and their absolute timing. *International Journal of Earth Sciences*, **100**, 415–429, <https://doi.org/10.1007/s00531-010-0573-7>
- Van Schijndel, V., Cornell, D.H., Hoffmann, K.H. and Frei, D. 2011. Three episodes of crustal development in the Rehoboth Province, Namibia. *Geological Society, London, Special Publications*, **357**, 27–47, <https://doi.org/10.1144/SP357.3>
- Vieira, D.T., Koester, E., Ramos, R.C., Porcher, C.C. and Barbosa, L.D.O. 2019. Sistema de zonas de cisalhamento transcorrentes Ayrosa Galvão–Arroio Grande, sudeste do Cinturão Dom Feliciano, RS. *17th Simpósio Nacional de Estudos Tectônicos, 11th International Symposium on Tectonics and 11th Simpósio Sul-Brasileiro de Geologia*, 26–29 May, Bento Gonçalves, Brazil. Abstracts, 64, <http://sbgeo.org.br/assets/admin/imgCk/files/Anais/ANAIS-XVIISNET-XISSBG-2019.pdf>
- Vieira, D.T., Koester, E., Ramos, R.C., Porcher, C.C. and Fernandes, L.A.D. 2020. SHRIMP U–Pb zircon ages for the synkinematic magmatism in the Dorsal de Canguçu Transcurrent Shear Zone, Dom Feliciano Belt (Brazil): tectonic implications. *Journal of South American Earth Sciences*, **100**, article 102603, <https://doi.org/10.1016/j.jsames.2020.102603>
- Vieira, D.T., Ramos, R.C., Koester, E., Lenz, C. and Klein, F.G. 2021. Peraluminous magmatism in the southernmost Dom Feliciano Belt (Brazil): magmatic evolution process, sources and tectonic implications. *Journal of South American Earth Sciences*, **106**, article 103081, <https://doi.org/10.1016/j.jsames.2020.103081>
- Vieira, T.A.T., Schmitt, R.S. *et al.* 2022. Contrasting P–T paths of basement and cover within the Búzios Orogen, SE Brazil: tracking Ediacaran–Cambrian subduction zones. *Precambrian Research*, **368**, article 106479, <https://doi.org/10.1016/j.precamres.2021.106479>
- Vinagre, R.C., Trouw, R.A.J., Kussama, H., Peternel, R., Mendes, J.C. and Duffles, P. 2016. Superposition of structures in the interference zone between the southern Brasília belt and the central Ribeira belt in the region SW of Itajubá (MG), SE Brazil. *Brazilian Journal of Geology*, **46**, 547–566, <https://doi.org/10.1590/2317-4889201620160034>
- Vinagre, R.C., Trouw, R.A.J., Marimon, R.S., Nepomuceno, F., Mendes, J.C. and Dantas, E. 2020. São Bento do Sapucaí Shear Zone: constraining age and P–T conditions of a collisional Neoproterozoic oblique shear zone, Ribeira Orogen, Brazil. *Journal of South American Earth Sciences*, **98**, article 102418, <https://doi.org/10.1016/j.jsames.2019.102418>
- Will, T.M., Gaucher, C., Ling, X.X., Li, X.H., Li, Q.L. and Frimmel, H.E. 2019. Neoproterozoic magmatic and metamorphic events in the Cuchilla Dionisio Terrane, Uruguay, and possible correlations across the South Atlantic. *Precambrian Research*, **320**, 303–322, <https://doi.org/10.1016/j.precamres.2018.11.004>
- Zanardo, A., Morales, B., Oliveira, M.A.F. and Del Lama, E.A. 2006. Tectono-lithologic associations of the Alterosa paleo suture zone southeastern Brazil. *Revista UNG – Geociências*, **5**, 103–117.
- Ziegler, U.R.F. and Stoessel, G.F.U. 1988. K–Ar dating of the Marienhof and Billstein formations in the Rehoboth Basement Inlier, SWA/Namibia. *Communications of the Geological Survey of South West Africa/Namibia*, **4**, 53–58.
- Zuquim, M.P.S., Trouw, R.A.J., Trouw, C.C. and Tohver, E. 2011. Structural evolution and U–Pb SHRIMP zircon ages of the Neoproterozoic Maria da Fé Shear Zone, central Ribeira Belt – SE Brazil. *Journal of South American Earth Sciences*, **31**, 199–213, <https://doi.org/10.1016/j.jsames.2011.02.002>